HAL
open science

Robust localization system using Visible Light Communication technology for underground mines

Fabián Seguel

To cite this version:

Fabián Seguel. Robust localization system using Visible Light Communication technology for underground mines. Networking and Internet Architecture [cs.NI]. Université de Lorraine; Universidad de Santiago de Chile, 2020. English. NNT : 2020LORR0012 . tel-02863495

HAL Id: tel-02863495

https://hal.univ-lorraine.fr/tel-02863495v1

Submitted on 10 Jun 2020

HAL is a multi-disciplinary open access archive for the deposit and dissemination of scientific research documents, whether they are published or not. The documents may come from teaching and research institutions in France or abroad, or from public or private research centers.

L'archive ouverte pluridisciplinaire **HAL**, est destinée au dépôt et à la diffusion de documents scientifiques de niveau recherche, publiés ou non, émanant des établissements d'enseignement et de recherche français ou étrangers, des laboratoires publics ou privés.

UNIVERSITÉ DE LORRAINE

AVERTISSEMENT

Ce document est le fruit d'un long travail approuvé par le jury de soutenance et mis à disposition de l'ensemble de la communauté universitaire élargie.

Il est soumis à la propriété intellectuelle de l'auteur. Ceci implique une obligation de citation et de référencement lors de l'utilisation de ce document.

D'autre part, toute contrefaçon, plagiat, reproduction illicite encourt une poursuite pénale.

Contact : ddoc-theses-contact@univ-lorraine.fr

LIENS

Code de la Propriété Intellectuelle. articles L 122. 4
Code de la Propriété Intellectuelle. articles L 335.2- L 335.10
http://www.cfcopies.com/V2/leg/leg_droi.php
http://www.culture.gouv.fr/culture/infos-pratiques/droits/protection.htm

École doctorale IAEM Lorraine

Robust localization system using Visible Light Communication technology for underground mines

THÈSE

présentée et soutenue publiquement le 12 Mars 2020

pour l'obtention du

Doctorat de l'Université de Lorraine

(Mention Automatique, Traitement du signal et des images, Génie informatique)

par

Fabián Esteban SEGUEL GONZÁLEZ

Composition du jury

Rapporteurs :	Professeur Millaray Curilem	Universidad de La Frontera
	Professeur Francois Spies	Université de Franche-Comté
Examinateurs :	Professeur Pablo Adasme	Universidad de Santiago de Chile
	Professeur Ismael Soto (*Directeur de thèse*)	Universidad de Santiago de Chile
	Professeur Patrick Charpentier (*Directeur de thèse*)	Université de Lorraine
	aître de Conférences Nicolas Krommenacker (*Co-directeur de thèse*)	Université de Lorraine

Centre de Recherche en Automatique de Nancy — UMR 7039

Remerciements

First and foremost, I want to thank my supervisors Ismael Soto, Patrick Charpentier and Nicolas Krommenacker. This work would not have been possible without their immense support, guidance and knowledge. But, most important without their friendship and the excellent work environment that we were involved during the preparation of this thesis. I hope sincerely our collaboration will not stop once this document is submitted.

I would also like to express my sincere gratitude to the reviewers of my thesis Prof. Millaray Curilem and Prof. Francois Spies, for the time and effort they have put in reviewing and assessing my work. Their ideas, feedback and questions have been invaluable.

My most sincere thanks also goes to Prof. Pablo Adasme, Prof. Hector Kaschel and Prof. Iván Jirón for evaluating my work throughout the whole PhD period. Their guidance and directions help me to finish my work in time.

I also want to thank all of my lab friends for the exchanges of knowledge and skills and, most important, *les apéros* and unforgettable moments we have enjoyed and shared inside and outside the lab.

Last but by no means least, I would like to thank my family. There are no words to express how grateful I am to them. They are the most important people in my world and I dedicate this thesis to them.

Contents

List of Figures v

List of Tables viii

Chapter 1
Introduction

1.1 Visible light positioning systems for indoor environments . . . 1
1.2 Motivation . . . 4
1.3 Contributions . . . 4
1.4 Publications . . . 6
1.4.1 Journal ISI articles . . . 6
1.4.2 Conference articles . . . 7

Chapter 2
Current positioning technologies in underground mines **9**

2.1 Introduction . . . 9
2.2 Importance and challenges of positioning in underground mines . . . 11
2.3 Requirements of positioning systems . . . 12
2.3.1 Accuracy . . . 12
2.3.2 Output data . . . 13
2.3.3 Precision . . . 14
2.3.4 Coverage . . . 15
2.3.5 Cost . . . 15
2.3.6 Required infrastructure . . . 15
2.3.7 Robustness . . . 16
2.3.8 Scalability . . . 16
2.3.9 Update rate . . . 17
2.3.10 Number of users . . . 17
2.3.11 Market maturity . . . 17

2.3.12 Intrusiveness . . . 17
2.3.13 Approval . . . 18
2.4 Classification of positioning systems for underground mines . . . 18
2.4.1 Technological principle . . . 19
2.4.2 System topology . . . 24
2.4.3 Deployment . . . 25
2.5 Systems proposed in literature . . . 26
2.6 Conclusions . . . 32

Chapter 3
Visible light communications channel modelling in underground mines **34**

3.1 Introduction . . . 34
3.2 Illumination standards . . . 36
3.3 Mathematical model . . . 38
3.3.1 Visible Light Communications System Configuration . . . 39
3.3.2 Light sources . . . 40
3.3.3 Light detectors . . . 43
3.3.4 Light propagation model . . . 44
3.4 Conclusions . . . 52

Chapter 4
Visible light positioning methods **53**

4.1 Introduction . . . 53
4.2 Main characteristics of VLP for their underground mine application . . . 54
4.2.1 Characteristics based on detector technology . . . 54
4.2.2 VLC characteristics for different positioning topologies implementation . . . 55
4.3 Visible light positioning methods classification . . . 56
4.3.1 Range based methods . . . 56
4.3.2 Range free methods . . . 64
4.3.3 Fingerprinting (FP) . . . 66
4.4 Robustness and characteristics analysis of VLP methods . . . 67

Chapter 5
Design and implementation of a low-cost/large-scale visible light positioning system **68**

5.1 Introduction . . . 68
5.2 Uplink for remote positioning . . . 68

5.3 Visible light communications downlink 70
5.4 Visible light communications receiver 71

Chapter 6
Design and implementation of a novel range free positioning method for robust visible light positioning in underground mines **75**

6.1 Introduction 75
6.2 System description 76
6.3 Network architecture based positioning method: Convex polygon positioning (CPP) 77
6.4 Enhance of position accuracy using imaging receivers (IR-CPP) 83
6.5 Simulation results 85
6.5.1 Square room 86
6.5.2 Tunnel section 92
6.6 Real implementation of CPP method using VLP testing platform 94

Chapter 7
Conclusions and perspectives **100**

7.1 Conclusion 100
7.2 Perspectives 101
7.2.1 Reduce the size of proposed receiver 101
7.2.2 Energy efficiency 102
7.2.3 Mobility and Tracking 102

Bibliography **104**

List of Figures

1.1 Visible light positioning classification based on receiver hardware and signal measurement used for position determination with the main contribution of this thesis highlighted in green . . . 3
1.2 Process diagram of contributions in this thesis . . . 5

2.1 Blockage of GNSS signal in (a) deep open cast mine and (b) underground mine . 10
2.2 Different types of mines based on their excavation (a) room-and-pillar and (b) longwall mining . . . 12
2.3 Estimated positioning error from CDF with a 90% of confidence level . . . 13
2.4 Different localization estimation (a) accurate and precise (b) accurate but not precise (c) not accurate but precise and (d) neither accurate nor precise . . . 14
2.5 Proposed taxonomy for the analysis of positioning systems . . . 16
2.6 Proposed taxonomy for the analysis of positioning systems . . . 18
2.7 Classification based on technological principle . . . 19
2.8 Different localization system topologies (a) Remote positioning, (b) Self positioning and (c) Indirect Positioning . . . 25

3.1 Current to Luminous flux curve of the LED light Cree XLamp CXB1512 [Des15] 35
3.2 Block diagram of an IMDD optical wireless communication system . . . 35
3.3 Typical light output comparison between white LED and incandescent light bulb as function of operating hours [Lum] . . . 37
3.4 El Teniente underground mine light deployment (a) Transportation tunnel (b) Machinery working inside the tunnel(images by Codelco) . . . 38
3.5 Different systems configurations for VLC link, PD is placed in the miner's helmet: (a) directed LOS, (b) nondirected LOS, (c) diffuse, and (d) tracked . . . 40
3.6 Electromagnetic spectrum [Min] . . . 41
3.7 Huma eye's response based on the 1978 CIE data (http://www.ecse.rpi.edu/ schubert/ Light-Emitting-Diodes-dot-org) . . . 42
3.8 . . . 43
3.9 . . . 44
3.10 Line of sight (LOS) VLC link . . . 45
3.11 Visible light communications channel model with tilted and rotated receiver . . . 46
3.12 Visible light communications channel model with tilted and rotated transmitter . 47
3.13 Diffuse and specular reflection from a glossy surface (Image retrieved from Juds et.al. (1988) [Jud88]) . . . 48
3.14 non-Line of sight (n-LOS) VLC link . . . 49

3.15 Walls geometry (a) traditional plane wall and (b) underground mine wall with randomly oriented surface . . . 49
3.16 Signal blockage due to shadowing in underground mines . . . 50
3.17 Scattering patterns (a) Rayleigh, (b) Mie, and (c) Non-selective scattering . . . 51

4.1 Advantages of indoor VLP systems . . . 54
4.2 Positioning method process diagram for (a) range based methods, (b) range free methods and, (c) fingerprinting . . . 57
4.3 Visible light positioning system topology classification . . . 58
4.4 Ranging information from RSS measurements (a) ideal ranging and (b) ranging estimation with uncertainty σ_d . . . 59
4.5 Power versus distance measurements of ED light Cree XLamp CXB1512 . . . 59
4.6 Lateration method in two dimensions based on RSS ranging . . . 60
4.7 Lateration method in two dimensions based on TOA ranging . . . 61
4.8 Hyperbolic lateration method in two dimensions based on TDOA ranging . . . 62
4.9 Angle of arrival based positioning method in two dimensions . . . 63
4.10 Angle of arrival based positioning method in two dimensions with unknown receiver orientation . . . 64
4.11 Convex position estimation . . . 66

5.1 Single chip transceiver nRF905 . . . 69
5.2 Packet error rate versus distance for nRF905 . . . 70
5.3 Transmitter design schematic . . . 71
5.4 Real implementation of VLC transmitter (a) general overview and (b) modulator in detail . . . 71
5.5 Random time slot access schematic . . . 72
5.6 Frequency access schematic . . . 73
5.7 PDA36A2 photodetector . . . 73
5.8 Oscilloscope used as digital to analog converter . . . 73
5.9 Proposed receiver architecture . . . 74

6.1 Different LED arrangements for VLC networks (a) Lattice architecture and (b) Tunnel architecture . . . 76
6.2 Sample graph with blue (dotted), green solid) and red (dashed) lines . . . 77
6.3 Difference height distance measurements (a) raw measurements and (b) filtered measurements . . . 78
6.4 Broadcast VLC Packet . . . 79
6.5 Convex bounding box for the mobile node position . . . 80
6.6 Overlapped cell to bounding box with binary indicator of Equation (6.6) equals to one . . . 81
6.7 Unfeasible point elimination based on connectivity feasibility check . . . 82
6.8 New feasible vertices using overlapped non-connected cells . . . 82
6.9 Set of vertices found by using connectivity and infrastructure information . . . 82
6.10 Convex polygon for feasible positioning area . . . 83
6.11 Detector architectures: (a) single photodetector and (b) imaging receiver . . . 84
6.12 Intersection pattern of feasible localization area based on (a) single PD and (b) imaging receiver . . . 84
6.13 CPP performance using a single PD for (a) Δh_{ji}=2 m and (b) Δh_{ji}=1.5 m . . . 87

6.14 CPP performance using a imaging receiver for (a) Δh_{ji}=2 m and (b) Δh_{ji}=1.5 m 87
6.15 Comparison of best PD architectures for (a) Δh_{ji}=2 m and (b) Δh_{ji}=1.5 m . . . 88
6.16 Two dimensional coverage representation for Δh_{ji}=2 m (a) FOV=60°, (b) FOV=80° and (c) FOV=100° . . . 89
6.17 Method performance using an 80° FOV detector for (a) RSS trilateration and (b) CPP . . . 90
6.18 Impact of mismatch measurements on receiver's heigth using PD(IR_3) architecture for (a)$\Delta h_{ij} = 1.5$ meters and (b)$\Delta h_{ij} = 2$ meters . . . 91
6.19 Impact of tilting and rotation angles using PD(IR_3) architecture for (a) $\Delta h_{ij} = 1.5$ meters and (b)$\Delta h_{ij} = 2$ meters . . . 92
6.20 CPP performance using a single PD in tunnel scenario for (a) Δh_{ji}=2 m and (b) Δh_{ji}=1.5 m . . . 93
6.21 CPP performance using a imaging receiver in tunnel scenario for (a) Δh_{ji}=2 m and (b) Δh_{ji}=1.5 m . . . 93
6.22 Comparison of best PD architectures for (a) Δh_{ji}=2 m and (b) Δh_{ji}=1.5 m . . . 94
6.23 Two dimensional coverage representation in tunnel scenario for Δh_{ji}=2 m (a) FOV=60°, (b) FOV=80° and (c) FOV=100° . . . 95
6.24 Real square room VLC platform for VLP testing . . . 96
6.25 Photodetector receiver in the testing grid for CPP VLP method validation . . . 97
6.26 Two dimensional received power representation in testing platform for Δh_{ji}=2.25 m and FOV=60° (a) ID1 VLC beacon and (b) ID2 VLC beacon . . . 98
6.27 Performance of CPP method using the testing VLP platform . . . 99

7.1 Portable helmet mounted device for VLP in underground mines . . . 102
7.2 Zero energy mobile VLC receiver . . . 103

List of Tables

2.1 Miners tracking systems requirements based on MINERS Act [10906] 20
2.2 Proposed positioning systems for underground mines 31
2.3 Pros and cons of visible light positioning technology in underground mines 32

3.1 Illumination requirements for different working zones of underground mines (Table adapter from [Com]) 36
3.2 Comparison between proposed and state-of-art VLC underground mines channel models 39
3.3 Comparison of different VLC system configurations 41
3.4 Effect of special underground tunnel characteristics in VLC channel model 52

4.1 Comparison of VLP based on receiver characteristics 55
4.2 Topologies and technologies for VLP in underground mines 55
4.3 Summary of range based, range free and fingerprinting positioning methods (Table adapted from [AIA+17]) 67

6.1 Parameters for computational simulation 86
6.2 Frequencies of VLC beacon nodes 95

Chapter 1

Introduction

Sommaire

1.1 Visible light positioning systems for indoor environments **1**
1.2 Motivation **4**
1.3 Contributions **4**
1.4 Publications **6**
1.4.1 Journal ISI articles 6
1.4.2 Conference articles 7

1.1 Visible light positioning systems for indoor environments

The aperture of Global Positioning system (GPS) for civilian usage and the discontinuance of selectivity availability (SA) in May 2000 produced a boost in positioning industry and location based services(LBS). Although contemporary Global Navigation Satellite System (GNSS) outdoor positioning has become precise and ubiquitous, it has not been capable to overcome different issues when dealing with indoor or dense metropolitan environments. Line of sight (LOS) signal can be blocked in metropolitan areas by high buildings and. Moreover, in indoor scenarios, such as, interior of buildings and tunnels, complete signal lost is experienced since GNSS signals are not capable to penetrate concrete, metal or ground [Van08].

Indoor positioning market is expected to obtain revenues for a value of US$ 10 billion by 2020 [Bus15]. Whilst satellite based navigation dominates outdoor scenarios, no overall single technology alternative exist for indoor environments and, many different technologies have been proposed as feasible solutions. Most of the indoor positioning systems (IPS) that can be found in literature are based on radio frequency (RF) technology, magnetic fields, or acoustic signals [LLY+15]. Among them, Wireless Fidelity (Wifi) based IPS have been preferred since this technology is commonly integrated in off-the-shelf devices and it re-uses already available infrastructure (Wifi access points) to provide position information [LDBL07, HNP+15]. The main disadvantage of Wifi based IPS is the large positioning errors can be always found (e.g. $6 \sim 8$ m) in purely Wifi-based positioning even though, reasonable accuracy can be achieved [LYS+14].

In the recent years, visible light communications (VLC) has gained attention of researchers. This, mainly because of the recent advances in the manufacture of lighting emitting diodes (LEDs) [HCWZ15].

The rapid development of VLC networks has encouraged researchers to propose positioning solutions based on this technology. Visible light positioning (VLP) systems or VLC based positioning has several advantages compared to RF based IPS. LEDs can be modulated at high frequencies. Due to this, VLC systems are capable to provide high data rate wireless communication, using already deployed lighting infrastructure [PFHM15]. LED lights are energy efficient, they have a longer life expectancy than other lighting devices and, they are a cost effective solution [HNP+15]. Moreover, joint illumination/VLC is perceived as a green technology [TWL+15, JWLL18]. VLC has a larger unlicensed spectrum compared to RF systems. It has a high spatial reuse (privacy) and does not interfere with RF waves. VLC systems can be used in RF-denied environments, such as, hospitals and air planes [WWY14, PFHM15]. One of the most important characteristics of VLP is the high accuracy that can be achieved in indoor environments compared to RF based systems [DY16].

Visible light positioning systems are often classified in two different groups based on the receiver hardware used for signal detection (as shown in Figure 1.1), i.e, image sensor (IS) based VLP and, photo detector (PD) based VLP [HY16].

Image sensors provide more useful LED position information than PD counterpart. In addition to this, light sources can be directly separated using the spatial multiplexing of the image and no complementary technique is required [DY16]. Most of the off-the-shelf devices have already incorporated cameras. Due to his, IS-based positioning methods are easy to implement and inexpensive [ZHQ+18, KZKP15]. The main disadvantage of IS-VLP systems is that IS-based VLC networks have a very limited data rate. Due to this, IS-based networks are not expected to be massively implemented for future wireless networks (no infrastructure re-use) which are supposed to deliver high data rates [DY16]. In addition to this, VLP demands a high computational effort to process the image stream.

On the other hand, PD-based VLC systems can provide high data rate communication [HY16, HLC+15]. Moreover, PDs are inexpensive and easy to install. In order to separate the signal from multiple sources, the usage of multiplexing techniques is required. Depending on the multiplexing technique used to separate the sources, the required hardware for the system can increase in complexity and affect the performance of positioning method [YNA+17, HNP+15].

Localization methods can be classified in two types. This classification is based on whether they use distance estimation (range based) or other type of information to compute mobile node's position (range free) [Mau12]. Range based methods use a distance estimation to perform positioning. Some range based methods are trilateration, multilateration and angulation. Distance estimation is derived from received signal characteristics, such as, signal strength, time of propagation and received phase/angle. Among them, receiver signal strength (RSS) is the simplest method to estimate ranging information. RSS measurements are relatively easy to obtain and, most of the devices are built with the required hardware to measure the received signal power level in dBm or a received signal strength indicator (RSSI). In order to estimate the distance from RSS measurements, a precise model of signal propagation is required. Due to this, model precision has high impact in the algorithm performance. On the other hand, despite provide a more precise distance estimation than RSS methods, time of propagation and received phase/angle measurements have several drawbacks on its hardware implementation. Time of propagation measurement can be divided in time of arrival (TOA) and time difference of arrival (TDOA) methods. TOA measurements require precise synchronization of transmitters and receivers. This synchronization is very difficult to provide. On the other hand, TDOA and phase/angle measurements require synchronization at the receiver side to estimate the range. In addition to this, in order to perceive the difference in time of arrival, the receiver must be equipped with a high sampling frequency device.

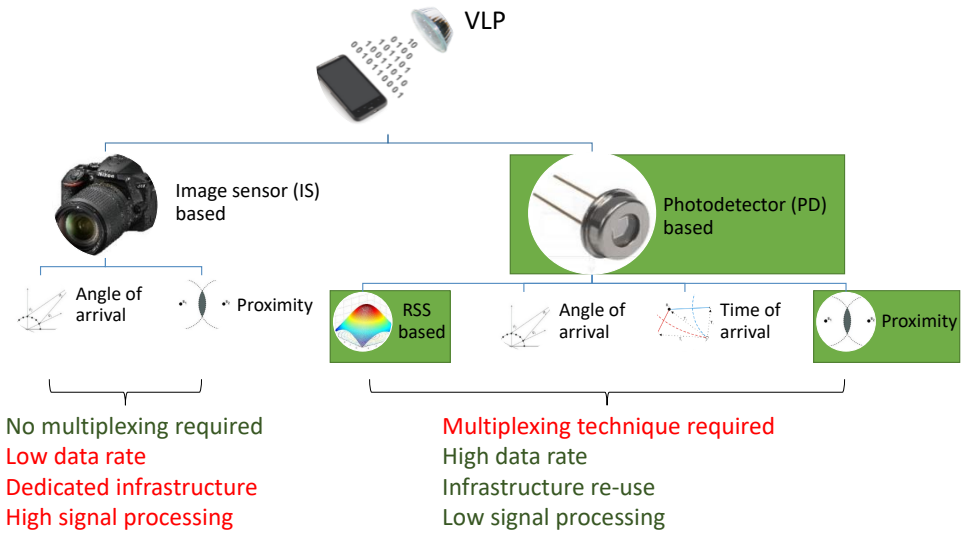

Figure 1.1: Visible light positioning classification based on receiver hardware and signal measurement used for position determination with the main contribution of this thesis highlighted in green

Once range measurements are performed, range based methods estimate the position of mobile node by trilateration/multilateration/angulation algorithms. For doing this, information of multiple anchor nodes (position-aware transmitters) is required.

On the other hand, range free algorithms use the available connectivity information to estimate the position of unknown node. Since different techniques such as equalization and coding can be used to successfully deliver the message from beacon node to the mobile user, signal perturbations do not severely affect position estimation [LYWJ10]. In addition to this, these methods can be inexpensively deployed. In order to retrieve connectivity information no extra hardware is required. As a result, they provide a more robust approach compared to range based algorithms [SGY+16]. Nevertheless, there exist a trade-off between their high robustness, low hardware complexity and their accuracy. Range free algorithms provide coarse-grained localization whilst range based algorithms can provide a fine-grained localization. Traditional range free algorithms, proposed mainly for RF-based wireless sensor networks (WSN), have been implemented straightforward for VLC networks. These algorithms are convex position estimation (CPE) [SGY+16] and centroid algorithm [SKS+16].

In Figure 1.1 the main methods of VLP systems are summarized. Advantages and characteristics of each class of VLP system are delivered. The main contributions of this thesis are highlighted in green.

Typically, low positioning error (or high localization accuracy), is a desirable attribute of IPS designs. Nevertheless, there exist a number of different requirements parameters that must be analysed when designing IPS. Determination of application requirements is a crucial step for any initiative to design indoor positioning systems since here, research and development of solution is underpinned.

1.2 Motivation

Underground mining is expected to lead the mining industry in the near future. Due to the advance of electronic devices and communications technologies, new safety regulations must be accomplished in order to operate underground mines safely and optimally. In 2006, US government update their safety policies and introduce the PUBLIC LAW109-236 [10906]. Because of this, underground tracking is nowadays mandatory for underground mine operations. This new regulation establishes that current, or immediately pre-accident location of all underground personnel must be delivered over ground. Despite the recent advances of tracking and positioning systems for indoor environments, underground mines are a unique scenario which poses different constraints to current technologies. Due to this, it is important to analyse in detail the main characteristic of different localization systems for underground mines (UM) that can be found in literature.

Most of the VLP methods have been evaluated in highly controlled scenarios were a dense and well deployed VLC network exist, i.e., interior of buildings, supermarkets, office and car parking. On the contrary, underground mine is a dynamic and hazardous environment by nature. As ore exploitation continues, mine expands. Therefore, it can be considered as a semi-structured environment [FFCM17] where some assumptions of tunnel geometry can be made. Moreover, due to the characteristics of mining tunnels, low control on communication infrastructure exist and, a strategic deployment of required devices can not always be done. Additionally, underground mines are considered by several researchers as one of the most difficult scenarios. Underground mining operations involve various hazardous conditions, such as, in-mine vehicular/human accidents, fire and explosions, collapses, toxic gases emanation and floods, among others. In addition to this, workers, machinery and in-mine equipment are exposed to extreme conditions, such as, high levels of humidity (up to 90 % or above [YGAM09]), airborne dust and extreme heat. These conditions have not only an impact on workers performing labours inside the tunnel but also on the functioning of electronic devices. The feasibility of using a VLP system under such conditions capable of fulfilling positioning requirements remains an open question. We address this question in our work.

1.3 Contributions

Based on the classification of VLP systems in Figure 1.1 we present the main contribution of this thesis. The focus of this thesis is to provide a VLP system for underground mines capable of fulfilling the special requirements present in this hazardous environment. Our main contribution are summarized below:

(1) Evaluation of current positioning technologies for underground mines environment. We propose, for the first time in literature, an analytical study of current technologies that have been proposed to provide positioning in underground mines. Throughout a rigorous classification and analysis of several technologies, main advantages and disadvantages of each system are delivered.

(2) Evaluation of user's requirements for underground mine positioning systems. We derive the main user's requirements for VLP systems in underground mines based on the particular characteristics of this environment and, using U.S. public law 109-236 of 2006 [10906]. From this analysis, the main performance evaluators to asses VLP results will be obtained.

(3) Implementation of an underground mine VLC channel model simulator. We propose a generic model for VLC channel in underground mines. This channel model takes into account several characteristics of underground mines that are not present in traditional models (higher temperatures, non orthogonality of walls, partial and total signal blockage, etc.). The simulator can be used not only to evaluate VLP systems but also the performance of VLC in underground mines.

(4) Analytical study of VLP in underground mines environment. Using the proposed channel model for underground mines we develop, for the first time in literature, an analytical study of VLP performance in underground mines.

(5) Design of a positioning system topology optimized for VLP in underground mines. We design a positioning system topology in order to fulfil the user's requirement of VLP in underground mines. This design is used in order to develop real hardware implementation of a VLP system. This contribution is detailed in Chapter 4.

(6) Implementation of a low-cost/large-scale VLP system. We implement a low-cost/large-scale VLP system for underground mines. Different VLP systems are evaluated using this hardware implementation. The platform can be used to test not only the proposed methods in this thesis but also further developments.

(7) Design and implementation of a robust range free VLP method. We provide the first range free VLP method designed using spatial reuse characteristics of VLC systems. We implemented and evaluate our method using the low-cost/large-scale hardware proposed in this thesis. Our proposition is compared with traditional others range free methods designed for RF communications. Contributions **(1)** and **(2)**, detailed in Chapter 2, deliver user requirements and positioning characteristics in underground mines.

(8) Evaluation of VLP robustness requirements. We study the robustness of several positioning methods under the scenario of underground mines. We compare the results of our proposed systems with a traditional RF based positioning method. Our evaluation provide essential insights to choose the adequate VLP system in underground mines environment.

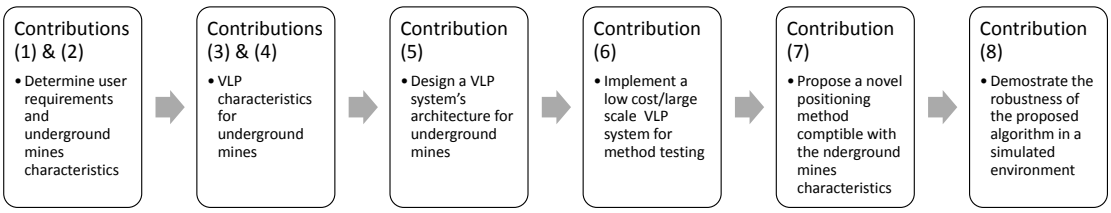

Figure 1.2: Process diagram of contributions in this thesis

In Fig. 1.2 a process diagram showing step-by-step construction of this thesis is presented.

Contribution **(1)** presented in Chapter 2 aims to detect the bottleneck of current positioning technologies when they are applied in underground mines environment. Then, contribution

(2), delivered in the same chapter, is used to determine user's specifications for this particular scenario. Proper design of a VLP system must be done after a rigorous evaluation of requirements.

Further on, once underground positioning requirements and characteristics are established, an evaluation of VLC performance in underground environment is delivered. Contributions **(3)** and **(4)** are used to determine the limitations of several VLP systems in underground mines. These results will be compared with the requirements derived from contributions **(1)** and **(2)** in order to determine the best architecture to can guarantee positioning service in the proposed scenario. Contributions **(3)** and **(4)** are presented in Chapter 3 and 4 respectively.

Once the main limitations of VLP in underground mines are determined and user's requirements are established, a VLP positioning system is designed and implemented. Contribution **(5)** uses limitations, capabilities and users requirements detailed in Chapters 2, 3 and 4 to design a low-cost/large-scale hardware architecture for underground mines, which is detailed in Chapter 5. Contribution **(6)**, delivered in the same chapter, exploits this design to implement a real world platform that will be used to evaluate the performance of visible light positioning methods.

Contribution **(7)** present a novel robust range free positioning method. Contrary to most of the methods existing in literature, our proposal has not been derived straightforward from RF based methods. The proposed algorithm uses special characteristics of VLC to enhance the position estimation performance. Insights of our method are delivered in Chapter 6.

Finally, contribution **(8)** evaluates the performance of our proposal using the large scale/low cost method testing platform of contribution **(6)**.

1.4 Publications

1.4.1 Journal ISI articles

1. Fabian Seguel, Ismael Soto, Cesar Azurdia, Pablo Palacios, Nicolas Krommenacker, Patrick Charpentier, Underground mine positioning: A survey, *To be submitted to:* IEEE communications surveys and tutorials

2. Soto I., Nilson Rodrigues R., Massuyama G., Seguel F.,Palacios Játiva P., Azurdia-Meza C.A., Krommenacker N, A Hybrid VLC-RF Portable Phasor Measurement Unit for Deep Tunnels. Sensors 2020, 20, 790, DOI: https://doi.org/10.3390/s20020367

3. Palacios Játiva P., Román Cañizares M., Azurdia-Meza C.A., Zabala-Blanco D., Dehghan Firoozabadi A., Seguel F., Montejo-Sánchez S., Soto I., Interference Mitigation for Visible Light Communications in Underground Mines Using Angle Diversity Receivers. Sensors 2020, 20, 367, DOI: https://doi.org/10.3390/s20020367

4. Fabian Seguel, Nicolas Krommenacker, Patrick Charpentier, Ismael Soto, A novel range free visible light positioning algorithm for imaging receivers, Optik, Volume 195, 2019, 163028, ISSN 0030-4026, DOI: https://doi.org/10.1016/j.ijleo.2019.163028

5. Seguel, Fabian; Krommenacker, Nicolas; Charpentier, Patrick; Soto, Ismael: 'Visible light positioning based on architecture information: method and performance', IET Communications, 2019, 13, (7), p. 848-856, DOI: 10.1049/iet-com.2018.5623

6. Dehghan Firoozabadi, Ali and Azurdia-Meza, Cesar and Soto, Ismael and Seguel, Fabian and Krommenacker, Nicolas and Iturralde, Daniel and Charpentier, Patrick and Zabala-Blanco, David, A Novel Frequency Domain Visible Light Communication (VLC) Three-

Dimensional Trilateration System for Localization in Underground Mining, Applied Sciences, Volume 9 (7), 2019, ISSN 2076-3417, DOI: https://doi.org/10.3390/app9071488

7. F. Seguel, A. Dehghan Firoozabadi, P. Adasme, I. Soto, N. Krommenacker, Cesar Azurdia-Meza, A novel strategy for LED re-utilization for visible light communications, Optik, Volume 151, 2017, Pages 88-97, ISSN 0030-4026, DOI: https://doi.org/10.1016/j.ijleo.2017.10.121.

8. D. Iturralde, F. Seguel, I. Soto, C. Azurdia and S. Khan, "A new VLC system for localization in underground mining tunnels," in IEEE Latin America Transactions, vol. 15, no. 4, pp. 581-587, April 2017. DOI: 10.1109/TLA.2017.7896341

1.4.2 Conference articles

1. Convex polygon positioning for homogeneous optical wireless networks F Seguel, N Krommenacker, P Charpentier, V Bombardier, I Soto 2018 International Conference on Indoor Positioning and Indoor Navigation (IPIN) DOI: 10.1109/IPIN.2018.8533863

2. A range free localization method for overlapped optical attocells using neighbor's information F Seguel, I Soto, N Krommenacker, P Charpentier, P Adasme 2018 11th International Symposium on Communication Systems, Networks and Signal processing (CSNDSP) DOI: 10.1109/CSNDSP.2018.8471895

3. Seguel, Fabian; Soto, Ismael; Adasme, Pablo; Krommenacker, Nicolas; Charpentier, Patrick; Potential and challenges of VLC based IPS in underground mines, 2017 First South American Colloquium on Visible Light Communications (SACVLC) DOI: 10.1109/SACVLC.2017.8267610

4. Multiple speaker localization and identification through multiple camera and visible light communication L Florent, F Seguel, K Nicolas, C Patrick, P Bertrand 2018 Global LIFI Congress (GLC), 1-4 DOI: 10.23919/GLC.2018.8319102

5. Spatial time division multiple access for visible light communication networks P Adasme, F Seguel, I Soto, E San Juan 2017 First South American Colloquium on Visible Light Communications (SACVLC) DOI: 10.1109/SACVLC.2017.8267605

6. New Formulations for an Optimal Connectivity Approach for Mobile Ad-hoc Networks P Adasme, I Soto, F Seguel International Conference on Mobile Web and Information Systems, 250-262 Proposed energy based method for light receiver localization in underground mining D Aguirre, AD Firoozabadi, F Seguel, I Soto 2016 IEEE International Conference on Automatica (ICA-ACCA) DOI: 10.1109/ICA-ACCA.2016.7778460

7. Comparison between FastICA and InfoMax for the blind separation of audio signals E San Juan, I Soto, P Adasme, L Cañete, F Seguel, W Gutierrez, 2018 11th International Symposium on Communication Systems, Networks and Signal processing (CSNDSP) DOI: 10.1109/CSNDSP.2018.8471822

8. Probabilistic Constrained Approach for Clustering in Multi-Cell Wireless Networks P Adasme, I Soto, E San Juan, F Seguel, N Krommenacker 2018 11th International Symposium on Communication Systems, Networks and Signal processing (CSNDSP) DOI: 10.1109/CSNDSP.2018.8471847

9. Optical Wireless Communications for Ubiquitous Computing Fabián Seguel, Ismael Soto, Pablo Adasme, Belarmino Núñez. 17th International Conference on Informatics and Semiotics in Organisations (ICISO) DOI: 10.1007/978-3-319-42102-5

Chapter 2

Current positioning technologies in underground mines

Sommaire

2.1 Introduction **9**
2.2 Importance and challenges of positioning in underground mines . . **11**
2.3 Requirements of positioning systems **12**
2.3.1 Accuracy 12
2.3.2 Output data 13
2.3.3 Precision 14
2.3.4 Coverage 15
2.3.5 Cost 15
2.3.6 Required infrastructure 15
2.3.7 Robustness 16
2.3.8 Scalability 16
2.3.9 Update rate 17
2.3.10 Number of users 17
2.3.11 Market maturity 17
2.3.12 Intrusiveness 17
2.3.13 Approval 18
2.4 Classification of positioning systems for underground mines **18**
2.4.1 Technological principle 19
2.4.2 System topology 24
2.4.3 Deployment 25
2.5 Systems proposed in literature **26**
2.6 Conclusions **32**

2.1 Introduction

The rapid advance of wireless communications technologies as well as personal devices has allowed the deployment of different positioning systems. Positioning systems were originally created by

the need of mobile users to orient in unknown environments [Wer14]. Nowadays, the most used positioning system is the Global Positioning Systems (GPS). GPS is capable to provide a large coverage and low cost positioning for outdoor environment. This technology has been used to enable different services in areas such as transportation, gaming, health and disaster management, among others [RGKR07]. In particular, open pit (also named open cast) mining operations have been using global navigation satellite systems (GNSS) based location based services (LBS) for many applications in the last 20 years. Some of these GNSS-based LBS are: drill positioning for precisely excavation of blast holes, fleet management for process optimization, collision avoidance and, transit control for safety management, among others [ER02]. Positioning systems used in open cast mines have reached a high level of trustworthiness in the industry. Systems such as, Computer Aided Earthmoving System (CAES) and Aquila Drill Management provided by Caterpillar-Minestar, Wenco and Modular fleet management systems are nowadays widely used in mining industry. Despite the large usage of GNSS-based LBS in open cast mining, this type of system suffers from different issues when facing more complex environments, such as, deep mining pits or confined areas. Satellite's signal is partially blocked in deep mining pits due to the presence of relatively high obstacles. Moreover, complete signal lost is experienced in underground miens and confined environments since the signal is not capable to penetrate concrete, metal or ground as shown in Fig. 2.1 [Van08].

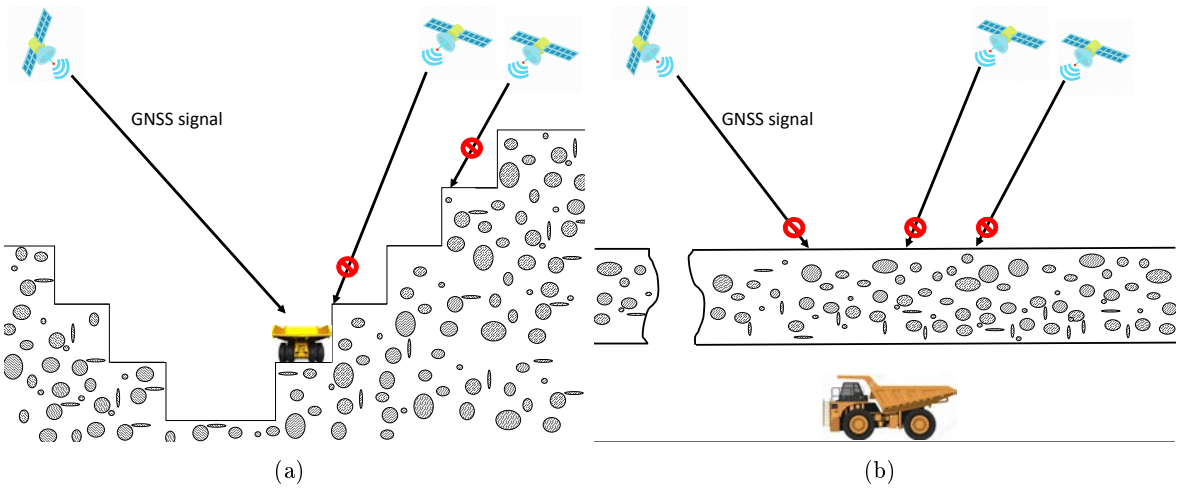

Figure 2.1: Blockage of GNSS signal in (a) deep open cast mine and (b) underground mine

As ore exploitation continues, shallow deposits are becoming exhausted and new veins containing high grade mineral are encountered in deeper layers of earth. Underground mining is, therefore, becoming more attractive due to their merits in terms of safety, production rates, decreasing costs and environmental friendly production [RNSA14]. Commonly, the deposits exploited by open pit mining are shallow and they have a relatively uniform geology. On the contrary, underground operation is preferred for deeper deposits which are not necessarily uniformly distributed. Due to this, underground mines are typically extensive labyrinths that employ a huge number of employees working over an area on many square kilometres [MP78].

In the recent years, due to the current advance of wireless technologies, new safety standards have been appointed in order to operate underground mines safely.In January of 2006, an explosion occurred at the Sago mine in Buckhannon, West Virginia. The rescue team had no way to communicate with the trapped miners, and did not know where they were located

(Twelve miners died in this disaster). Following these disasters, the U.S. government changed their safety policies for underground mines. In June 15, 2006 the congress introduced the PUBLIC LAW 109–236(M) Mine Improvement and New Emergency Response (MINER) [10906] to amend the mine safety and health act of 1977. The main goal of this new standard is to provide wireless communications and, position information of personnel inside the mine following an underground accident. The implementation of such systems has encountered various challenges due to the particular conditions of underground mines.

In the literature, only few surveys on localization systems for underground mines can be found. In [TNH+15] the authors briefly discuss the enabling technologies to provide positioning in underground mines. In this article the performance of the methods is not delivered. In addition to this, the main requirements of positioning systems for underground mines are not analysed. In [BMC10] the capability of different wireless communications systems to provide positioning in underground mines are compared. In this book a Zigbee-enabled active RFID tracking and monitoring system for miners and equipment is presented. The systems provided the position of mobile devices inside the tunnel by means of a proximity-method. In addition to this, the mobile node can alert the central station via text message in case of emergency or other requirements. Nevertheless, no exhaustive literature review can be encountered in this work and it is mainly focused on the proposed system.

In [TNH+15] different positioning technologies for underground tunnels are presented. Although in this work the authors do not deal with the particular characteristics of underground mines, a brief state-of-art analysis is done. Details of the methods and the used taxonomy for comparison are not presented. In addition to this, no performance indicators and, systems requirements are discussed. In this Chapter, an intensive survey on different positioning systems for underground mines is delivered. Several technologies proposed in literature are analysed in terms of their particular performance in a highly demanding and hazardous environment such as underground mines. Moreover, this work proposes a brief tutorial in localization methods focusing, mainly, in their characteristics and requirements.

2.2 Importance and challenges of positioning in underground mines

Underground mines can be classified in two types based on the manner it is excavated. The first type, room-and-pillar mining, is a cyclical and step-by-step mining sequence in which, pillars of mineral are left while excavating in order to support the roof from possible collapse as shown in Fig. 2.2 (a). On the other hand, longwall mining consist on the excavation of a non-interrupted and continuous tunnel as shown in Fig. 2.2 (b).

The type of method used for mine excavation has an impact on the localization technology used to determine the position of a mobile node. For instance, when using wireless technologies based on radio frequency signals to provide positioning, room-and-pillar mines poses more challenges in terms of coverage than longwall mines. Underground mine environment is dynamic by nature. As ore exploitation continues, mine expands. Therefore, it can be considered as a semi-structured environment [FFCM17] where some assumptions on the geometry of the tunnel can be made. Moreover, due to the characteristics of the mining tunnels, low control on the localization infrastructure exist and strategic deployment of required devices for positioning cannot always be done. From a positioning system perspective, semi-structured environments pose huge challenges in terms of system scalability (to expand the coverage of localization system) and precision. In addition to this, the evolution of the tunnel must be followed closely in order to update maps of the mine site. Additionally, underground mines are considered by several re-

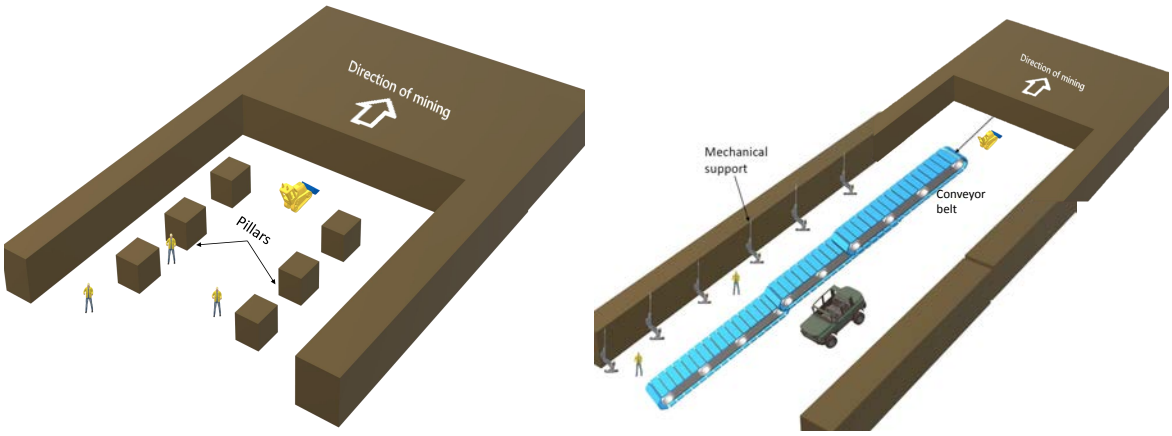

(a) (b)

Figure 2.2: Different types of mines based on their excavation (a) room-and-pillar and (b) long-wall mining

searchers as one of the most difficult scenarios. Underground mining operations involve various hazardous conditions, such as, in-mine vehicular/human accidents, fire and explosions, collapses, toxic gases emanation and floods, among others. In addition to this, workers, machinery and in-mine equipment are exposed to extreme conditions, such as, high levels of humidity (up to 90 % or above [YGAM09]), airborne dust and extreme heat. These conditions have not only an impact on workers performing labours inside the tunnel but also on the functioning of electronic devices. Due to the above described conditions of underground operations, accidents are more dangerous than those in other activities. Mine operation, as any other industrial labour, tries to achieve maximum productivity by working safely. As a result, positioning systems must be designed to fulfil their special requirements and, overcome a huge number of challenges in terms of design and implementation. In [YGAM09] different considerations for underground communication devices, such as, safety, immunity and protection, size, design and reliability are presented. The analysis of these requirements is done by taking into account the extreme conditions in which the devices must operate when they are used in underground environments. Positioning technology for underground mines must be designed taking into account the same special requirements of communications devices since they will be exposed to the same conditions.

2.3 Requirements of positioning systems

In this particular section, different positioning systems requirements are detailed and analysed specifically for underground mines.

2.3.1 Accuracy

Accuracy of a localization system can be defined as the deviation between position estimation and true value. The concept "measurement accuracy" cannot quantified numerically. A position estimation is said to be "more" accurate when it offers a smaller estimation error. In order to classify methods by its accuracy, statistical information of estimation error is used. Accuracy of a system is obtained by using the cumulative distribution function (CDF) of positioning errors. In Figure 2.3 the PDF of two different position estimation are shown.

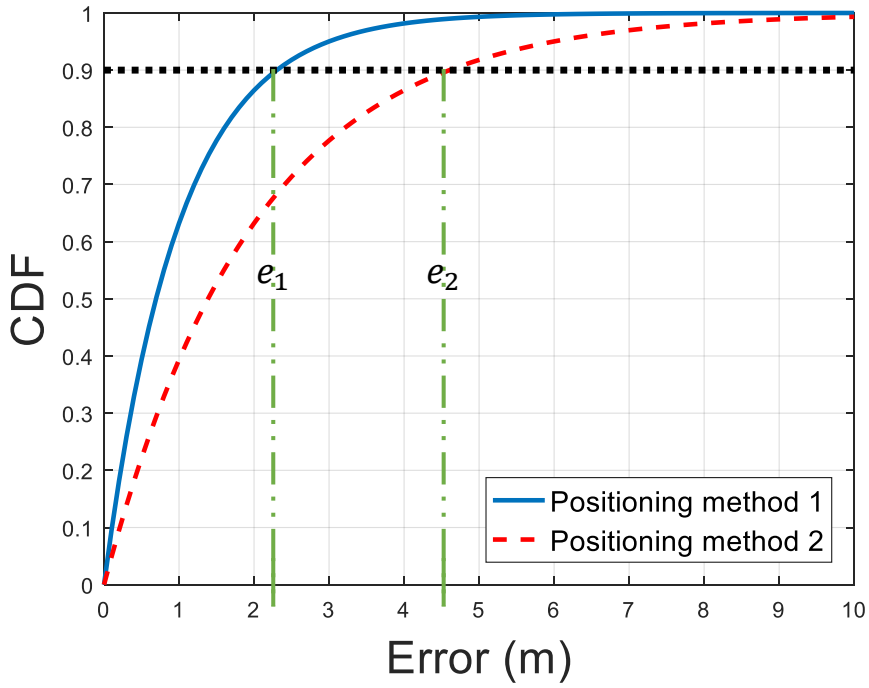

Figure 2.3: Estimated positioning error from CDF with a 90% of confidence level

Herein, positioning method 1 is said to be more accurate than method 2, since, for the same confidence level (90% of probability in CDF), it achieves lower error in position estimation ($e_2 < e_1$). Typically, positioning error is measured by taking the euclidean distance between real and estimated position as follows

$$e = \|\hat{\mathbf{x}} - \mathbf{x}\| \tag{2.1}$$

where $\hat{\mathbf{x}}$ is the estimated position and $\mathbf{x}$ is the real position.

Some positioning systems provide only "room level" position information. This means that, the mobile user is localized somewhere inside a room without 2-D or 3-D information. When the indoor positioning system provides this type of position information, its error (or accuracy) can be measured using ratio of correct room level estimations to the total number of targets. This, will deliver a percentage of correct estimates as follows

$$Accuracy = \frac{N_{correct}}{N_{attempts}} 100\% \tag{2.2}$$

where $N_{correct}$ and $N_{attempts}$ are the number of correct estimates and the total attempts of position estimation respectively.

2.3.2 Output data

Depending on specific requirements of the positioning system, different types of data can be used to represent the position of the mobile node within an environment. The most used data position representation types are 2-D and 3-D coordinates. These coordinates can be delivered using a relative or absolute positioning. In the first, coordinates are expressed as a function of

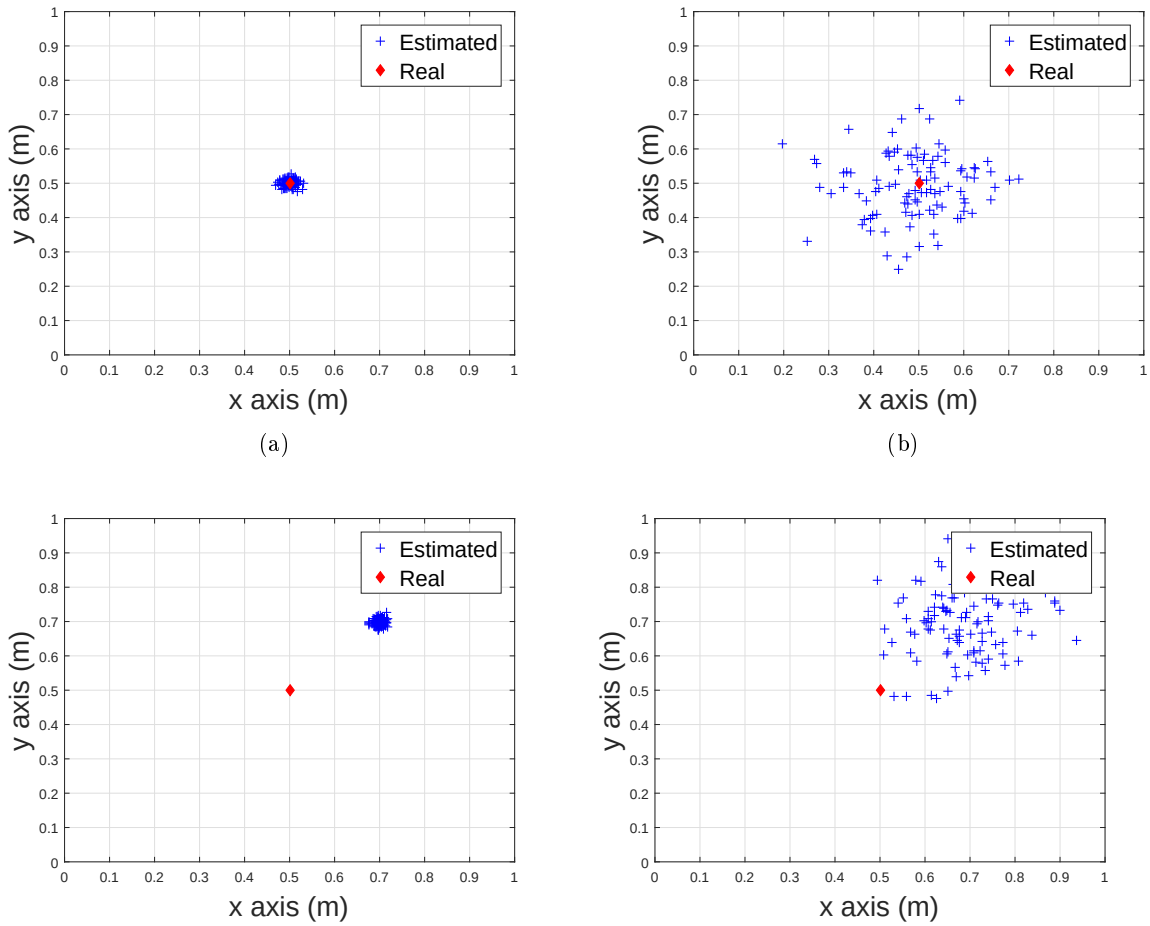

(a) (b) (c) (d)

Figure 2.4: Different localization estimation (a) accurate and precise (b) accurate but not precise (c) not accurate but precise and (d) neither accurate nor precise

an arbitrary point within the space. The second, presents the position coordinates based on an absolute reference system. When "room level" positioning is used, output data is frequently the address in which mobile node is connected or, purely and simply the name or number of the corresponding room in which mobile node is located.

Some other information can be added. For example, velocity and orientation are the data output required for IMU based positioning systems. Some other less common data output for positioning systems are uncertainty and variance.

2.3.3 Precision

Precision measures the deviation of position estimates for the same location. Precision and accuracy are often assumed as the same concept in real life situations. However, there are fundamental differences between the two concepts. In Figure 2.4 the concept of precision is graphically shown and differentiated from accuracy.

As it can be seen, four different position estimation are displayed in this figure. In Figure 2.4(a) the estimation is precise and accurate. In Figure 2.4(b) the estimation is precise since

but not accurate since the exist a high dispersion in position estimations. On the other hand, Figure 2.4(c) shown precise but not accurate estimations since the dispersion is low but the error between the real position and the estimated position is high. Finally, Figure 2.4(d) shows position estimation that is neither accurate or precise since the error and dispersion of estimates are high.

2.3.4 Coverage

The coverage of a positioning system can be defined as the spatial extension in which the performance of the system must be guaranteed [Mau12]. Three categories of coverage are available:

- Local coverage: Local coverage is refereed to a small and well-defined area which could be a room or a building. Local coverage is not extendable (or scalable). Its coverage is defined in m, m^2 or m^3.
- Scalable coverage: This type of systems have the ability of extend the area of coverage by adding hardware infrastructure. In addition to this, the system must not compromise its accuracy when extending its coverage.
- Global coverage: Is a system that can perform worldwide. Only GNSS system and celestial navigation can be considered in this category.

2.3.5 Cost

The cost of a positioning system can be divided in different sub-categories where not only monetary price is considered.

- Time cost: considers the time required to install and administrate the positioning system.
- Capital cost: The capital cost considers the infrastructure cost (prices per mobile and static devices) and salaries of support personnel.
- Maintenance cost: Is the cost for maintain the system functioning.
- Space cost: Takes into account the amount of required infrastructure and hardware's size.

2.3.6 Required infrastructure

The required infrastructure refers to the deployed hardware needed to perform positioning. The required infrastructure may vary depending on the localization solution. As an example, no infrastructure is required for pedestrian dead reckoning. On the other hand, dedicated infrastructure must be deployed for RFID and some Bluetooth based solutions. In these applications hardware is deployed in order to provide exclusively location services. Finally, Wifi and visible light communications (VLC) based positioning solutions are considered as pre-deployed infrastructure since they use the already deployed network to provide communication and positioning. In section 2.4.3 a more detailed insight of required infrastructure is delivered.

2.3.7 Robustness

The robustness of a positioning system refers to its resistance against perturbations. This perturbation can be of various types. For example resistance to physical damage, jamming, dust and heat can be considered for robustness analysis. This definition will be important through the thesis. In particular, for underground mines several perturbations can be pointed out as the most significant. These perturbations are listed and highlighted in Figure 2.5.

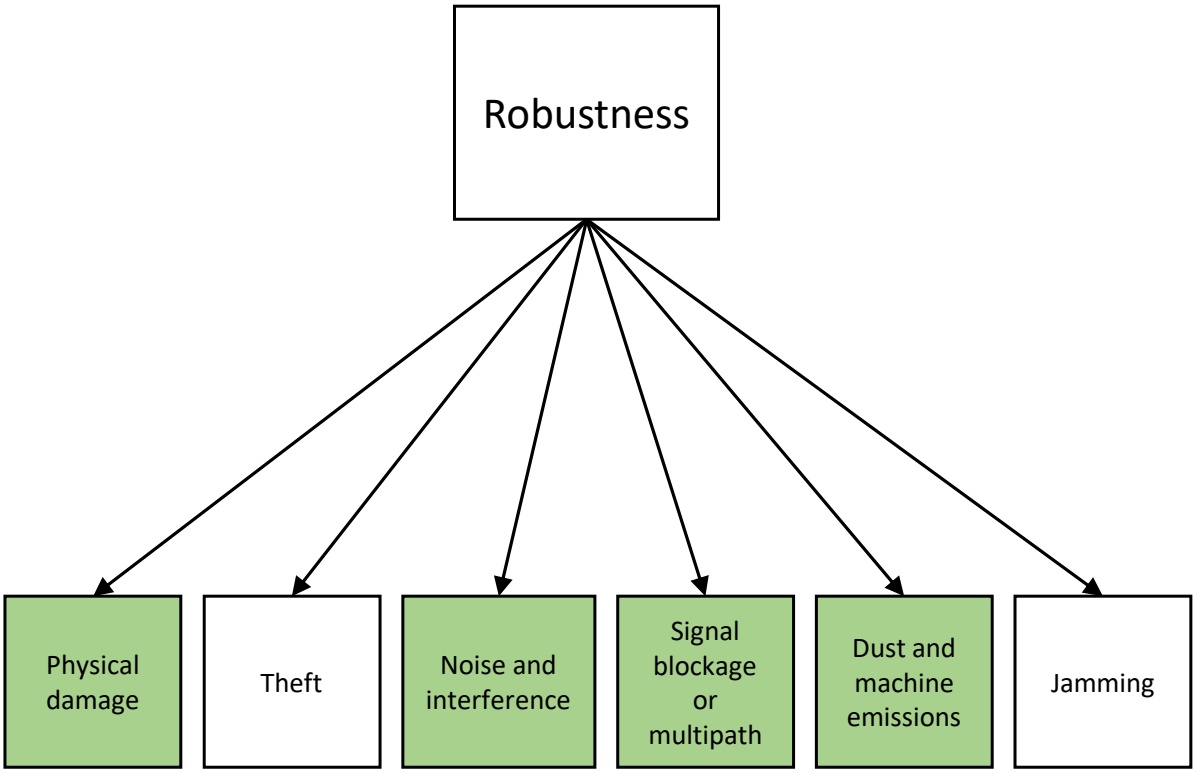

Figure 2.5: Proposed taxonomy for the analysis of positioning systems

In this thesis we study the robustness of different VLP methods to **Physical damage**, **Noise**,**interference**, **Signal blockage**, **dust** and **multipath**.

2.3.8 Scalability

The scalability refers to the ability of the positioning system to increase its coverage area. The positioning system is not scalable if it is not capable to provide position estimation in a larger area than the originally designed. On the other hand, scalable systems can increase its coverage area. For doing this, increment of required infrastructure may be needed. Moreover accuracy lost could be experienced as size effect of increasing the coverage.

2.3.9 Update rate

The update rate is the maximum time in which the position of mobile node must be refreshed. Traditionally, real time localization services for pedestrian usage have an update rate of 1 Hz (position estimation each second). This parameter strongly depends on the mobile node's speed. For example, a vehicle driving at 16 km per hour travels 16.7 meters in a second. Due to this, when faster mobile node's must be localized, higher frequency update rate is required in order to ensure positioning with higher accuracy. In particular, for underground mines the update rate is set by safety regulations as shown in Table 2.1.

2.3.10 Number of users

The number of user is often based on the type of user the systems can support. In underground mines, position information of all workers inside the tunnel must be available for the overground monitoring station. Regular workers, visitors and people inside cars must be identified and localized.

2.3.11 Market maturity

The market maturity states the current development of the proposed technology. Different maturity levels can be identified to classify the positioning system based on the work don by Mautz [Mau12]. In particular there are three main market maturity levels

- Concept: Concept is the early stage on the development of an indoor positioning system. In this stage simulations, as well as, evaluation of different system's aspects are carried out. Requirements analysis is expected to be done in this stage.
- Prototype: A second step in the development od an positioning system is the implementation of a prototype. In this stage of the development a real platform in which the system is tested must be provided. Performance of the prototype should be tested using lab conditions, a simulated environment or real conditions. The latter, provides the most useful information about the positioning system and is often identified as a necessary step to move on and advance to the next stage.
- Product: Is the final stage in a positioning system develpment. In this stage, the proposed system is available in the market.

In general, mining industry is opposed to the changes. Due to this, only product level technologies are preferred when implementing positioning systems for underground mines.

2.3.12 Intrusiveness

Intrusiveness of a positioning system is refereed to the act of interrupting and disturbing. The positioning system is generally composed by one or several devices. These devices are installed in mobile nodes or as deployed infrastructure. Due to the particular characteristics of underground mines, the fixed infrastructure deployed inside the tunnel must be as low as possible. It means that this infrastructure must be imperceptible.

On the other hand, intrusiveness of mobile devices must comply some other requirements. In Mardonova et.al. [MC18] different wearable devices are analysed for its usage in underground mines. Is important to notice that the mobile device used for positioning must be imperceptible for performing labours safely.

2.3.13 Approval

Some regulations stablish the need of approval from governmental or private agencies for the implementation of positioning systems in some environments. As an example, the MINERS-Act of 2006 [10906] establishes the need of approval from Mine Safety and Health Administration (MISHA) in order to be capable of functioning in an underground mine.

2.4 Classification of positioning systems for underground mines

Positioning systems are used to determined the position of a person and/or device relative to a kwown position or within a coordinate system [ZB11]. Basically, any Positioning system has two main components, i.e., "known" nodes and "unknown" nodes. Known nodes are aware of their position. On the other hand, position of unknown nodes is to be determined by the positioning system. Known nodes are also named as anchor nodes, reference nodes or beacon nodes in the literature whilst unknown nodes are often named as dumb nodes, target node or to-be-located nodes [LYWJ10].

In this section, some basic working principles and requirements of UM positioning systems will be deliver. First, different requirements as well the most important performance indicators will be explained in detail. Hereinafter, positioning systems that can be found in literature are detailed for the reader. In order to classify them, we proposed a taxonomy shown in Fig. 2.6.

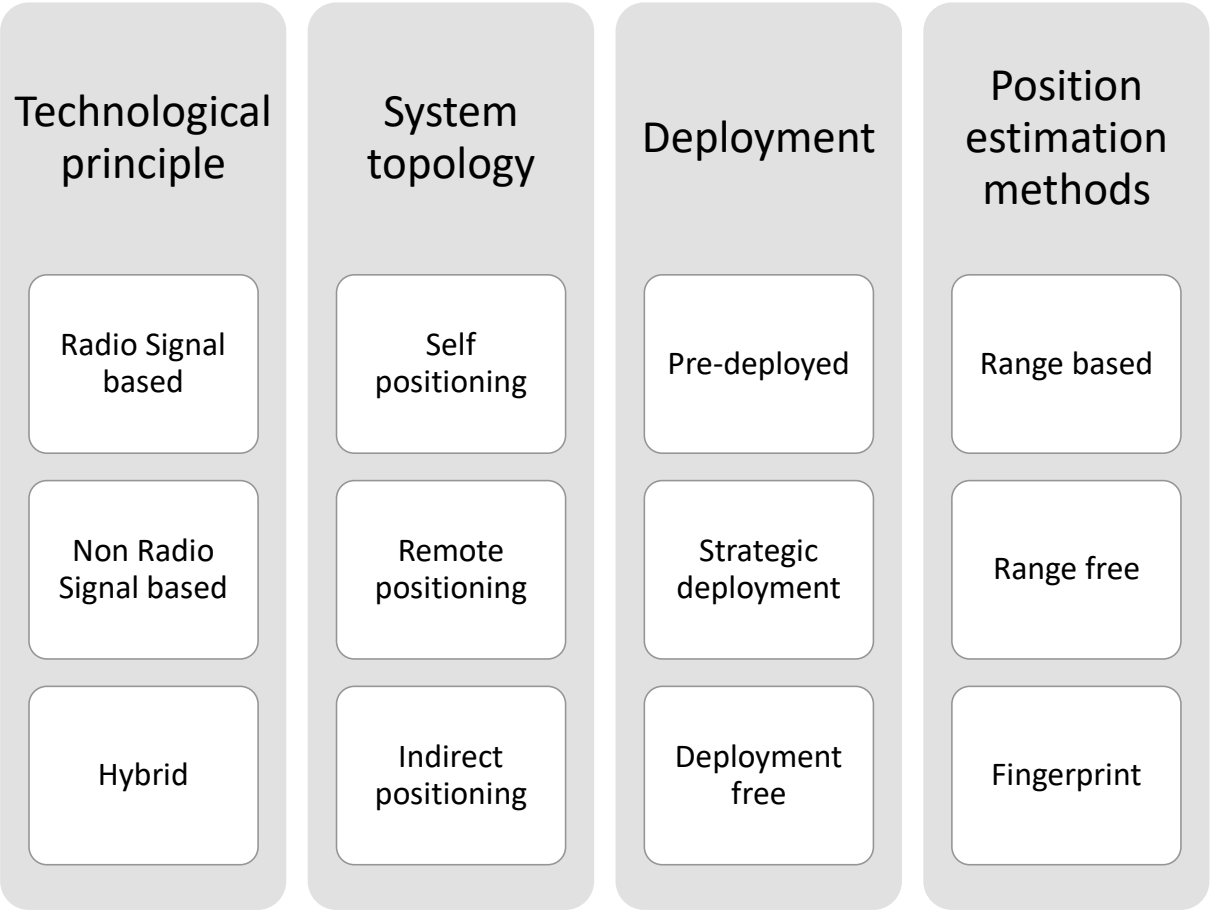

Figure 2.6: Proposed taxonomy for the analysis of positioning systems

The proposed taxonomy classifies positioning systems by using four different characteristics. Each element of the proposed taxonomy is explained in detail below.

2.4.1 Technological principle

For classifying different types of localization systems based on their technological principle, three main categories are proposed. The first category covers the entire range of systems using radio frequency signals to determine the position of mobile nodes. On the other hand, non-radio signal based systems cover the spectrum of system that does not require a wireless-radio based network to determine the position of the mobile node. A third technological approach are hybrids systems who use both technologies to provide localization. The three types of technologies that are described in detail bellow based on research conducted by several authors. In addition to this, to summarize the analysis a table of different localization systems proposed in literature is presented at the end of this section.

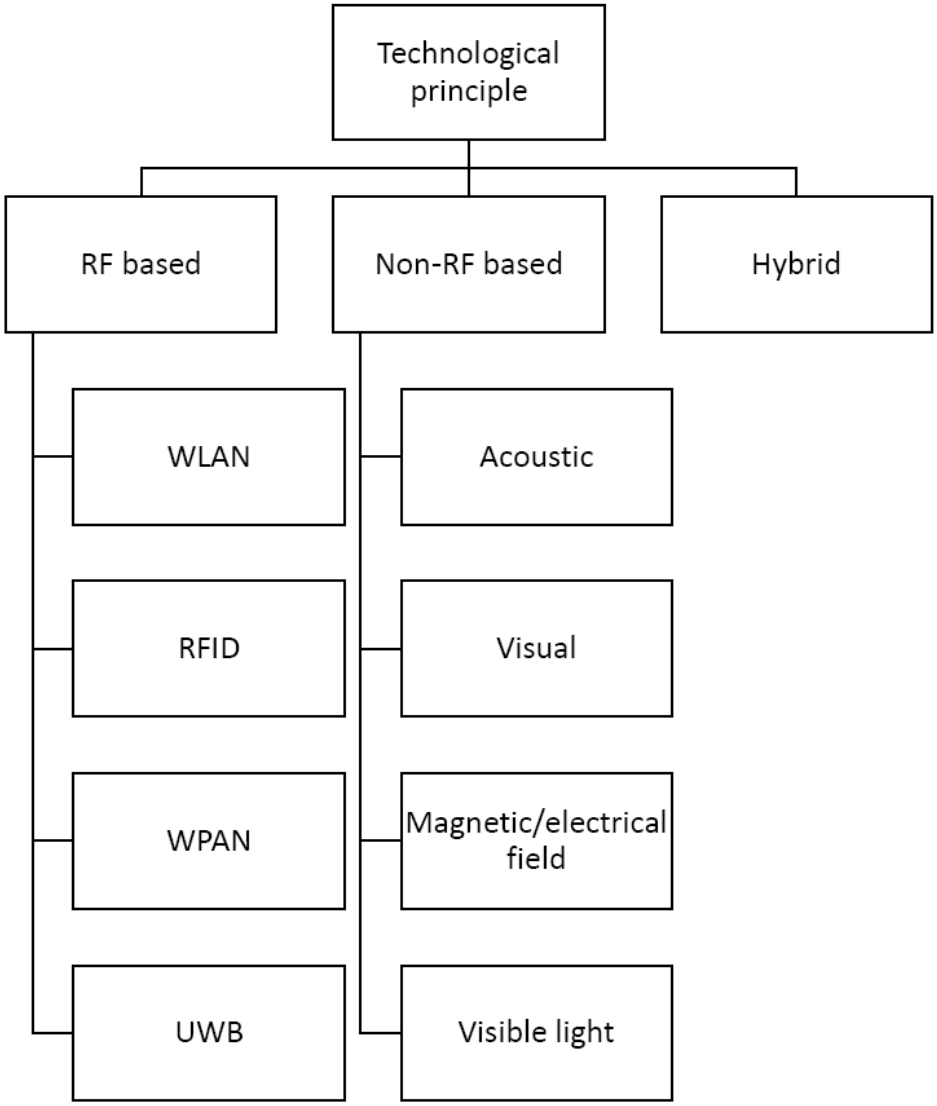

Figure 2.7: Classification based on technological principle

Parameter	Accuracy	Output data	Precision	Coverage	Cost	Required infrastructure	Robustness
Requirement	60.96 m relative to a fixed point	2-D coordinates, absolute positioning	Not defined	Scalable coverage	Low	Ambient without conditions to allow high infrastructure deployment	High robustness to tunnel conditions
Parameter	Scalability	Update rate	Number of users	Market maturity	Intrusiveness	Approval	Privacy
Requirement	Yes with possible accuracy lost	Up to 60 seconds	maximum number of persons, including visitors expected to be in the coverage area	Product	Non intrusive	Requires approval of Mine Safety and Health Administration (MSHA), U.S.	Position of workers must be available in a central station. Each miner should be uniquely identified

Table 2.1: Miners tracking systems requirements based on MINERS Act [10906]

Radio signal based systems

Radio signal based systems are those that use the radio-frequency spectrum of the electromagnetic waves to determine the position of the mobile node. Radio signal based systems has the advantage that they can be used to provide two main pillars of location based services, i.e., help in the position estimation process and the capability to transmit wireless information allowing mobility of the unknown node. Underground mines are a very challenging environment for radio frequency based signals. Behaviour of RF signals is different in mine tunnels than in any other regular environment. This, due to the physical shape of the tunnel can cause signal scattering, multipath propagation and blockage (pillars, U turns, etc.). Moreover, tunnel walls are composed by different materials depending on the mine site. Due to this, electromagnetic characteristics such as dielectricity and conductivity of each tunnel are unique and they have an effect on the radio frequency signal propagation. The proposed radio signal based system must cope with these challenges.

- Wireless Local Area Networks (WLAN): WLAN (IEEE 802.11) is a well stablish wireless communications technology in various industry sectors. WLAN standards use the Industrial, Scientific and Medical (ISM) bands in 5 and 2.4 GHz to provide full-duplex wireless communications. This type of networks are thought to deliver data transmission within a rate between 1 to 108 Mbps and a coverage range between 50 and 150 meters depending on the characteristic of the environment and line-of-sight (LOS) is not required for data transmission. Experimental demonstration of WLAN , in particular IEEE 802.11b standard has been conducted in [YGAM09]. The mine site where WLAN was tested correspond to a longwall tunnel. Ranges up to 150 meters were achieved, whereas 802.11b devices are expected to provide a maximum range of 50 meters. In case WLAN is provided as already-deployed communications infrastructure, localization systems can be rapidly delivered without requiring any further deployment. WLAN standards provide the capability to implement diverse position estimation methods. Particularly, proximity and lateration methods are preferred since off-the-shelf devices are equipped with the required hardware.

- Radio Frequency Identification (RFID): This type of systems are capable to store and retrieve data using radio waves. RFID systems comprise two main components i.e., RFID reader and RFID tags. RFID reader is capable to obtain the information stored in RFID tags using a pre-defined protocol. RFID tags can be classified in three groups, these are: passive tags,semi passive tags and active tags. Active tags transmit their information to reader previous to a query or independently. Since active tags are equipped with batteries they are capable to working with low-power received signals. In addition to this, they can be associated easily with different type of sensors. Nevertheless, due to the usage of batteries, tey are more expensive and have a more limited lifetime compared to passive and semi passive tags. Semi passive tags are known also as battery-assisted tags use their battery prior to a reader query in order to increase its communication range. They have a battery life of about five years and once it is drown they acts as passive tags. Their coverage range is between active and passive tags ($<$10 meters). Passive RFID tags are capable to operate without a battery. The RF signal coming from the reader power ups an integrated circuit that generates the response to the reader's query. Their main drawback is its short communication range (3-5 meters). Usually, RFID reader and tags are not pre-installed as communication infrastructure. Due to this, this type of system needs to be deployed for a specific purpose. Moreover, due to its short coverage range, strategic deployment of readers is required in order to provide full coverage.

- Wireless personal area networks (WPAN): WPAN, standardized in IEEE 802.15 have been extensively investigated in underground environments. These networks offer bi-directional wireless communications. Compared to WLAN their coverage range is much shorter and they do not posses pre-deployed infrastructure. Standards such as IEEE 802.15.4a and ECMA-368 (which will be discussed next) include positioning features. Nevertheless, they have not been used extensively in positioning systems intended for underground mines. In particular, two standards are preferred for using in underground scenarios, i.e., Bluetooth (IEEE 802.15.1) and ZigBee (IEEE 802.15.4). Each WPAN standard differs significantly in their physical layer. Due to this, each standard will be detailed separately below.

  Bluetooth: This type of systems have a maximum coverage range of up to 10 m depending on the propagation conditions of the environment when a class 3 transmitter with a power output of 1 mW are used. They use the ISM band in 2.4 GHz to provide wireless communication with a rate between 1 and 3 Mbps. In general, off-the-shelf bluetooth devices are not equipped with the necessary hardware to provide lateration-based positioning. Due to this, proximity methods are preferred in this type of systems since no extra hardware is required.
  |*ZigBee*: ZigBee technology is a low data rate WPAN standard with data rate up to 250 Kbps operating in the band of 2.4 GHz. This standard is also specified for 868–870-MHz and 902–928-MHz bands at 20 and 40 kbps, respectively. ZigBee networks are principally intended for low cost and low power monitoring and control applications. The coverage range of ZigBee nodes in indoor environments is 20 to 30 meters. ZigBee technology is capable to provide lateration and cell of origin based positioning using off-the-shelf devices.

- Ultra Wide Band (UWB): Ultra wide band systems have been subject of extensive research as a promising candidate for WPAN applications, sensor networks and ubiquitous computing [CFT12]. Due to its large bandwidth usage, regulation of these type of systems required a completely different approach. For instance, frequency channels assignation of such large widths to specific users are not feasible because free spectrum is not available. For instance, ECMA-368 standard for WPAN uses the frequency band of 3 to 10 GHz. IEEE 802.15.4a include for the first time UWB and designated operating frequencies in three ranges: bellow 1GHz, between 3 and 5 GHz, and between 6 and 10 GHz. UWB technology has extensively adopted for localization systems where accuracy on the order of 1 meter is required. Its high accuracy is due to the precise time-of-flight range estimation achieved by its large bandwidth. IEEE 802.15.4a is an example of a standard capable to provide ranging accuracy of 1 meter or better.

Non-radio signal based systems

- Acoustic systems: In contrast to electromagnetic waves used by RF systems, acoustic signals are mechanical waves. Mechanical waves are transmitted by the oscillation pressure in a medium such as air or building materials. Acoustic position estimation can be based on ultrasound or audible sound. The estimated range of acoustic based positioning systems is about 10 meters due to the specific decay profile of the airborne acoustic channel. Lateration based methods can be easily implemented using this type of systems using a microphone array at the receiver side. Acoustic systems are severely affected by multipath propagation, directivity of transducers and noise. In addition to this, increasing the power of the signal is not a feasible alternative since loud sound signals from nodes to be localized

are energy-demanding which decreases the battery lifetime.

- Inertial Navigation Systems: INS estimate the mobile node position, velocity and orientation from an Inertial Measurement Unit(IMU). The inertial measurement unit consist of three motion sensors (orthogonally arranged accelerometers), three angular rate sensors (Gyroscopes) and/or a magnetometer (measuring the strength and/or direction of a magnetic field). This type of systems provides independent operability. Due to this, they do not required a deployed infrastructure to estimate the mobile node position. When initial position and orientation of the mobile device are known, subsequent positions, orientations and velocities can be updated continuously via Dead Reckoning (DR) without the need for external reference positions. The accuracy of the propagated position depends heavily on the quality of the initially provided position and orientation. Accelerometer measurements are also corrupted by noise. Due to this, INS decrease their accuracy over the travelled distance.

- Signage and Maps: Signage and maps are traditionally the most available approach for human navigation in indoor environments. Actual position is provided by using static signalling and, in order to help the mobile user to reach his destination, a partial or complete map display of the environment is provided. Nowadays, new signs and maps are replacing this traditional approach. For instance, cameras and mobile devices can replace user's sight and reasoning to provide positioning and navigation. In [XYY+17] the usage of a camera to scan unique "markers" is proposed. By doing so, the unique mark provides information to a mobile phone application to determine actual position. On the other hand, the approach proposed in [DAMG15] tries to match the complete acquired images with a database of the building's floor plan. If a match is found, the current location is displayed.

- Magnetic/electrical field: Contrary to electromagnetic waves (RF systems), magnetic waves are capable to penetrate walls inside buildings without propagation error. Due to this, magnetic field based localization systems does not suffer from several drawbacks encountered in electromagnetic systems, such as, multipath and signal delay effects among others. When using magnetic fields for indoor positioning, a distinction on the nature of the magnetic field must be done. Two different types of systems can be considered, natural magnetic field based system and artificial magnetic field based system. Additionally, natural can be classified in two sub-types, geomagnetism and permanent magnets. Geomagnetism based systems use the natural earth's magnetic field to provide positioning. Inherent structure on interior tunnels produce disturbances on the natural field. These variations can be used as a fingerprint to determine the mobile node position. On the other hand, permanent magnets can be used in the mobile node. Magnetic field sensors place at known places measure the magnetic density flux produced bu the magnet in order to determine its position. The second type of localization systems based on magnetic fields use artificially generated magnetic fields. In this type of systems, a variable electrical current circulating in concentric coils is used to create the artificial and controlled magnetic field (Lenz effect). Usually, the artificially induced magnetic fields have a short coverage range (less than 3 m) and, due to this, their application is limited to small volumes.

- Visible light communications (VLC): These systems use the visible spectrum of electromagnetic waves to provide communication. This type of systems have recently emerged and has been subject of extensive research for the research community. The recent advances

in lighting technology, in particular lighting emitting diodes (LED) have transformed VLC system in a feasible and applicable technology. VLC technology transmits information by modulating the intensity of an optical source at a rate much more faster than the response time of human's eye making the change on the optical source unnoticeable. As a consequence, VLC systems are capable to provide illumination and wireless communication at the same time. As the lighting infrastructure is assume to be pre-deployed, only a few modification on the lighting devices is required. These systems used require mostly line-of-sight (LOS). In addition to this, VLC link is used mostly to provide the downlink and, hybridization with RF and Infra-red (IR) systems is proposed to provide full-duplex communication. In literature, the term visible light positioning (VLP) stands for localization systems that use VLC to provide positioning. In general, many of the approaches that used in RF based positioning systems can be encountered in VLP.

Hybrid systems

as it can be seen, numerous technologies can be used to provide positioning. Each technology posses their own *pros* and *cons* in terms of performance, coverage, etc. Due to this, the idea of combining different types of localization technologies to overcome difficulties and/or improve the system's performance arises. The main problem of this type of systems is that there does not exist an unified systematic evaluation on the possible trade-offs and drawbacks of using different technologies simultaneously for localization purposes. In the literature, diverse hybrid localization systems be encountered. They are mainly focused in increase the performance (mainly accuracy) and coverage of traditional single-technology approaches.

2.4.2 System topology

The deployment of anchor nodes as well as the mobility of dumb nodes has an important effect on the performance of the localization system. [DMS98]. Localization systems can be classified in three different groups considering the topology of the system, i.e., self-positioning, remote-positioning and indirect-positioning. This classification is useful when evaluating a positioning system for a particular application. Different approaches will be classified based on where the position measurements are performed and where the obtained position information is used. [DMS98]. The three categories are detailed below.

- Remote positioning: In this type of systems the anchor nodes receive the signal originated from or reflecting off the dumb node. Measurements of the signal are transmitted to a central station where they are used to estimate a position as shown in Fig.2.8(a). These type of positioning systems are used in centralized LBS.

- Self Positioning: In self positioning systems the dumb node performs the measurement of the signal sent by the anchor nodes and uses these measurements to perform localization. Using this type of topology the mobile node or user is aware of its position. Nevertheless, this position information can be only used in distributed applications as shown in Fig.2.8(b).

- Indirect Positioning: When the networks used to perform localization is capable to transmit data indirect positioning topology can be used. In this scheme the estimated position by self-positioning or remote-positioning can be re-transmitted as illustrated in Fig.2.8(c). When the self positioning system sends its information to a remote or central station is referred to as indirect remote-positioning. On the other hand, when a remote positioning

system delivers to the dumb node its positioning information is referred to as indirect self-positioning.

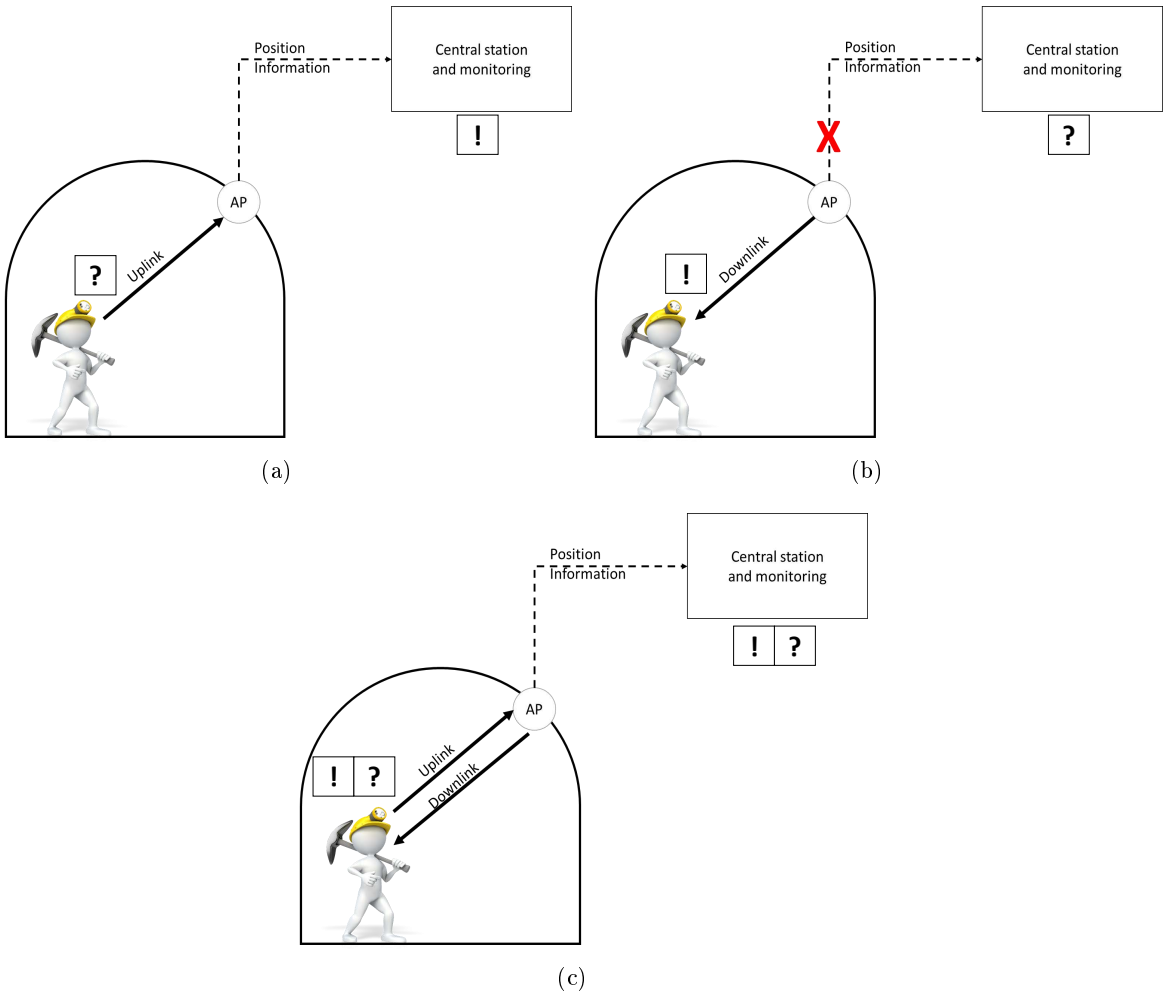

Figure 2.8: Different localization system topologies (a) Remote positioning, (b) Self positioning and (c) Indirect Positioning

As it can be seen from Fig.2.8 the system topology will impose a major constraint on the LBS that can be provided. For example, navigation systems are thought to be enabled by self-positioning systems since the mobile node must be aware of its position in order to be guided. On the other hand, dispatch software use remote-positioning topology since they require position information of every dumb node in order to optimize the instructions. In the following section, different enabling technologies are analysed. Their potential to provide self-positioning, remote-positioning or indirect positioning will be delivered as part of this investigation.

2.4.3 Deployment

This characteristic of the localization system defines the deployment of required infrastructure to provide positioning. The infrastructure deployment is classified in three categories detailed bellow

- Pre-Deployed: In this type of localization systems the required infrastructure is already deployed in the scenario. In particular, systems that uses the wireless communication infrastructure (WLAN, VLC, etc.) to provide localization are the most representative systems.
- Strategic Deployment: This type of systems require special deployment of localization infrastructure to provide positioning. Systems such as RFID, magnetic, acoustics and WPAN based systems are some examples of localization technologies that require the installation of dedicated infrastructure to determine the position of the mobile node.
- Deployment-Free: These systems do not require infrastructure deployment to provide positioning. Usually, inertial sensors and map knowledge are used in indoor scenarios.

2.5 Systems proposed in literature

In current literature, different systems have been proposed to deal with the problem of underground mine positioning. In this section each proposal is presented and analysed.

In Table 2.2 the main contributions existing in literature are presented. These underground mine positioning systems have been evaluated based on their technological principle, topology, infrastructure requirements, accuracy and implementation.

When RF technology is used for underground positioning Zig-bee technology is preferred among the others. Different range based and range free methods can be implemented by using this technology. In particular TOF and RSS based range free methods are preferred since this type of networks are capable to provide signal strength measurements and propagation time measurements without requiring additional hardware. The main problem of using Zig-bee technology to provide localization services is that this type of networks have a low data rate. Due to this, communications applications are constrained to low data-rate demanding services. Some proposals have been evaluated in real scenario reaching level meter accuracy.

On the other hand, WLAN networks are capable to provide higher data rates. Due to this WLAN architecture can be used as a pre deployed networks that provides wireless communications with localization capabilities. RSSI based range based and fingerprinting methods are preferred since WLAN devices do not require extra hardware to measure the signal strength.

UWB and Bluetooth technology have been also proposed to face the positioning problem in underground mines. Despite achieving a high accuracy in real scenarios, these techniques are not cost effective. In general, UWB devices are expensive and Bluetooth solution requires a high number of devices deployed inside the tunnel to reach acceptable coverage and accuracy.

[h]

Article	Technological principle	System topology	Infrastructure deployment	Estimation method	Accuracy	Implementation
Li et al (2009)	RF Zig-bee	Indirect remote positioning	Strategic deployment	Range based RSSI	2.6m static 4.5m dynamic (average error)	Real scenario
Guan-zhu (2009)	RF Zig-bee	Self positioning	Strategic deployment	Not specified	Not specified	Computational Simulation
Cheng (2015)	RF Zig-bee	Remote positioning	Strategic deployment	Range based RSS	Not specified	Real scenario
Srikanth (2016)	RF wireless sensor network	Self positioning	Strategic deployment	Range based RSSI	3.67 m to 6.972 m (average error)	Computational Simulation
Qin (2012)	RF Zig-bee	Indirect remote positioning	Strategic deployment	Range based RF-TOF	3 m CDF 86.4%	Real scenario
Tahir (2018)	RF Zig-bee	Self-positioning	Strategic deployment	Range based RSSI	2 m 100% CDF	Computational Simulation
Moridi (2015)	RF Zig-bee	Remote positioning	Strategic deployment	Range free Cell ID	Room level	Real scenario
Xu (2012)	RF Zig-bee	Remote positioning	Strategic deployment	Not specified	Not specified	Computational simulation
Guo (2011)	RF Zig-bee	Remote positioning	Strategic deployment	Range based not specified	Not specified	Not specified
Wu (2014)	RF Zig-bee	Self positioning	Strategic deployment	Range based TOF	5 m	Real scenario
El Assaf (2015)	RF not specified	Remote positioning	Strategic deployment	Range free hop-count method	3m normalized root mean square error	Computational Simulation

Dayekh (2014)	RF not specified	Not specified	Strategic deployment	Fingerprint	50cm controlled environment 1.28 m when method is challenged CDF	Real scenario
Song (2017)	RF nanoPAN 5375	Self positioning	Strategic deployment	Range based TOA	$\leq$ 2 m CDF	Real scenario
Nerguizian (2006)	RF WLAN	Remote positioning	Pre deployed	Fingerprinting	2 m average error	Real scenario
Ralston (2005)	RF WLAN	Indirect remote positioning	Pre deployed	Fingerprinting	2-10 m error	Real scenario
Lin (2013)	RF WLAN	Indirect remote positioning	Pre deployed	Fingerprinting	3-5 m	Real scenario
Cypriani (2013)	RF WLAN	Indirect remote positioning	Pre deployed	Fingerprinting	$\leq$ 20 m mean error	Real scenario
Guo (2012)	RF WLAN	Self positioning	Pre deployed	Fingerprinting	1.6 m	Computational simulation
Baouche (2008)	RF low power WPAN	Remote positioning	Strategic deployment	Range free hop-count method	Not specified	Computational Simulation
Minhas (2017)	RF low power WPAN DASH-7	Indirect remote positioning	Strategic deployment	Range Based RSS	2-4 meters	Real scenario (tunnel with low cross section)
Liu (2010)	RF (leaky feeder)	self positioning	Strategic deployment	Range based (RSS or TOA)	Depends on number of connected nodes and user's speed	Computational Simulation
Pereira (2012)	RF GSM leaky feeder	Indirect self positioning	Pre deployed	Fingerprint	160 m 90% CDF	Real scenario

Chehri (2009)	RF UWB	Indirect remote positioning	Strategic deployment	Fingerprint	Not specified- feasibility study	——
Cheng (2012)	RF UWB	Self positioning	Strategic deployment	Range based TOA	not measured	Computational simulation
Qin (2015)	RF UWB	Self positioning	Strategic deployment	Range based TOF	0.3 m CDF	Real scenario
Baek (2017)	RF Bluetooth	Indirect self positioning	Strategic deployment	Range free Cell ID	Depends on network deployment	Real scenario
Rusu (2011)	RFID	Self-positioning	Strategic deployment	Range free	From centimetres to few meters	Real scenario
Hammer (2015)	Acoustic	Self positioning	Strategic deployment	Range based bilateation AOA and range free proximity supported	25 cm mean absolute error	Real scenario
Lin (2017)	Magnetic field	Indirect remote positioning	Strategic deployment	Range based received magnetic field strength	0.767 RMSD	Computational Simulation
Abrudan (2016)	Magnetic field	Self-positioning	Strategic deployment	Range based RSSI	$<$1.2 m several tries	Real scenario
Pfeil (2015)	Hybrid Acoustic/UWB	Indirect self positioning	Strategic deployment	Range based TOF	3 cm CDF	Real scenario
Savic (2013)	Hybrid UWB/INS	Indirect self positioning	Strategic deployment	Range based TOA	15 cm CDF	Real scenario
Hawkins (2006)	Hybrid RF/INS	Self positioning	Strategic deployment	Range based RF technique/INS particle filter	Not delivered	Computational simulation

Niu (2018)	Hybrid INS/image	Indirect self positioning	Strategic deployment	Image positioning and dead reckon	5 m CDF	Real scenario
Ke-Fei (2009)	Hybrid RFID/INS	Indirect self positioning	Strategic deployment	Fingerprint and INS based method	1.7 m RMS error	Real scenario
Lavigne (2006)	Hybrid INS/scanning laser/RFID	Self positioning	Strategic deployment	INS based method supported by range based RFID	Not specified	Real scenario
Haidery (2016)	Hybrid RFID/WLAN	Remote positioning	Pre deployed	Cell ID like method	Not specified	Real scenario
Xu (2017)	Camera	Self positioning	Strategic deployment	Range based image processing based method	0.381 m curved tunnel and 0.1242 straight tunnel	Real scenario
Li (2018)	Laser	Self positioning	Deployment free	SLAM	Not specified	Real scenario (public dataset)
Thrun (2004)	Laser	Self positioning	Deployment free	SLAM	Not specified	Real scenario
Wu (2016)	VLC	Indirect remote positioning	Pre deployed	Range free Cell ID	Not specified	Real scenario
Krommenacker (2016)	VLC	Self positioning	Pre deployed	Range free Cell ID based method	From meter-level to centimetre-level	Computational simulation
Iturralde (2014,2017)	VLC	Self positioning	Pre deployed	Range based RSS trilateration	$\leq$1 m	Computational simulation

Dehghan Firoozabadi (2019)	VLC	Self positioning	Pre deployed	Range based RSS trilateration	$\leq$1 m CDF	Computational simulation

Table 2.2: Proposed positioning systems for underground mines

Table 2.3: Pros and cons of visible light positioning technology in underground mines

Technology	Pros	Cons
VLC based positioning	- High accuracy - Pre-deployed infrastructure - Low cost - Scalable	- Remote positioning not supported

Acoustic based method proposed by Hammer et al. [HPF+15] uses an AOA based algorithm for high positioning accuracy. This proposal also support range free localization. The main problem of this proposal is that strategic deployment of infrastructure is required and only self positioning topology is supported.

Another technology that has been used for underground mine positioning is magnetic field based localization. Lin et al. [LAWA17] proposed an indirect remote positioning topology. This proposal is uses a magnetic field RSS based method to estimate the position of mobile node inside the tunnel. This methods shows promising accuracy when the system is evaluated through computational simulation. On the other hand Abrudan et al. [AXMT16] proposed a magnetic field based positioning which has been implemented in real scenario. The main drawbacks of this proposal is that only self positioning topology is supported and strategic deployment of magnetic beacons is required.

Different hybrid positioning methods can be found in literature. Mainly, different low cost high precision positioning technologies are hybridized with RF technology in order to support remote positioning or indirect self positioning. As it can be seen INS are used frequently in hybrid approach due to their capability to provide position information with deployment-free infrastructure.

SLAM based approaches are mostly used for inspection of abandoned or unsafe tunnels. These solutions are deployment free in terms of infrastructure. Nevertheless, they require a high number of sensors and computational capacity to perform localization making these approaches more expensive and difficult to implement for day to day operation.

Visible light communications based positioning has also being proposed for underground mine environment. This approach uses the already pre deployed lighting infrastructure and achieves a high accuracy. The main problem of this approach is that they only provide self positioning topology. Furthermore, the overground station is not aware of the position of underground personnel. Range based and range free methods are supported when using VLC for localization purpose.

2.6 Conclusions

In this Chapter an in depth analysis of different current localization technologies for underground mine positioning was delivered. An important number of solutions have been proposed after the entry into force of the new MINER act in 2006. Due to the special characteristics of underground tunnels only few approaches can be highlighted as potential solutions capable to meet the requirements established by this new safety standard. Most of the proposed localization systems achieves the minimum-accuracy requirement ($\leq 60m$) shown in Table 2.1. Among all, WLAN, VLC and INS based systems have the advantage of using low or non required infrastructure to provide position information of personnel inside the tunnel. In particular, WLAN approach has the capability to provide indirect and remote positioning topologies to comply with the require-

ment of overground monitoring along with high speed wireless communications. On the other hand, INS and VLC solutions can only provide self positioning. Due to this, they require to be hybridized with some other wireless communication technology in order to report the position estimation to the overground central monitoring station for emergency response.

In Table 2.3 the main pros and cons of VLC technology are summarized. These features will be taken into account to design a feasible visible light positioning solution for underground mine localization. As it can be seen this novel technology has the potential to be implemented in underground environment since it fulfils cost, infrastructure, scalability and accuracy requirements. The main drawback to be solved in order to reach the topology requirement of MINER act [10906] is the lack of uplink communication. This problem will be addressed later on in Chapter 5.

Chapter 3

Visible light communications channel modelling in underground mines

Sommaire

3.1 Introduction **34**
3.2 Illumination standards **36**
3.3 Mathematical model **38**
3.3.1 Visible Light Communications System Configuration 39
3.3.2 Light sources 40
3.3.3 Light detectors 43
3.3.4 Light propagation model 44
3.4 Conclusions **52**

3.1 Introduction

Any optical communications link consist in two basics elements. The first is a light source which is used at the transmitter side to transport digital information to the receiver. Then, at receiver side, an electronic element transforms and demodulate the optical signal in order to recover the transmitted data.

There are a bunch of methods to transmit information by using optical sources. Among them, intensity modulation with direct detection (IM/DD) appears as the de facto method of implementing optical wireless communications due to its reduced cost and complexity [Bar12, KB97].

In IM/DD systems, the optical intensity of the source is directly modulated by varying the drive current I_{LED} since the transmit optical power, P_t, is proportional to I_{LED} as see in Figure 3.1.

At the receiver side, a photodetector element is used in order to integrate tens of thousands of very short wavelengths of the incident optical signal which generates a photocurrent. The photocurrent is directly proportional to the power of the incident optical signal.

In Figure 3.2 and IM/DD scheme is presented. At the transmitter side and LED light is used to convey information. At the receiver side a photodetector (PD) is used.

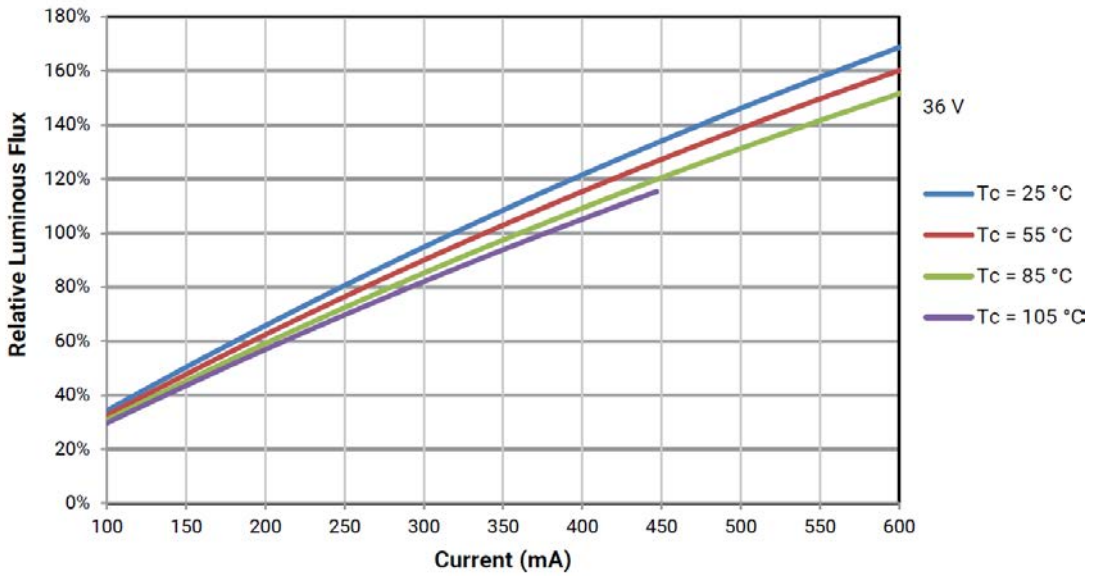

Figure 3.1: Current to Luminous flux curve of the LED light Cree XLamp CXB1512 [Des15]

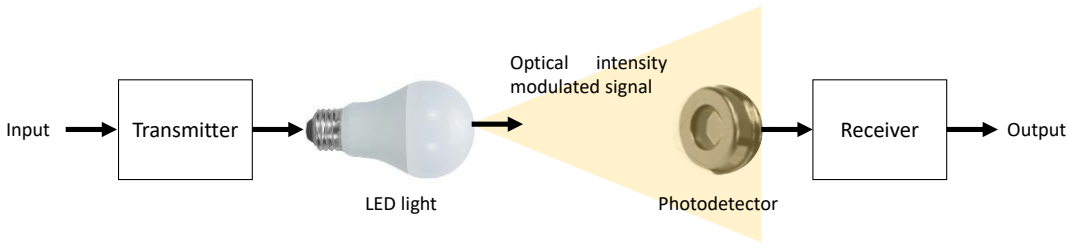

Figure 3.2: Block diagram of an IMDD optical wireless communication system

Basically, in order to model visible light communications inside the tunnel, three different components of the VLC channel must be analysed, These are: LED lights, environment conditions and detector properties. These characteristics are analysed in this section.

Underground mines are one of the most complex environments for communications and positioning due to their particular characteristics. Underground mines can have a massive extension. The largest operation can be found in Chile. El Teniente mine is considered as the largest underground mine with an extension of 3000 km of tunnels. This extension impose a huge challenge in terms of coverage for a communication and the positioning systems. They must be scalable and have a very large coverage if the complete extension of the tunnel must be endowed with communication and positioning. Moreover tunnels inside the mine have different sizes and geometries, often depending on its usage and space requirements to perform different labours.

Another important issue to be considered that may affect underground mine communications and positioning is that, extreme conditions are present throughout the tunnel. Some of them are high levels of humidity (up to 90 % or above [YGAM09]), airborne dust and extreme heat.

In order to properly analyse the performance of our proposed positioning method, a visible light communications channel model is developed in this section. This model, takes into account

several factors present in underground mines that are not considered in traditional VLC channel modelling.

In order to develop VLC channel model that analyse the particular characteristics of underground mines, we must take into consideration the illumination standards of underground mining and the environmental conditions that will affect the communication link.

In the next sections, these parameters will be analysed and, a visible light communication channel model for underground mines will be provided.

3.2 Illumination standards

Illumination standards will provide an insight on deployed infrastructure and artificial illumination constraints inside an underground mine. Illumination is a key factor in VLC networks since the coverage is strongly related to lighting infrastructure. Due to this, deployed infrastructure of the application scenario must be study in order to verify its feasible implementation.

Commonly, illumination in indoor environments is regulated by safety and health governmental institutions. In particular for underground mines many different regulations in terms of illumination requirements can be found. Each country has their own regulations in terms of safe illumination. In addition to this, illumination criteria is not uniform for every underground operation. The level of illumination in a mine zone changes depending on the labour carried out as shown in Table 3.1. Some countries does not have a clear threshold on illumination requirements. As an example, Chilean regulation for safety and heath remove underground mines from the illumination regulations in the Article 103: "*"Every workplace, with exception of underground mines or similar workplaces, must be illuminated with natural or artificial light*".

Table 3.1: Illumination requirements for different working zones of underground mines (Table adapter from [Com])

Country	Mine zone (lx)					
	Shafts	Loading	Around machines	Haulages	Headings	Workshop
Belgium	20-50	20	25	10	-	-
Hungary	41-100	40-80	20-50	2-10	-	20-50
Canada	21	-	-	21	53	-
Poland	30	30	10	2-10	5-15	30
UK (British Coal)	70	30	-	2.5	-	50-150
European Coal and Steel community	40-90	15-80	-	5-15	10-30	-

Proper illumination in underground mines is important due to different safety and health aspects. In particular the The National Institute for Occupational Safety and Health (NIOSH) of U.S. states that many of the higher frequency risks in mining are related to the challenge of inadequate lighting. These include slip, trip, and fall (STF) hazards which can be more difficult to detect in low light [The15]. In addition to this, the worker age is another important factor to take into account since 40% less light reaching the retina of a 45-yr-old person compared to a 24-years-old person.

In addition to the standardization issue on lighting infrastructure, there is another condition for the deployment of VLC based networks, i.e., the usage of LED lights as the main illumination device. The selected device for illumination purposes must comply with some properties in order

to be suitable for its application in underground mines. Lighting devices must have a low rate of maintenance and reposition. Moreover, due to the increasing costs of energy, they must be energy efficient. Traditionally, fluorescent lights have being used in mining environment. Fluorescent lights are still a more cost effective solution than LED lights as evaluated in Chueco et. al. [CLB15]. Nevertheless, the research on this novel technology have made their prices fall. Between 2008 and 2016 the price of a LED light bulb dropped in 90% and it is expected that market tendency will remain the same. Besides its decreasing cost, LED lights other benefits such as low-energy consumption, long useful life, and low maintenance rates making this technology applicable in underground mines. In Figure 3.3 the light output of each mentioned technology based on their operating hours is shown.

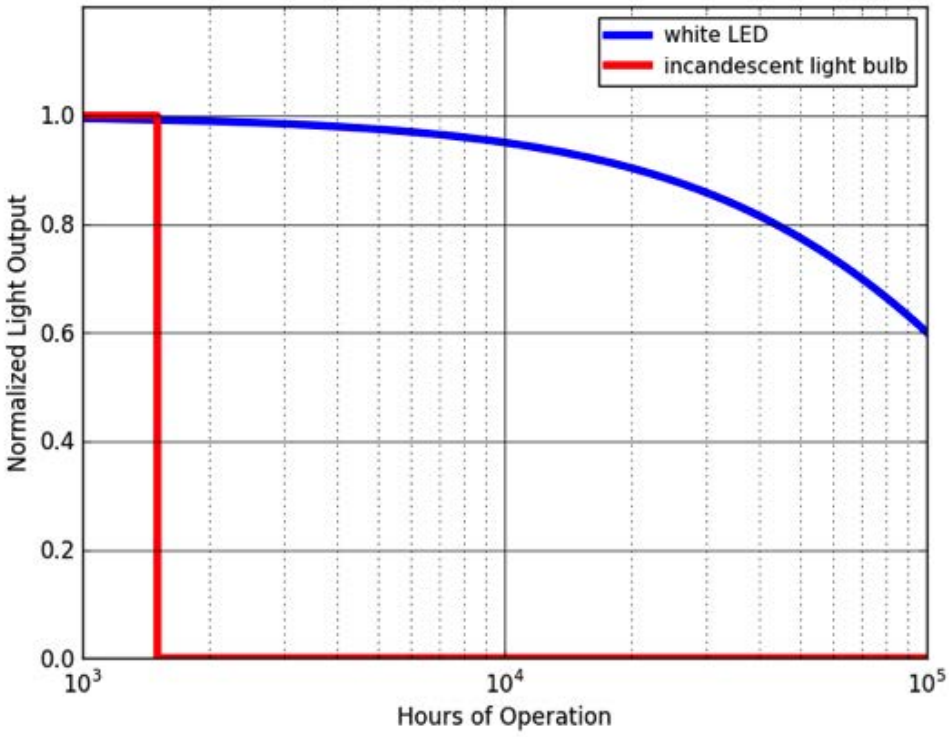

Figure 3.3: Typical light output comparison between white LED and incandescent light bulb as function of operating hours[Lum]

As it can be seen, LED lights have a lower maintenance rate and a larger life-span than traditionally used incandescent light bulbs. Moreover, an acceptable lighting output is provided for up to 100000 hours. A decrease in the lighting out may have an impact in the positioning system if the method used for localization uses the received power to estimate the position of the mobile node. The robustness of different positioning methods to this perturbation will be analysed in latter sections.

3.3 Mathematical model

Underground mines consist in tunnels as shown in Section I. Inside the mine, different sections can be identified. Each section will provide different conditions. In Figure 3.4 different sections inside the underground mine are presented.

(a) (b)

(c) (d)

Figure 3.4: El Teniente underground mine light deployment (a) Transportation tunnel (b) Machinery working inside the tunnel(images by Codelco)

A number of different characteristics can be pointed out when compared with traditional indoor environments. Luminaries deployed inside the tunnel can be placed in the ceiling or in walls. In order to facilitate maintenance and replacement labours, walls placement is preferred over ceiling installation. When luminaries are placed in the tunnel's walls, randomly tilt transmitters condition has to be considered for channel modelling. In addition to this, machinery inside the mine can cause shadowing as shown in Figure 3.4 (d). Due to this, the signal received by workers inside the mine will be provided by the reflection of light inside the tunnel (diffuse link).

As it can be seen in Figure 3.4 (b), inside the tunnel a physical separation between pedestrians and machinery is often done to prevent accidents.

A traditionally use assumption made when studying indoor positioning systems is that walls are perpendicular to the floor and ceiling. This assumption is not valid in underground tunnels. Furthermore, walls inside the tunnel are not flat. This also must be considered when modelling the channel impulse response (CIR) of the visible light communication system.

Table 3.2: Comparison between proposed and state-of-art VLC underground mines channel models

Model	**Characteristic**				
	Tilted LED	Tilted PD	Shadowing	Dust	Walls geometry
Wang et. al. 2018 [WAKZ+18]			x	x	
Wang et. al. 2017 [WWC+17]					
Wang et. al. 2017 [WAKS+17]					
Our proposal	x	x	x	x	x

In current literature, only a few VLC models for underground mines have been proposed [WAKZ+18, WWC+17, WAKS+17]. These channel models do not consider several factors present in underground mines environments presented in Table 3.2.

This section will be organized as follows: First,visible light system configuration is analysed. Then light source model will be presented. Detector response (receiver) and functioning are detailed next. Finally, light propagation model will be delivered and analysed. A comparison between traditional indoor VLC channel model and underground mine model is carried out in this section.

3.3.1 Visible Light Communications System Configuration

There are great number of considerations which must be taken into account when designing VLC networks. When VLC is used for confined environments, light will be reflected by the ceiling, walls and most of the objects inside the room. In addition to this, the optical signal will not pass through opaque barriers. Due to this, there are numerous ways to physically configure an optical link. Typically, They are grouped into four system configurations as shown in Figure 3.5.

Direct LOS path is commonly used in point-to-point communication links. The link is concentrated in a very narrow beam, this leads to a low power requirement. In addition to this, LOS link offers higher data rates with a transmission range from few meters to kilometres. LOS link is almost not affected by multipath signal distortion. Its usage for indoor applications could be limited because of its small coverage area [BL05]. Direct LOS path needs the alignment between emitter a receiver, because of this, this link configuration cannot be used in mobile applications. On the other hand, non-direct LOS is commonly used for indoor applications. This link configuration is considered as the most flexible configuration. A combination of a wide light beam transmitters and a wide FOV receiver is used. Signal scattered from surfaces ca be used to increase the coverage area. This link configuration is suitable for point to multipoint broadcast applications because it offers robustness against shadowing and blockage. Transmitter must not be necessarily aligned with the receiver to perform the communication. Nevertheless, this type of link can may be affected by a high path loss and multipath distortion which leads to a detrimental effect on the performance of the system when dealing with high data rates. Besides, inter-cell interference increases when multiple sources are arranged in a small area due to the wide light beam of the transmitters. Non-direct LOS link is not suitable to operate in environments with intense ambient light [GPR12], nevertheless, underground mines are far from being intensively illuminated.

Diffuse configuration proposed in [GB79a] consists on a transmitter pointing directly towards the ceiling or any surface within the room as shown in Figure 3.5 c). This link is the most suitable for optical WLAN and optical ad-hoc networks. Alignment between emitter and receiver is not necessary and is immune to blockage. It suffers from a multipath distortion and a high path

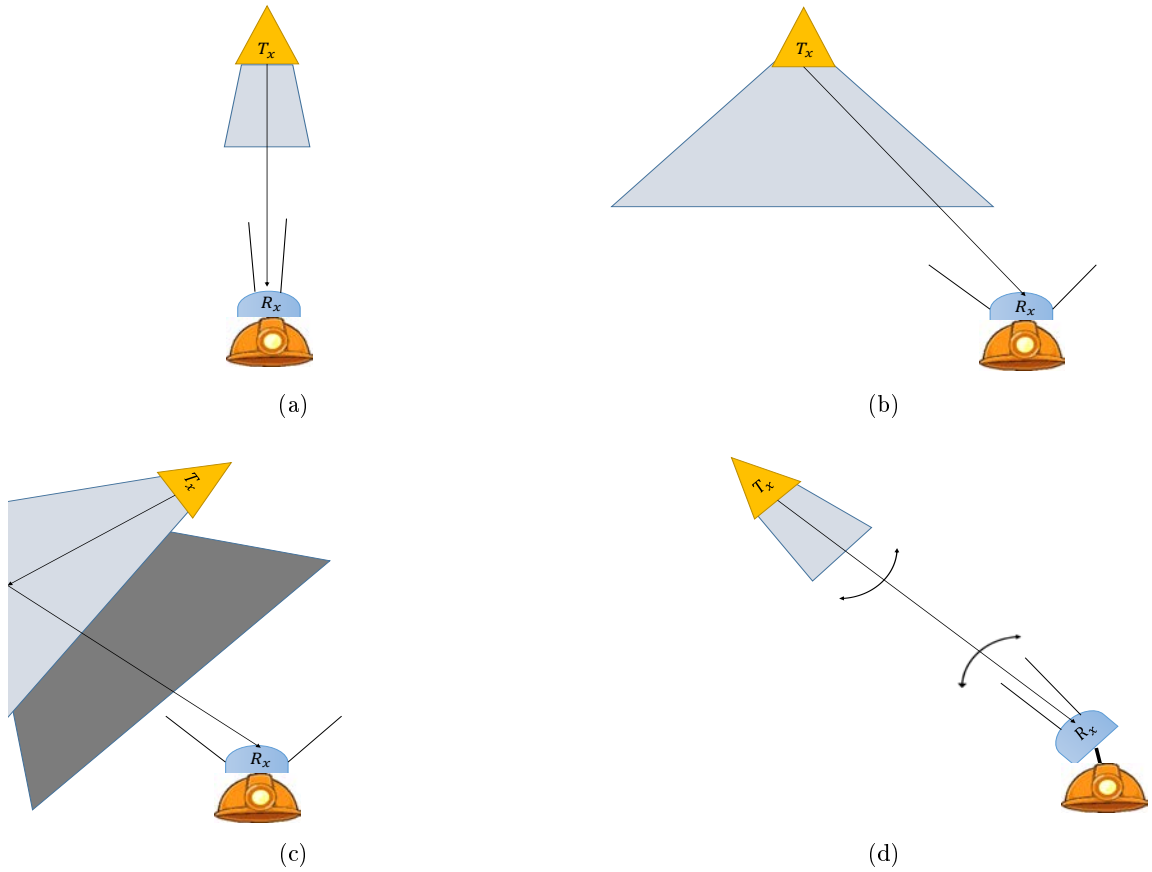

Figure 3.5: Different systems configurations for VLC link, PD is placed in the miner's helmet: (a) directed LOS, (b) nondirected LOS, (c) diffuse, and (d) tracked

loss which is increased by temporary obstructions [KKC95]. The bit rate is limited and its performance is severely affected by ambient light.

In tracked systems emitter and receiver are aligned automatically by an electro-mechanical device. Nevertheless, these electro-mechanical devices are expensive. Electronic tracking schemes for this type of communication scheme has been previously proposed in [Wis96]. In table 3.3 the main characteristics of each link configuration for enabling VLC based IPS are presented, i.e., mobility, coverage and cost. Diffuse and non-directed LOS link configurations have higher mobility and coverage compared to others configurations. Moreover, the cost of implementing a VLC system using nondirected LOS or diffuse link is low.

3.3.2 Light sources

In optical wireless communications systems, lights sources are used as transmitters to convey digitalized information. In general, light sources used for digital communications the following features must be considered for proper selection of the source [GPR12]. Some of the characteristics are: Source wavelength, Fast response time, energy efficiency, reliability, cost, lifespan, linear current-power conversion, ability to be directly modulated by varying driving current just to name a few.

As mentioned before, there are a number of sources available in the market and, selection of

Table 3.3: Comparison of different VLC system configurations

System Configuration	Mobility	Coverage	Cost
Directed LOS	none	low	low
Nondirected LOS	high	high	low
Diffuse	very high	very high	low
Tracked	high	high	high

the technology is based on technical and economical criteria. The most commonly used lighting devices in indoor optical wireless communications are lighting emitting diodes (LED). LEDs are solid-state devices the emit incoherent light when an they are subject to an electronic excitation [SN07]. This excitation is achieved by applying a forward bias voltage across the p-n junction.

LEDs lights can be fabricated to emit light across a wide range of wavelengths (colours) from the visible to the infrared (IR) region of the electromagnetic (EM) spectrum [GPR12]. The LED's peak wavelength (colour) depends mostly on the band-gap energy of the semiconductor material (E_g) used in the p-n junction.

In Figure 3.6 the entire electromagnetic spectrum is shown.

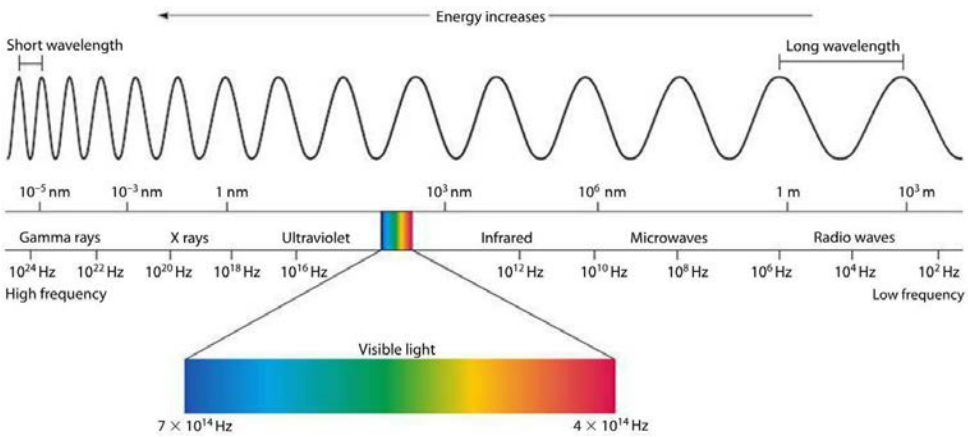

Figure 3.6: Electromagnetic spectrum [Min]

As it can be seen, visible light, which is the portion of the EM spectrum that can be seen by the human eye, extends from 400 to 700 nm as shown in Figure 3.7.

Visible light plays a key role in modern optical wireless communications since this technology is used to provide high data rate wireless communication using the deployed lighting infrastructure. This novel technology is known as visible light communications (VLC). There are three main characteristics that must be taken into account when selecting the light source. There are: Power efficiency, luminous efficiency and light bandwidth.

The power efficiency of a LED light is the ratio between the optical power output ($P_{optical}$) and the electrical power input (P_e). This is expressed as follows:

$$\eta_{power} = \frac{P_{optical}}{P_e} \tag{3.1}$$

The luminous efficiency (η_{lu})is used to describe the LED characteristics within the visible spectrum. This parameters normalize the power efficiency η_{power} by a factor related with the radiation pattern within human eye sensitivity shown in Figure 3.7.

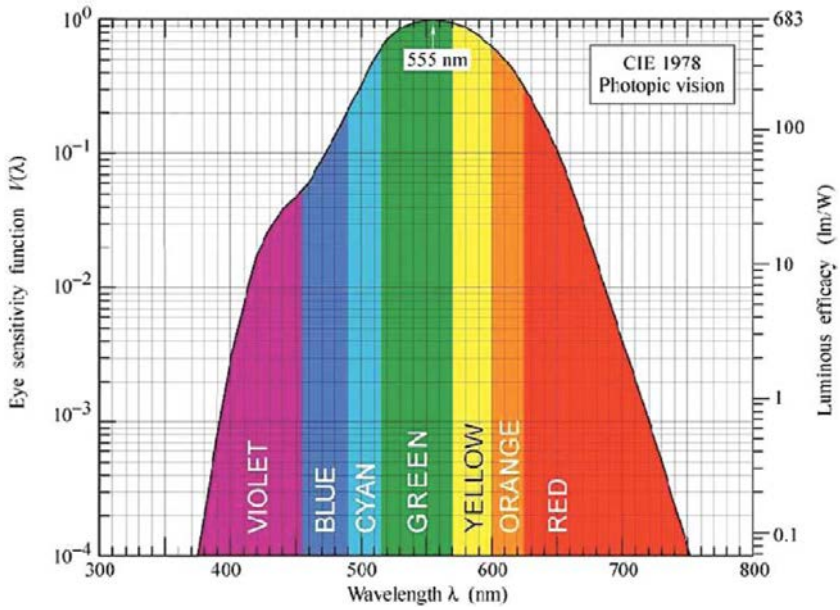

Figure 3.7: Huma eye's response based on the 1978 CIE data (http://www.ecse.rpi.edu/ schubert/ Light-Emitting-Diodes-dot-org)

The luminous flux (lumens) can be defined as the total emitted flux scaled in order to reflect the human eye's sensitivity to different light wavelengths. The luminous flux is given by:

$$\phi_{flux} = 683 \int V(\lambda) P_{optical}(\lambda) d\lambda \tag{3.2}$$

where $V(\lambda)$ is the normalization factor based on the eye response shown in Figure 3.7 and $P_{optical}(\lambda)$ is the radiation power spectrum of the LED light.

The luminous efficiency of the LED is given by

$$\eta_{lu} = \frac{683 \int V(\lambda) P_{optical}(\lambda) d\lambda}{P_e} \tag{3.3}$$

Finally, the light bandwidth will determine the modulation bandwidth and, as a consequence, the maximum data rate the system can achieve. This parameter depends on several factors which can be found in [GPR12]. In general, LEDs have a low pass transfer function modelled as:

$$H(jw) = \frac{1}{1 + jwRC} \tag{3.4}$$

This, is an equivalent first-order jRC low-pass filter. R and C are the resistance and junction capacitance of the LED. Hence, 3 dB modulation bandwidth of the LED is given by

$$f_c = \frac{1}{2\pi RC} \tag{3.5}$$

Generally, LED angular distribution of the radiation intensity pattern is modelled using a generalized Lambertian radiant intensity as shown in Figure 3.8.

In Figure 3.8 (a), angular distribution of the radiation intensity pattern of the LED light Cree XLamp CXB1512 [Des15] is shown. As it can be seen, the radiated power varies with the radiation angle ϕ_j as presented in Figure 3.8 (b).

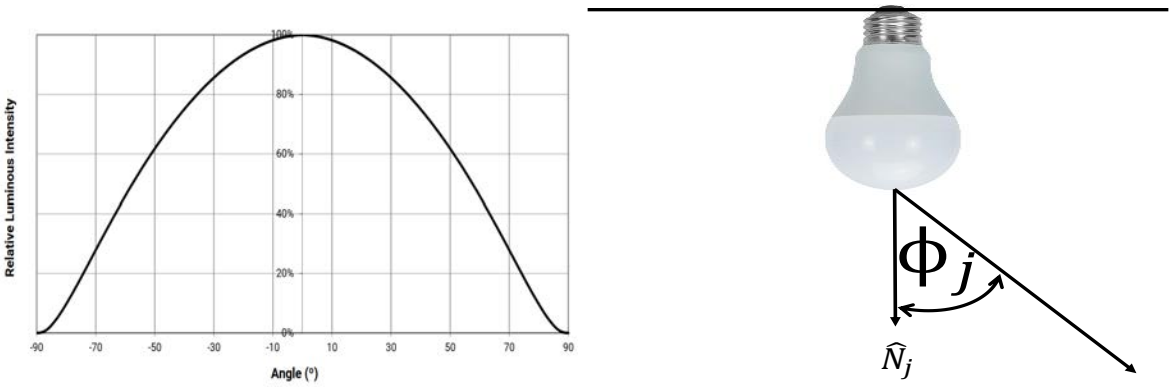

(a) (b)

Figure 3.8:

This radiation pattern is mathematically modelled as follows

$$R(\phi_j) = \begin{cases} \frac{(m_l+1)}{2\pi} \cos^{m_l}(\phi_j) & -\pi/2 \leq \phi_j \leq \pi/2 \\ 0 & \text{elsewhere} \end{cases} \tag{3.6}$$

where m_l is the Lambert's mode number of the light sources, which is a constructive parameter of the LED. This parameter is related to the LED semi-angle at half power $\Phi_{1/2}$ by

$$m_l = \frac{-\ln(2)}{\ln(\cos(\Phi_{1/2}))} \tag{3.7}$$

By using the above expression of Equation 3.6, the radiation intensity of a LED light emitter with power P_t is given by

$$S(\phi_j) = \begin{cases} P_t \frac{(m_l+1)}{2\pi} \cos^{m_l}(\phi_j) & -\pi/2 \leq \phi_j \leq \pi/2 \\ 0 & \text{elsewhere} \end{cases} \tag{3.8}$$

This equation will be used to represent the transmitted power of the source.

3.3.3 Light detectors

At the receiver side of a VLC link, an element capable to transform the modulated light intensity into and electrical signal is used,i.e., a photodetector (PD).

The PD is a square law optoelectronic transducer that generates an electrical current which is proportional to the square of the incident optical field to its surface. Due to this, the current generated at the PD (I_p) is proportional to the received optical power P_r as given by

$$I_p = \eta_{qe} \frac{qP_r}{hf} \left(1 - e^{-\alpha l}\right) \tag{3.9}$$

where η_{qe} is the quantum efficiency, l is the length of the photoactive region, q is the electronic charge, and α is the absorption coefficient. The absorption medium is commonly selected as the Si and gallium alloys for the visible light.

Mathematically, the photodetector is modelled as an active area collecting the radiation incident at angles ψ smaller than the detector FOV. The angular characteristics of the PD and

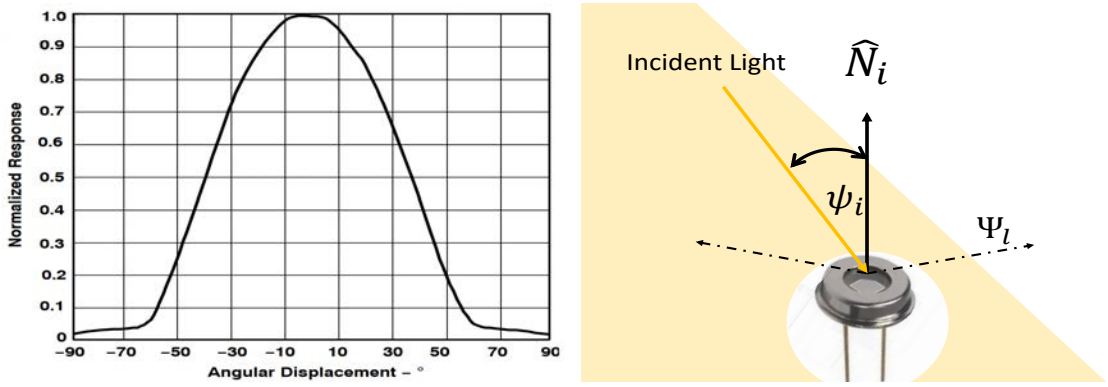

(a) (b)

Figure 3.9:

its FOV are shown in Figure 3.9 (a). In this case, the FOV angle of the TSL257-LF PD is approximately 120°. The effective collection area of the detector is given by

$$A_{eff}(\psi_i) = \begin{cases} A_d \cos(\psi_j) & -\Psi_l/2 \leq \psi_i \leq \Psi_l/2 \\ 0 & \text{elsewhere} \end{cases} \tag{3.10}$$

The incident light angle to the PD surface and FOV angle are graphically shown in Figure 3.9 (b).

It is obvious that a large area detector would collect more power than a small area PD. Nevertheless, it would cause a number of problems, such as increased manufacturing cost, narrow receiver bandwidth, and increased receiver noise. Due to this, the use of an optical concentrator preferred to increase the overall effective collection area. The fain og an ideal non-imaging concentrator is expressed as

$$g(\psi_i) = \begin{cases} \frac{n_i^2}{\sin(\Psi_l)} & -\Psi_l/2 \leq \psi_i \leq \Psi_l/2 \\ 0 & \text{elsewhere} \end{cases} \tag{3.11}$$

where n_i is the internal refractive index of the concentrator. Finally, an optical filter with a gain $T_s(\psi_i)$ can be considered. Typically, this parameters is taken as $T_s(\psi_i) = 1$.

3.3.4 Light propagation model

In the previous sections, light sources and detectors for VLC link have been mathematically modelled. In this section, we use them in order to construct our VLC channel model for underground mines.

In general, the received power of the line-of-sight (LOS) signal from each LED light [KN04] is expressed as

$$P_i = R_{PD} P_j (H_{LOS} + H_{n-LOS}) + N \tag{3.12}$$

where P_i is the received power by the mobile node i, R_{PD}, P_j and H_{LOS} are the responsivity of photo detector, the transmitted power by LED source j and the channel gain component of line of sight (LOS) link respectively. Finally, H_{n-LOS} is the non-line of sight (non-LOS)

component.The noise N is additive noise modelled as the sum of thermal noise $\sigma_{thermal}$ and shot noise σ_{shot} [LZZ+12].

$$N = \sigma^2_{thermal} + \sigma^2_{shot} \tag{3.13}$$

where $\sigma^2_{thermal}$ and σ^2_{shot} are the thermal and shot noise variances respectively modeled as

$$\sigma_{thermal} = \frac{8\pi k T_K}{G_{ol}} C_{PD} A I_2 B^2 + \frac{16\pi^2 k T_k \Gamma}{g_m} C^2_{PD} A^2 I_3 B^3 \tag{3.14}$$

$$\sigma_{shot} = 2qR_{PD}P_i B + 2qI_B I_2 B \tag{3.15}$$

Parameters of these equations are detailed as follow: q is the electronic charge, B is equivalent noise bandwidth of the electrical filter that follows the photo detector, I_B is background current, T_k is the absolute temperature, G_{ol} is the open-loop voltage gain, C_{PD} is the fixed capacitance of photo detector per unit area, Γ is the FET channel noise factor, g_m is the FET transconductance. The noise bandwidth factors I_2 and I_3 are $I_2 = 0.562.$ and $I_3 = 0.0868.$

The line of sight (LOS) channel gain component (H_{LOS}) of the VLC is link in Equation 3.12 graphically presented in Figure 3.10.

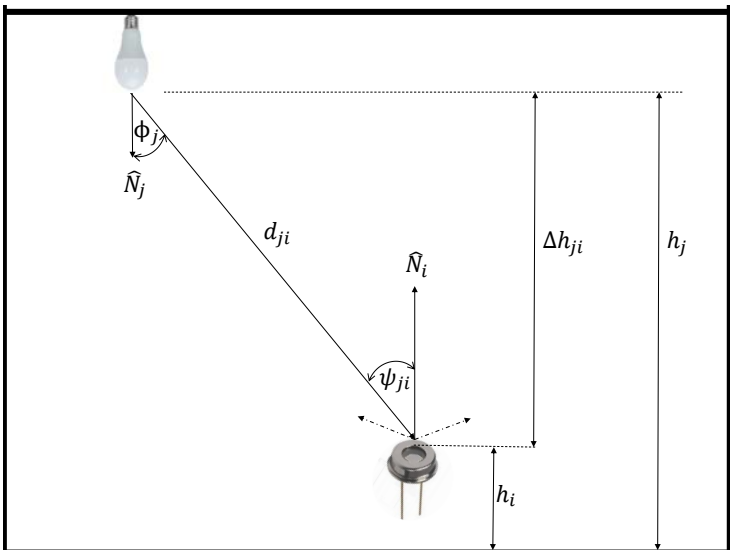

Figure 3.10: Line of sight (LOS) VLC link

As it can be seen, the LOS link depends on light sources and detector parameters explained earlier. The LOS channel gain of the optical wireless is formulated by merging Equation 3.8 at the transmitted side and Equations 3.10 and 3.11 as follows [KN04]

$$H_{ji} = \begin{cases} \frac{(m_l+1)A_{eff}}{2\pi d^2_{ji}} \cos^{m_l}(\phi_{ji}) G(\psi_{ji}) \cos(\psi_{ji}) & -\Psi_l/2 \leq \psi_{ji} \leq \Psi_l/2 \\ 0 & \text{elsewhere} \end{cases} \tag{3.16}$$

where m_l is the Lambertian order transmission of the LED light, A_{eff} is referred to the effective area of the PD, the distance between the transmitter j and receiver i is denoted as d_{ji}. Finally, ϕ_{ji} and ψ_{ji} are the angle of irradiance and the incidence angle correspondingly. The term $G(\psi_{ji}) = T_s(\psi_{ji})g(\psi_{ji})$ is the combined gain of the optical filter and the optical concentrator

respectively. The gain of the VLC channel is greater than zero if and only if the incidence angle of the signal ψ_{ji} is less or equal to the half field of view (FOV) angle of the optical receiver Ψ_l as described earlier.

When a tilt receiver is considered, PD normal vector $\hat{N}_i$ is not oriented vertically. Due to this, the incidence angle ψ_{ji} and irradiance angle φ_{ji} are not equal, as shown in Figure 3.11. In this figure, azimuthal rotation α_{PD} and horizontal tilting angle β_{PD} are displayed.

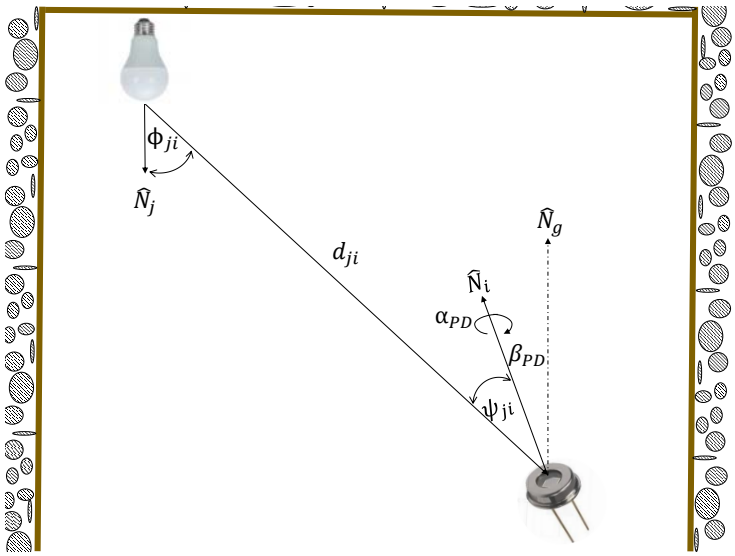

Figure 3.11: Visible light communications channel model with tilted and rotated receiver

When the tilting and rotation angles are considered, incidence angle ψ_{ji} is affected. Incidence angle depends on azimuthal rotation of the photodetector α_{PD} and horizontal PD tilt β_{PD}. Cosine of the incidence angle used in Equation (3.16) can be re-written as

$$\cos(\psi_{ji}) = \frac{\vec{v}_{PD2LED} \cdot \hat{N}_i}{\|\vec{v}_{PD2LED}\|_2 \left\|\hat{N}_i\right\|_2} \tag{3.17}$$

where $\vec{v}_{PD2LED}$ is the vector from PD to the LED source and $\hat{N}_i$ is the normal vector of the tilt receiver. Magnitude of the vectors are: $\|\vec{v}_{PD2LED}\|_2 = d_{ji}$ and $\left\|\hat{N}_i\right\|_2 = 1$. The normal vector of a PD which has been rotated and tilted in angles α and β respectively can be expressed as

$$\hat{N}_i = \frac{[\sin(\beta_{PD})\cos(\alpha_{PD}), \sin(\beta_{PD})\sin(\alpha_{PD}), \cos(\beta_{PD})]}{\|[\sin(\beta_{PD})\cos(\alpha_{PD}), \sin(\beta_{PD})\sin(\alpha_{PD}), \cos(\beta_{PD})]\|_2} \tag{3.18}$$

By replacing Equation 3.18 into Equation 3.17 we obtain the new formulation for the cosine of a tilted and rotated photodetector as follows

$$\cos(\psi_{ji}) = \frac{[x_{LED} - x_{PD}, y_{LED} - y_{PD}, \Delta h_{ji}] \cdot [\sin(\beta_{PD})\cos(\alpha_{PD}), \sin(\beta_{PD})\sin(\alpha_{PD}), \cos(\beta_{PD})]}{d_{ji}} \tag{3.19}$$

where $Z_{LED} - Z_{PD} = \Delta h_{ji}$ is the difference height between transmitter and receiver shown in Figure 3.10.

Similarly, due to the special conditions of underground mines, rotated and tilted LEDs must be considered. The graphical representation of a tilted transmitter is presented in Figure 3.12.

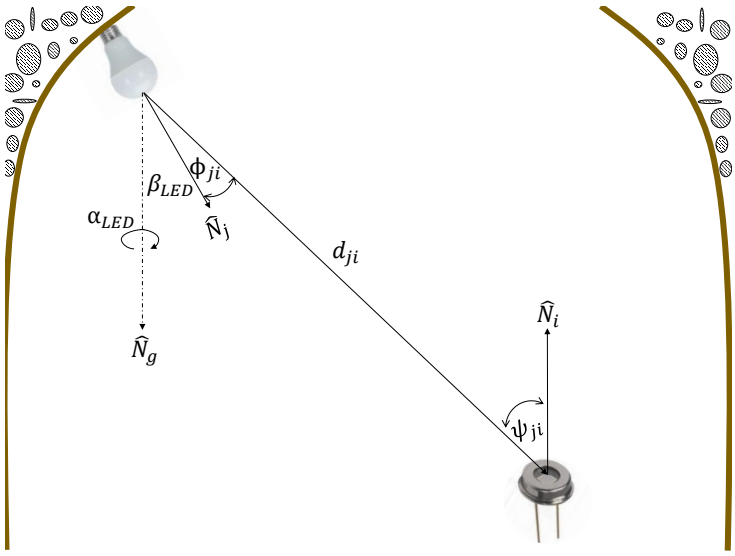

Figure 3.12: Visible light communications channel model with tilted and rotated transmitter

The tilting and rotation angles at the receiver side will affect the radiation angle ϕ_{ji} is affected. The new radiation angle depends now on azimuthal rotation of the LED light source α_{LED} and horizontal PD tilt β_{LED}. The cosine of the radiation angle used in Equation (3.16) can be re-written as

$$(\cos(\phi_{ji}))^{m_l} = \left(\frac{\vec{v}_{LED2PD} \cdot \hat{N}_j}{\|\vec{v}_{LED2PD}\|_2 \left\|\hat{N}_j\right\|_2} \right)^{m_l} \tag{3.20}$$

where $\vec{v}_{LED2PD}$ is the vector from LED source to PD and $\hat{N}_j$ is the normal vector of the tilted LED. Magnitude of the vectors are: $\|\vec{v}_{LED2PD}\|_2 = d_{ji}$ and $\left\|\hat{N}_j\right\|_2 = 1$. The normal vector of an LED that has been rotated and tilted in angles α_{LED} and β_{LED} respectively can be expressed as

$$\hat{N}_j = \frac{[\sin(\beta_{LED})\cos(\alpha_{LED}), \sin(\beta_{LED})\sin(\alpha_{LED}), -\cos(\beta_{LED})]}{\|[\sin(\beta_{LED})\cos(\alpha_{LED}), \sin(\beta_{LED})\sin(\alpha_{LED}), -\cos(\beta_{LED})]\|_2} \tag{3.21}$$

notice that, the Z-component of the LED normal vector ($\hat{N}_j$) is negative since the light source is pointing downwards as shown in Figure 3.12.

By replacing Equation 3.21 into Equation 3.20 we obtain the new formulation for the cosine of a tilted and rotated light source as follows

$$\cos(\phi_{ji}) = \frac{[x_{PD} - x_{LED}, y_{PD} - y_{LED}, -\Delta h_{ji}] \cdot [\sin(\beta_{LED})\cos(\alpha_{LED}), \sin(\beta_{LED})\sin(\alpha_{LED}), -\cos(\beta_{LED})]}{d_{ji}} \tag{3.22}$$

Finally, in order to measure the effect of tilted transmitters and receivers Equations 3.19 and 3.22 should be replaced into Equation 3.16.

The non-LOs component of Equation 3.12, h_{n-LOS} caused by the reflection of the light.

In general, reflection of light in a surface can be one of two types, i.e., *specular* or *diffuse*. In specular reflection, the angle at which the light-wave is reflected is equal to the angle of incidence to that surface as shown in Figure 3.13. On the other hand, in diffuse reflections, light reflecting from the surface is scattered at many angles rather than at just one angle. This, due to multiple reflections by the microscopic irregularities inside the material.

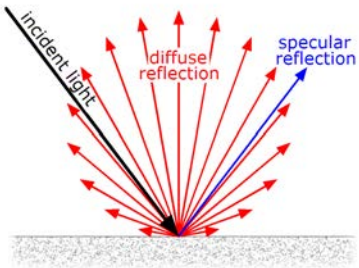

Figure 3.13: Diffuse and specular reflection from a glossy surface (Image retrieved from Juds et.al. (1988) [Jud88])

One common model for diffuse reflection is Lambertian reflectance, in which the light is reflected with equal radiance in all directions

In [GB79b] power distribution model for a diffuse optical wireless link is presented. This model is based on a single reflection. The channel impulse response is calculated by integrating the power of all the components arriving at the receiver after being reflected in a surface as shown in Figure 3.14.

The following recursive methods is used in order to evaluate diffuse reflections within an indoor environment. First, surfaces of the room are divided into K small reflecting elements with an area A_m. Then, channel response is calculated by a two steps method as follows: i) each element of the surface with area of A_m is considered as a receiver, and ii) each element is then considered as a point Lambertian source that re-emits the light scaled by reflectivity ρ_m.

Given a particular single source j and a single receiver in a square in a room, the impulse response can be written as an infinite sum of reflections. The n-LOS channel impulse response is evaluated using a recursive algorithm (shown in Equation 3.23) [LVd00]

$$H_{n-LOS} = \frac{(m_l+1)A}{2\pi} \sum_{m=1}^{K} \frac{\Delta A_m \rho_m}{d_{jm}^2 d_{mi}^2} cos^{m_l}(\phi_{jm}) \cos(\psi_{jm}) \cos(\phi_{mi}) \cos(\psi_{mi}) G(\psi_{mi}) \delta\Big(t - \frac{d_{jm}+d_{mi}}{c}\Big) \tag{3.23}$$

where ΔA_m is the area of the considered reflecting element, K is the total number of reflective elements considered in the algorithm, ρ_m is the reflecting coefficient of the surface area ΔA_m, d_{jm} is the distance between the source and the reflective element as shown in Figure3.14. Since $||H_{n-LOS}^{(k)}|| \to 0$ when $k \to \infty$ the channel impulse response can be modelled using only the first reflection. The first reflection is the most important component since it limits the data rate in LOS transmissions.

Usually, in traditional indoor environments, i.e., offices, commercial centres, hospitals, etc., walls are consider perpendicular to the ceiling as shown in Figure 3.14. Nevertheless, this as-

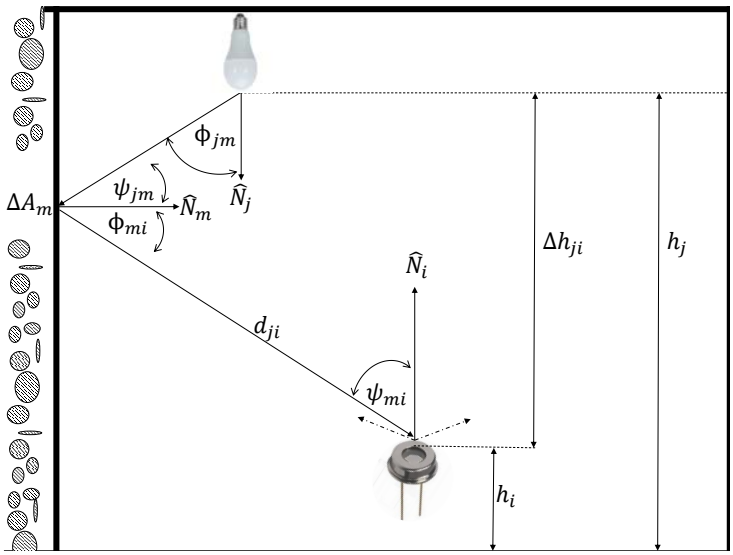

Figure 3.14: non-Line of sight (n-LOS) VLC link

sumptions is not valid for underground mines since most of then are U-shaped as shown in Figure 3.4. Moreover, in these traditional environments, plane walls as depicted in Figure 3.15 (a) are considered. However, walls in underground mines are not plane. Due to this, each surface area of reflection A_m has a different normal vector as shown in Figure 3.15 (b).

As mentioned before, reflections are considered as point Lambertian sources. The radiation intensity of these "sources" depends on the normal vector $\hat{N}_m$ as displayed in Figure 3.14.

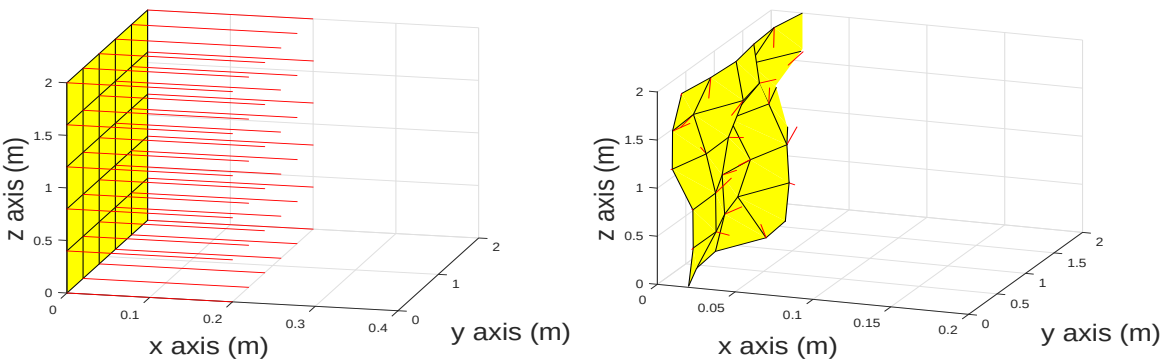

(a) (b)

Figure 3.15: Walls geometry (a) traditional plane wall and (b) underground mine wall with randomly oriented surface

Due to this, reflections inside underground mines are different from reflections studied in traditional environments and, as a consequence, the channel capacity will differ. In this thesis we do not study the channel capacity of underground mine VLC channel since we focused in underground mine positioning based on VLC. Nonetheless, the fact that reflection components of the channel inside mines differ from traditionally studied environments is a fact that can be considered for further research.

The mathematical analysis for specular reflection in non-plane surfaces is similar to the one

done for tilted/rotated transmitters and receivers. The rotated and tilted normal vector of the reflecting surface will affect the incidence angle from LED to surface, ϕ_{jm}, and the irradiance angle from the surface to the PD, ψ_{mj}, of Equation 3.23. The normal vector of a rotated and tilted surface is given by

$$\hat{N}_m = [\cos(\alpha_m)\cos(\beta_m), \sin(\alpha_m)\cos(\beta_m), \sin(\beta_m)] \tag{3.24}$$

where α_m and β_m are the rotation and tilted angles of the non-plane and non-parallel mining wall respectively.

Finally, as mentioned before, underground mines have two other particular characteristics that may affect the VLC communication link and must be modelled. These are: signal scattering produced by dust due to normal mining operation and shadowing due to infrastructure and mobile vehicles.

Shadowing and objects' presence is often analysed in traditional VLC channel modelling for indoor environments. The effect of furnitures and body induced signal blockage are mostly studied [CZHG15, MU15, BCS+17, JK04, WAKZ+18]. In Figure 3.16 signal blockage due to shadowing caused by an underground mine vehicle is depicted.

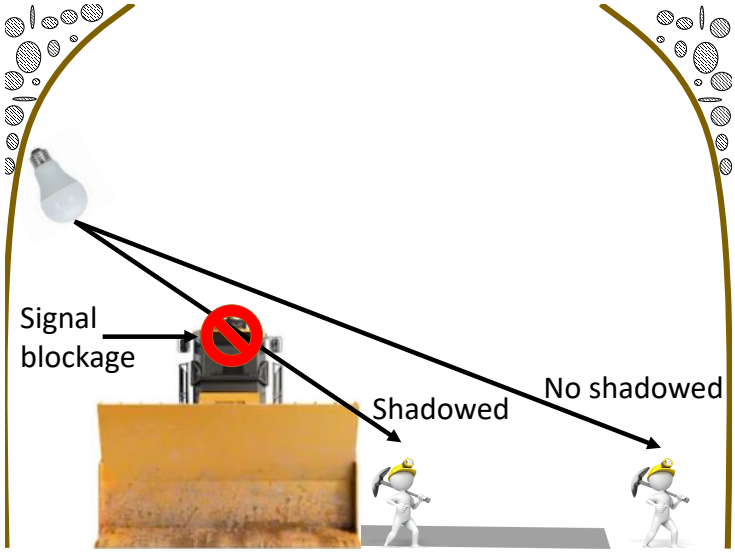

Figure 3.16: Signal blockage due to shadowing in underground mines

As it can be seen, for our link we consider helmet-mounted PD. Due to this, the effect of body induced signal blockage is neglected. In general, using this configuration, we must only take into account blockage caused by mobile vehicles inside the mine and deployed machinery infrastructure. Shadowing effect for VLC has been previously modelled by a Bimodal Gaussian distribution [WAKZ+18, WWC+17, WAKS+17] with the following probability density function (PDF).

$$f(z, \mu_0, \sigma_0, \mu_1, \sigma_1) = \frac{1}{2\sqrt{2\pi(\sigma_0^2)}} e^{\frac{-(z-\mu_0)}{2(\sigma_0^2)}} + \frac{1}{2\sqrt{2\pi(\sigma_1^2)}} e^{\frac{-(z-\mu_1)}{2(\sigma_1^2)}} \tag{3.25}$$

where μ_0, μ_1, σ_0, σ_1 are the mean and standard deviation values of the first and second Gaussian distributions respectively. Optical diffraction phenomenon is used in this type of systems to overcome shadowing effect on the VLC link. This is done by using a wide angle field of view (FOV) receiver.

On the other hand, scattering produced by dust in suspension is not often considered in traditional indoor environments since it is not applicable for nowadays VLC applications in offices, supermarkets, hospitals and non-hazardous industries. As for underground mines, dust is produced by the rock's crushing, grinding, blasting, and drilling inside the mine and must be taken into account.

Dust particles effects on VLC link have been mostly analysed in free space optical (FSO) links[EFA16, MPS19, AA14, MMJ18]. In this type of links, the atmospheric attenuation is given by the Beer's law equation [14]:

$$\frac{P_r}{P_t} = \tau = e^{-\beta_{abs}\beta_{scat}d_{ji}} \tag{3.26}$$

where d_{ji} is the distance between transmitter and receiver, β_{abs} is the molecular and aerosol absorption, and β_{scat} is the aerosol and molecular scattering. The attenuation due to absorption can be neglected in most of the cases (β_{abs} =1). Due to this, scattering produced by suspended molecules and particles (also known as aerosols) is often considered as the most important parameter to being model.

Aerosols can have a wide range of shapes, size and nature. Moreover, they can vary in distribution, concentration and constituents. Due to this, its interaction with the light beam can have a large dynamic. In general, the sizes of aerosol particles are comparable to the wavelength of interest in optical communications. Due to this, Mie scattering theory is used to describe the effect of aerosol particles with radius between 0.01–1 μm [AA14, GPR12].

Scattering is defined as *"the dispersal of a beam of radiation into a range of directions as a result of physical interactions"* [AA14]. When a aerosol particle intercepts an light wave, part of its energy is removed by the particle and re-radiated into a solid angle centred at the particle. The scattered light is polarized, and of the same wavelength as the incident wavelength, which means that there is no loss of energy to the particle.

There are three main types of scattering shown in Figure 3.17, i.e., Rayleigh, Mie, and non-selective scattering.

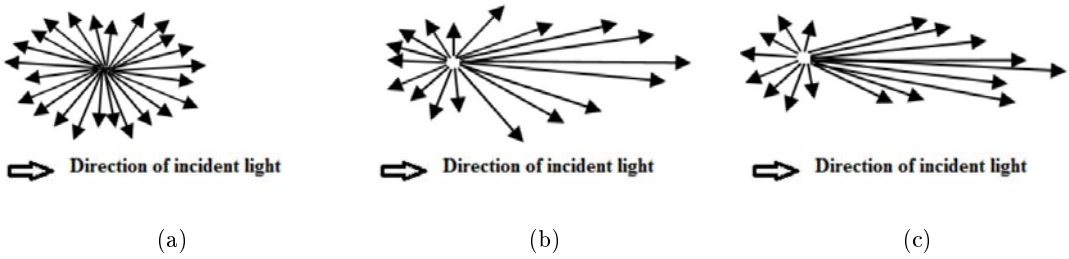

Figure 3.17: Scattering patterns (a) Rayleigh, (b) Mie, and (c) Non-selective scattering

Generally, aerosol and molecular scattering is modelled as follows

$$\beta_{scat} = \beta_R + \beta_M \tag{3.27}$$

where β_R and β_M are Rayleigh and Mie scattering contribution respectively. At terrestrial altitude, Rayleigh scattering can be neglected. Due to this, the total scattering is modelled as $\beta_{scat} = \beta_M$.

The attenuation due to Mie scattering is expressed by the Mie scattering coefficient as follows

$$\beta_M = \left(\frac{3.91}{V}\right)\left(\frac{0.55\mu}{\lambda}\right)^i \tag{3.28}$$

where V is the visibility range in Kilometres, λ is the light wavelength, and i is the size distribution of the scattering particles typically varying between 0.7 to 1.6 corresponding to visibility conditions.

$$\begin{aligned} i &= 1.6 \text{ for } V > 50 \text{ Km} \\ i &= 1.3 \text{ for } 6 \text{ Km} \leq V \leq 50 \text{ Km} \\ i &= 0.585V^{1/3} \text{ for } V < 6 \text{ Km} \end{aligned} \tag{3.29}$$

3.4 Conclusions

In this section an analysis of underground mine channel model has been delivered. Underground mines channel model for light propagation is not similar to traditional indoor model environment due to the special characteristics found in this scenario. In particular, three major factors make this channel model more unique. These characteristics are: randomly oriented LED lights, non-plane walls and the presence of aerosol particles which may produce mie scattering. These characteristics will affect the light propagation as shown in Table 3.4.

Table 3.4: Effect of special underground tunnel characteristics in VLC channel model

Characteristic	**Randomly oriented LEDs**	**Non-plane walls**	**Aerosol particles**
Effect on VLC channel	Channel gain of LOS-link	Multipath	Scattering

In order to evaluate the robustness of a localization method, the effect of above mentioned characteristics on method's performance must be evaluated. Thus, throughout this thesis, specifically in Chapter 6, an evaluation of the impact underground mine's channel model in position estimation will be delivered. Moreover, a novel localization methods robust to the above mentioned effects will be designed.

Chapter 4

Visible light positioning methods

Sommaire

4.1 Introduction **53**

4.2 Main characteristics of VLP for their underground mine application **54**

4.2.1 Characteristics based on detector technology 54

4.2.2 VLC characteristics for different positioning topologies implementation . 55

4.3 Visible light positioning methods classification **56**

4.3.1 Range based methods 56

4.3.2 Range free methods 64

4.3.3 Fingerprinting (FP) 66

4.4 Robustness and characteristics analysis of VLP methods **67**

4.1 Introduction

In the recent years, visible light communications (VLC) has gained attention of researchers due to its capability to provide high data rate wireless communication [PFHM15] and high accuracy positioning in indoor environments [DY16]. Moreover, VLC is a cost effective solution since it uses the already deployed lighting infrastructure to provide both, illumination and wireless communication.

The advantages of using VLC to provide indoor position systems have encouraged the researchers to propose numerous solutions. Some of the most important advantages are displayed in Figure 4.1. In particular, it is important for the development of our proposal to notice that VLP positioning systems are **immune to interference**. As mentioned in Section 2.3.7, this thesis search for a positioning system robust to interference.

Different VLP methods have been introduced in literature. Most of them have been adapted from existing methods in RF networks. In this section the main characteristics of different VLP methods are delivered. First, the main capabilities of VLC to provide positioning in underground tunnels are analysed. Then, main VLP methods are classified and explained in detail. Finally, the most suitable positioning method for underground mine tunnels is proposed.

4.2 Main characteristics of VLP for their underground mine application

As it was described in previous sections, there are many different requirements that must be fulfilled when designing a positioning system. In this section, the usage of VLP methods in underground mines is analysed. In order to do this, capabilities of VLC based positioning methods are analysed. First, characteristics of VLP based on the detector technology used to retrieve the communication signal are analysed. Finally, different possible positioning topologies are delivered in order to proposed the most suitable one to underground mine application.

4.2.1 Characteristics based on detector technology

Visible light positioning (VLP) systems can be classified in two different groups based on the receiver hardware used for signal detection, i.e, image sensor (IS) based positioning systems and, photo detector (PD) based positioning systems [HY16].

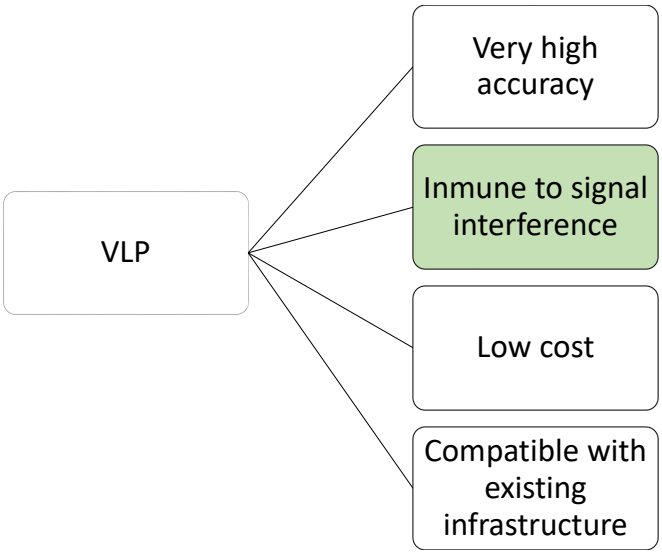

Figure 4.1: Advantages of indoor VLP systems

Image sensors provide more useful information related to the LED position than PD counterpart. In addition to this, different light sources can be directly separated from the image and no multiplexing technique is required [DY16]. Most of the off-the-shelf devices have already incorporated cameras, making IS-based positioning easy to implement and inexpensive [ZHQ+18, KZKP15]. The main disadvantage of this type of systems is that IS-based VLC networks have a very limited data rate. Due to this, IS-based networks are not expected to be massively implemented for future wireless networks since they are supposed to deliver high data rates [DY16].

On the other hand, PD-based VLC systems can provide high data rate communication [HY16, HLC+15]. Moreover, PDs are inexpensive and easy to install. In order to separate the signal from multiple sources, the usage of multiplexing techniques is required. Depending on the multiplexing technique used to separate the sources, the required hardware for the system can increase in complexity and affect the performance of the positioning method [YNA+17, HNP+15].

Table 4.1: Comparison of VLP based on receiver characteristics

Receiver type	Advantage	Disadvantage
Photodetector	Requires less complex analysis High data rate Energy-efficient	Requires multiplexing
Image sensor	Suitable for angle of arrival based positioning Minimally affected by multipath	Limited data rate High power consumption

The main advantages and disadvantages of VLP systems based on PD and IS are summarized in Table 4.1.

4.2.2 VLC characteristics for different positioning topologies implementation

The architecture of the deployed network has an important effect on the performance of localization algorithm. Localization can be arranged in three different topologies [DMS98] depending on where the localization is performed and the communication direction. These categories were presented in Section 2.4.2.

Table 4.2: Topologies and technologies for VLP in underground mines

Topology	Link Requirements	Technology	Issues
Remote Positioning	Uplink	RF or IR	VLC is not used in uplink due to low coverage compared to RF and IR solutions
Self Positioning	Downlink	VLC	No positioning information in central monitoring station overground
Indirect	Uplink and Downlink	VLC for downlink and RF or IR for uplink	Full duplex communication is required

Personnel's position inside the tunnel must be available in the control site overground. Due to this, **remote positioning** or **indirect remote-positioning** topologies are preferred. To perform direct/indirect remote positioning, uplink communication is required since mobile node must send information overground. In literature, uplink has been mainly provided by infrared (IR) or radio frequency (RF) in VLC systems [PJRQ+11, PFHM15, KZKP15].

Since VLC has been proposed mainly as downlink technology [ZWW+15, CBH16] only self-positioning or indirect remote-positioning are feasible alternatives. As mentioned above, position information must be available overground. Due to this, indirect remote-positioning is the suitable positioning topology in underground mines. In table 4.2 a summary of link requirements and main issues for implementing VLP in underground tunnels are shown.

As it can be seen in Table 4.2 two main technologies are proposed for uplink, these are, IR and RF. Taking into account particular characteristics of underground mines, RF technologies seems to be the most suitable to provide uplink due to its long range of coverage. As it was shown in Chapter 2, different RF technologies have been proposed to solve the positioning problem in underground mines. Each one of these technologies work in a particular band of the EM spectrum. In literature, different studies of RF link propagation in underground tunnels have

been carried out recently in order to determine the most suitable band for telecommunications applications.

There exist a bunch of literature about wireless communications and propagation modelling in underground mines. In particular Forooshani et al. [FBMN13] provides a deep survey for RF propagation in this scenario. Signal propagation is usually affected by several parameters such as operating frequency, mine tunnel size, and transmitter-receiver position. In this thesis we do not study the effect of this parameters for uplink propagation. Nevertheless our choices are supported by extensive literature that can be found throughout this thesis. In particular the following section the most proper frequency and configuration for underground application will be selected.

4.3 Visible light positioning methods classification

VLP methods can be classified in tree types [AJ19]. This classification is based on whether they require a distance (range) estimation or some other signal information to compute mobile node's position [Mau12].

In general, three main positioning approaches are used for VLP systems : (1) range-based methods, (2) range-free methods, and (3) fingerprinting.

Range based, range free and fingerprinting process diagrams are presented in Figure 4.2

As it can be seen, distance measurement dependent (range based) and fingerprinting methods require more information to estimate the position of mobile node than distance measurement independent methods (range free).

In this section the three types of visible light positioning methods will be analysed using the taxonomy presented in Figure 4.3. Each algorithm will be explained and the main pros and cons of their implementation in underground mines' VLP systems will be presented.

4.3.1 Range based methods

Range based algorithms determine the mobile node position by using a distance estimation. The three main range based methods are lateration, hyperbolic lateration and angulation. The before mentioned methods require a distance estimation to perform localization. This estimation is derived from signal characteristics, such as, received signal strength, time of propagation, and received phase/angle. Receiver signal strength (RSS) based ranging is the simplest method to derive distance estimation. RSS measurements are relatively easy to obtain and, most of the devices are built with the required hardware to measure received signal power level in dBm or a received signal strength indicator (RSSI). In order to estimate the distance from RSS measurements, a precise model of signal propagation is required. Due to this, model precision has high impact in algorithm performance. On the other hand, despite provide a more precise distance estimation than RSS methods, time of propagation and received phase/angle measurements have several drawbacks on their hardware implementation. Time of propagation measurement can be divided in time of arrival (TOA) and time difference of arrival (TDOA) methods. TOA measurements require precise synchronization of transmitters and receivers which is very difficult to provide. On the other hand, TDOA and phase/angle measurements require synchronization at the receiver side to estimate the range. In addition to this, to perceive the difference in time of arrival, receivers must be equipped with a high sampling frequency device. This, due to the high speed of optical signals.

Once range measurements are performed, range based methods estimate the position of the mobile node by trilateration/multilateration/angulation algorithms. For doing this, informa-

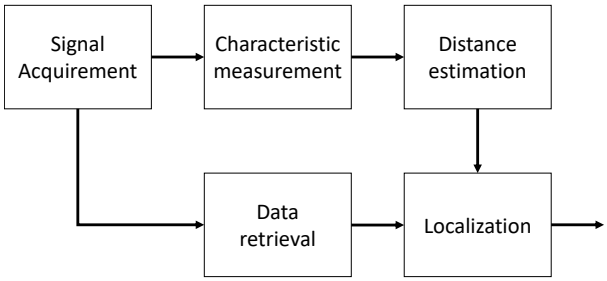

(a)

(b)

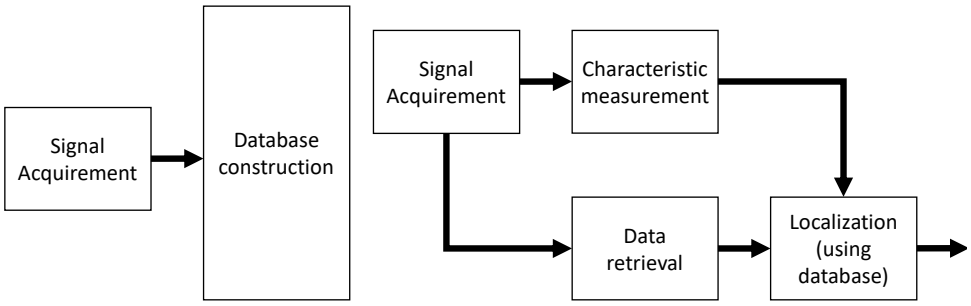

(c)

Figure 4.2: Positioning method process diagram for (a) range based methods, (b) range free methods and, (c) fingerprinting

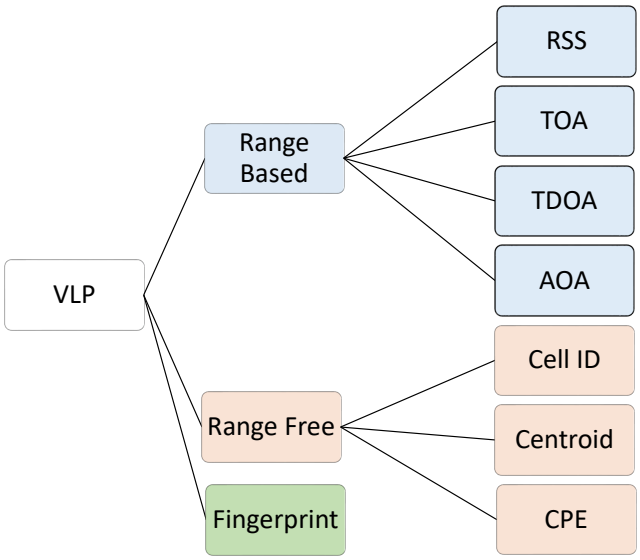

Figure 4.3: Visible light positioning system topology classification

tion of multiple anchor nodes (position-aware transmitters) is required. This, imposes another drawback on the implementation of type of algorithms.

Range based methods have been extensively studied in literature for VLP. A few number of surveys have been published and the performance in terms of accuracy has been analysed for the most significant methods [DY16, ZHQ+18, HCWZ15, HNP+15, KZKP15, YZXZ15, ASN13]. In this thesis we do not provide an in depth survey on VLP systems. For a complete analysis on VLP technology you may refer to the before mentioned surveys that have been published recently. In this section, main methods will be delivered and analysed in terms of their robustness and hardware requirements.

Received signal strength (RSS)

RSS measurements provide range information between two nodes based on path loss (PL) channel characteristics. If the relation between distance and power loss is known, then, RSS can be used to estimate the distance between receiver and transmitter, i.e., $d_{ji} = f(P_r)$. For doing that, transmit power is assumed to be known.

Due to the presence of noise, non-LOS effects and quantification errors in distance versus path loss relation, ranging estimates are subject to errors. Hence, in reality, each RSS measurement defines an uncertainty area, such as the one depicted in Figure 4.4 using a dashed line.

Ideally, taking the average RSS over a sufficiently long time interval would exclude the effects of multipath fading and shadowing.

As described in Section 3.2.2, the received power from the jth light source at the ith PD is expressed as

$$P_j i = R_{PD} P_j(H_{LOS}) + N_t otal \tag{4.1}$$

where P_j is the source power, N_{total} is the total noise that consider the contribution of thermal noise, shot noise and multipath reflections, and H_{LOS} is the channel log gain described

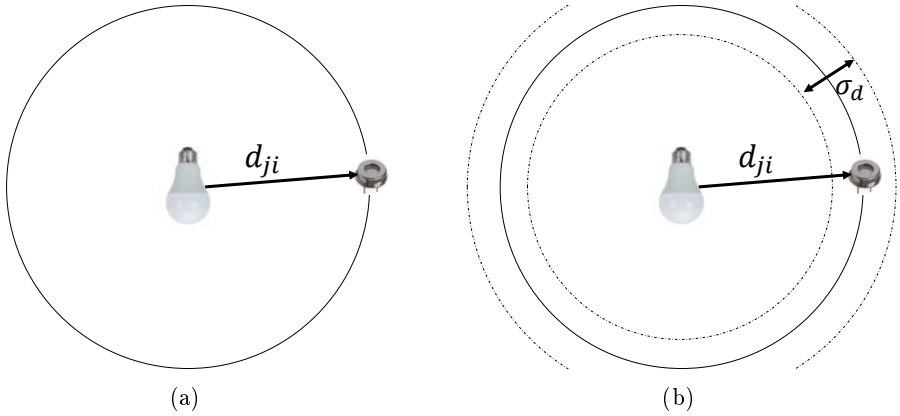

Figure 4.4: Ranging information from RSS measurements (a) ideal ranging and (b) ranging estimation with uncertainty σ_d

in Equation 3.16. In Figure 4.5, received power versus distance plot for a LED light model Cree XLamp CXB1512 is shown.

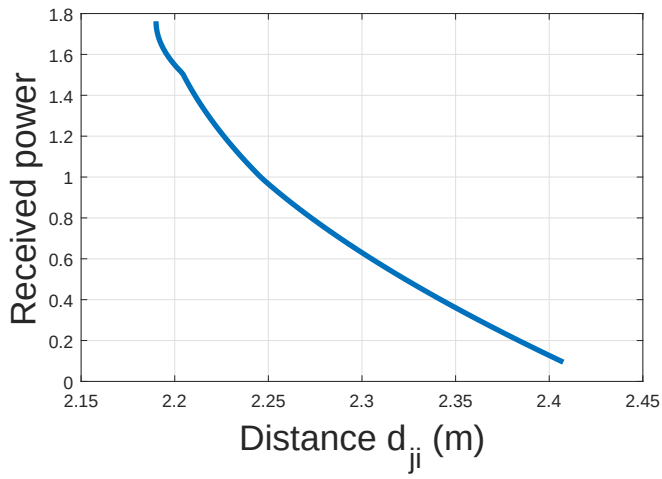

Figure 4.5: Power versus distance measurements of ED light Cree XLamp CXB1512

In this figure mean RSS value from 100 samples is taken instead instantaneous RSS value. As it can be seen, there exist a non-linear relation between the received power by the PD, and the distance between transmitter and receiver.

Notice that, the received power depends also on the signal's received angle (Equation 3.16). In order to solve this problem, a scaling factor RSS method was proposed in [KKY+13] when no other devices such as gyroscopes or accelerometers are incorporated at the receiver. Some other methods use PD arrays [SES13] and cross correlation function between transmitter and receiver [LYC+14] in order to deal with angle diversity at receiver's side. In general, RSS based method increases its accuracy when a large number of LEDs are perceived [NJM13], multipath effects are neglected and non-tilt receivers are considered.

In order to obtain a unique position estimation we require several estimated ranges. For example, in order to obtain an unique estimate for 2-D positioning, at least three range mea-

surements must be done as shown in Figure 4.6.

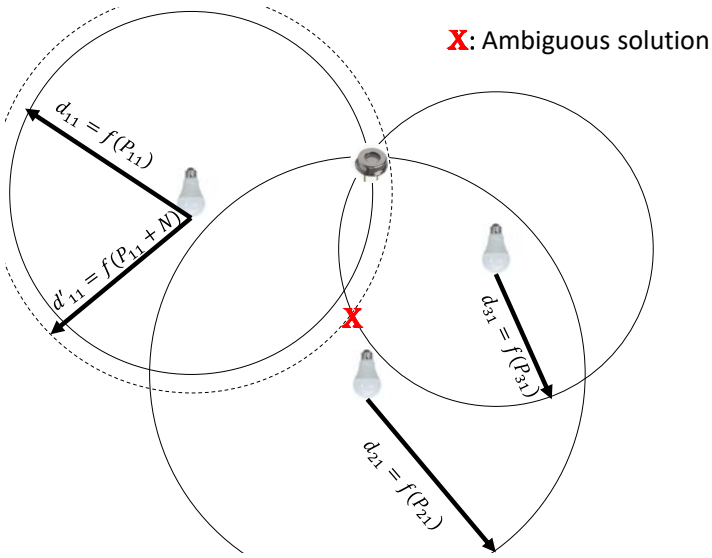

Figure 4.6: Lateration method in two dimensions based on RSS ranging

As it can be seen, distance estimations are done using the received signal strength. Ambiguous solutions are discarded by receiving at least three LED lights at the mobile node.

In order to determine the mobile node's position from RSS values, distance estimates form a system of M non-linear equation as follows

$$\begin{aligned} f(P_{11}) = d_{11} &= \sqrt{(\hat{x}-x_1)^2 + (\hat{y}-y_1)^2 + (\hat{z}-z_1)^2} \\ f(P_{21}) = d_{21} &= \sqrt{(\hat{x}-x_2)^2 + (\hat{y}-y_2)^2 + (\hat{z}-z_2)^2} \\ f(P_{31}) = d_{31} &= \sqrt{(\hat{x}-x_3)^2 + (\hat{y}-y_3)^2 + (\hat{z}-z_3)^2} \\ &\dots \\ f(P_{M1}) = d_{M1} &= \sqrt{(\hat{x}-x_M)^2 + (\hat{y}-y_M)^2 + (\hat{z}-z_M)^2} \end{aligned} \tag{4.2}$$

where (x_j, y_j, z_j) denotes the position of the LED lights. The unknown values of this equations system are the components of the mobile node's position $(\hat{x}, \hat{y}, \hat{z})$.

This method is called Lateration. In order to solve this non-linear equations system, a traditional non-linear least square optimization problem is proposed.

$$\begin{aligned} \underset{(\hat{x},\hat{y},\hat{z})}{\text{minimize}} \quad & \sum_{j=1}^{M} \left(d_{ji} - \sqrt{(\hat{x}-x_j)^2 + (\hat{y}-y_j)^2 + (\hat{z}-z_j)^2} \right)^2 \\ \text{subject to} \quad & (\hat{x}, \hat{y}, \hat{z}) \succeq 0 \end{aligned} \tag{4.3}$$

Time of arrival (TOA)

TOA calculates the distances between LED lights and mobile node by directly multiplying the propagation delay of the signal by the speed of light as follows

$$d_{ji} = c|(T_j - T_i)| = c\Delta T_{ji} \tag{4.4}$$

where T_j is the starting time of the transmission, T_i is the reception time, and c is the speed of light.

In Figure 4.7 ranging estimations from three independent sources are shown. This system also assumes direct LOS communication and, unlike RSS based methods, it does not suffer detrimental effect when tilt receivers are considered.

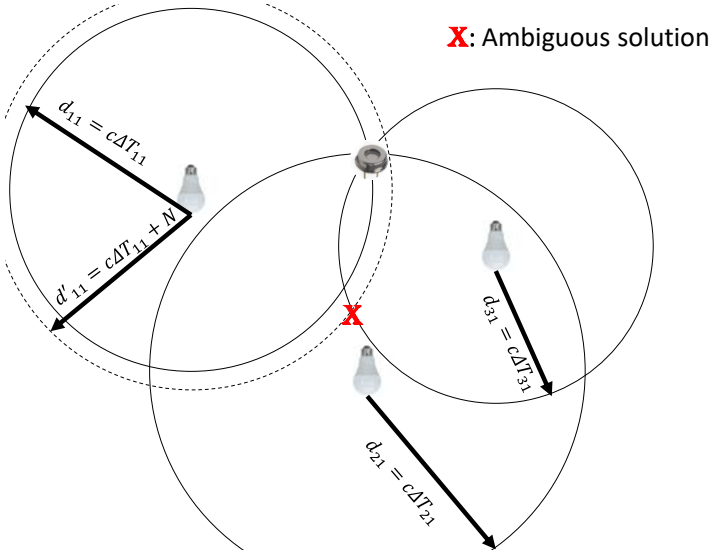

Figure 4.7: Lateration method in two dimensions based on TOA ranging

Similarly to RSS based positioning estimation, distance estimates form a system of M non-linear equation as follows

$$\begin{aligned} c\Delta T_{11} = d_{11} &= \sqrt{(\hat{x}-x_1)^2 + (\hat{y}-y_1)^2 + (\hat{z}-z_1)^2} \\ c\Delta T_{21} = d_{21} &= \sqrt{(\hat{x}-x_2)^2 + (\hat{y}-y_2)^2 + (\hat{z}-z_2)^2} \\ c\Delta T_{31} = d_{31} &= \sqrt{(\hat{x}-x_3)^2 + (\hat{y}-y_3)^2 + (\hat{z}-z_3)^2} \\ &\dots \\ c\Delta T_{M1} = d_{M1} &= \sqrt{(\hat{x}-x_M)^2 + (\hat{y}-y_M)^2 + (\hat{z}-z_M)^2} \end{aligned} \tag{4.5}$$

This non-linear system is solves by using the optimization problem of Equation 4.3.

In practical systems, measurement of distances based on signal propagation delay are noisy. Therefore, ranging uncertainty shown in Figure 4.4 (b) affects the distance estimation. In addition to time delay measurements uncertainty, the hardware implementation of TOA methods has another important drawback. In order to obtain the signal propagation delay ΔT_{ji}, the time bases in all light sources and mobiles nodes must be the same. This particular requirement is hard to achieve. Synchronization of time base will require network effort and highly stable clocks in both, transmitters and receivers.

Another option to solve this problem is measuring the asynchronism between transmitter and receiver to compensate the deviation in propagation delay estimation. However, there exist the problem of different time bases between transmitter and receivers which is not solve since mobile devices use low cost hardware components and they provide reasonable short-term stability only [SDM14].

Time difference of arrival(TDOA)

TDOA method uses the difference on arrival time of signals transmitted by fixed lights to a mobile node, or by measuring a single/multiple sources in a multiple PD array at receiver side. If the distance between transmitters is known, then, the ranging between each transmitter and receiver can be obtained and, subsequently, position of mobile node. Some methods assume a single PD receiver who measures the difference on arrival time from multiple light sources with known positions. In order to differentiate the signals, time division multiplexing (TDM) or frequency division multiplexing (FDM) techniques are used.

TDOA procedure can be summarized as follow: Signals from three LEDs, j, k and l, are transmitted synchronously at time instance T_0. At the ith receiver, these three light signals arrive at the time T_j, T_k and T_l respectively. The propagation distance difference is calculated from the propagation delays as follows.

$$\Delta d_{jl} = d_{ji} - d_{li} = c(T_j - T_l) = c\Delta T_{jl} \Delta d_{kl} = d_{ki} - d_{li} = c(T_l - T_l) = c\Delta T_{ll} \tag{4.6}$$

As it can be seen from Equation 4.6, the propagation distance difference depends on the signal propagation delay difference. By working with time of arrival differences from multiple sources, initial reference time unknown time T_0 is not required to be known at receiver side. Nevertheless, synchronization at transmitter side is required. Furthermore, there are no problems due to different time scales at anchor and mobile nodes since time instances, T_j, T_k and T_l, are measured at the mobile node.

In contrast to TOA and RSS based ranging methods, where the propagation delay defines circles around a LED light, the signal propagation delay difference measurement generates points of equal distance differences to the LED. This, defines a hyperbola in the two-dimensional case or a hyperboloid for the three-dimensional space [SDM14].

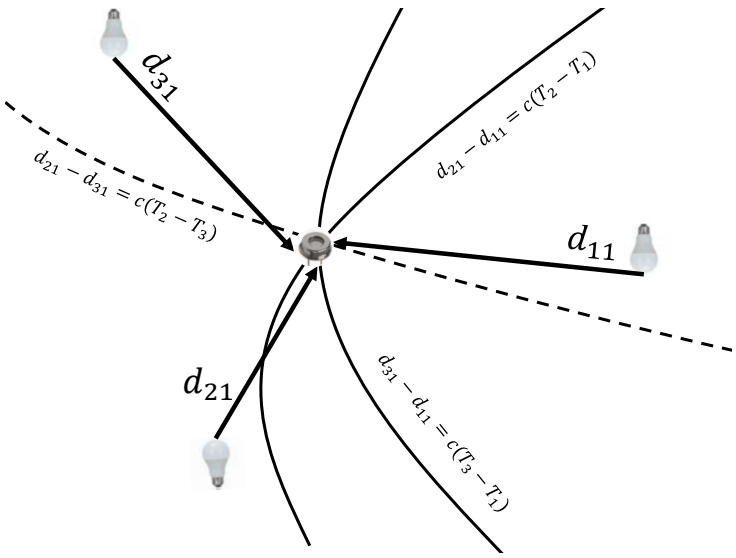

Figure 4.8: Hyperbolic lateration method in two dimensions based on TDOA ranging

The intersection between at least two hyperbolae, formed by three LED lights, provides an unique position estimation as shown in Figure 4.8. A further third hyperbola (dashed line) is constructed by subtracting the first two distance difference $d_{21} - d_{31} = d23$. Due to this, by

receiving information from M sources, we can form estimate the mobile node's position by solving the system of $M-1$ independent non-linear equations as follows

$$\begin{aligned} d_{21} - d_{11} &= \sqrt{(\hat{x}-x_2)^2 + (\hat{y}-y_2)^2 + (\hat{z}-z_2)^2} - \sqrt{(\hat{x}-x_1)^2 + (\hat{y}-y_1)^2 + (\hat{z}-z_1)^2} \\ d_{31} - d_{11} &= \sqrt{(\hat{x}-x_3)^2 + (\hat{y}-y_3)^2 + (\hat{z}-z_3)^2} - \sqrt{(\hat{x}-x_1)^2 + (\hat{y}-y_1)^2 + (\hat{z}-z_1)^2} \\ &\dots \\ d_{M-1} - d_{11} &= \sqrt{(\hat{x}-x_{M-1})^2 + (\hat{y}-y_{M-1})^2 + (\hat{z}-z_{M-1})^2} - \sqrt{(\hat{x}-x_1)^2 + (\hat{y}-y_1)^2 + (\hat{z}-z_1)^2} \end{aligned} \tag{4.7}$$

Angle of arrival (AOA)

For using AOA method the angle in which different optical signals arrive to a single PD receiver has to be measured or, alternatively, the angle of arrival of a single or multiple sources to a multiple PD array. For doing this, LOS link is considered as de-facto system configuration in VLC. Positioning using AOA can be obtained by using a minimum of 2 LED lights for 2-D localization unlike above mentioned methods where at least 3 sources are required. The difference on the AOA can be inferred from the difference of the received power from multiple sources in a single PD or by using a PD array.

In Figure 4.9 angle of arrival for downlink in two dimensions is shown.

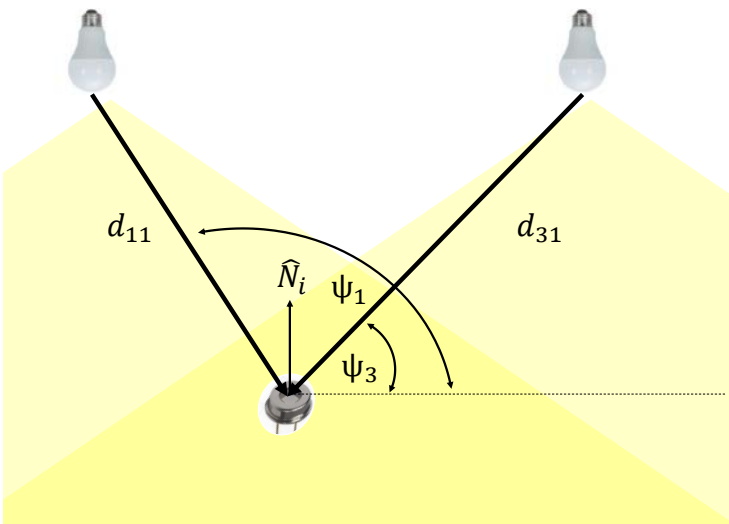

Figure 4.9: Angle of arrival based positioning method in two dimensions

As it can be seen from this figure, the angle in which the light signal arrives to the mobile node is strongly related with the distances between LED transmitters and PD receiver as follows

$$\begin{aligned} \hat{y} - y_1 &= \tan(\psi_1)(\hat{x} - x_1) \\ \hat{y} - y_2 &= \tan(\psi_2)(\hat{x} - x_2) \end{aligned} \tag{4.8}$$

By solving this linear equation system we find the intersection of two lines which provides the estimated mobile node's position.

Besides considering LOS link, some applications assumes that the transmitter and receiver are parallel, thus, incidence angles and irradiance angles are equal. Other sensors such as accelerometers can be used to compensate the effect of tilt receivers in combination with multiple PD array [YHV16]. Nevertheless, using these sensors at the receiver side will reduce the battery lifetime in mobile devices. In addition to this, AOA methods suffer high detrimental effect when non-LOS link and reflections are considered.

Another approach used to deal with tilted receivers (or unknown receiver orientation) in AOA based positioning systems is using the AOA difference $\Delta\psi_{21} = \psi_2 - \psi_1$, which is independent from the unknown orientation β_{PD} shown in Figure 4.10.

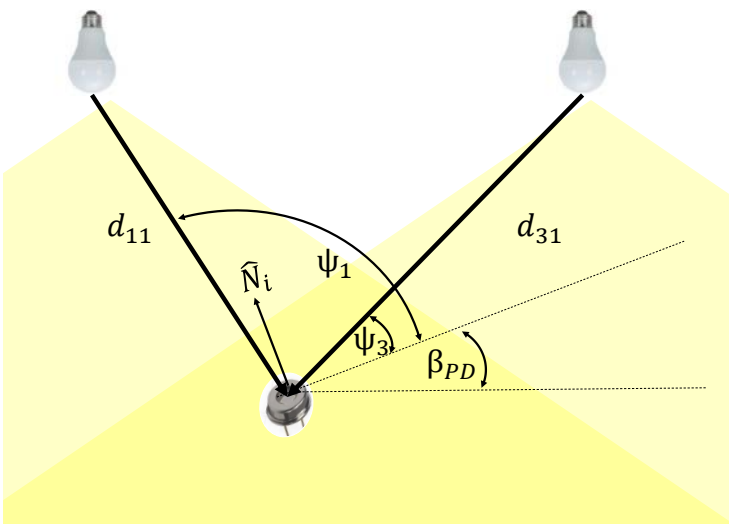

Figure 4.10: Angle of arrival based positioning method in two dimensions with unknown receiver orientation

According to the inscribed angle theorem, the angle $\Delta\psi_{21}$ and the two BS positions determine the major arc of a circle. For an unknown β_{PD} orientation the LED position may be anywhere on that arc [SDM14]. In order to solve this problem and find an unique solution for the mobile node's position, the AOA measurement to a further LED transmitters is required. By doing this, the equations system of 4.8 is transformed into

$$\begin{aligned} \hat{y} - y_1 &= \tan(\psi_1 + \beta_{PD})(\hat{x} - x_1) \\ \hat{y} - y_2 &= \tan(\psi_2 + \beta_{PD})(\hat{x} - x_2) \\ &\dots \\ \hat{y} - y_M &= \tan(\psi_M + \beta_{PD})(\hat{x} - x_M) \end{aligned} \tag{4.9}$$

where M is the total number of LED transmitters perceived by the mobile node.

4.3.2 Range free methods

Range free algorithms use only connectivity information to perform localization. Different techniques such as, equalization and coding can be applied in order to successfully deliver the message from beacon node to the mobile user. Due to this, signal perturbations do not severely affect position estimation [LYWJ10]. Moreover, no extra hardware is required to measure signal characteristics. As a result, they provide a more robust approach compared to range based algorithms

[SGY+16]. Nevertheless, there exist a trade-off between its high robustness, low hardware complexity and their achievable accuracy. Range free algorithms provide coarse-grained localization (low accuracy) whilst range based algorithms can provide a fine-grained localization (high accuracy).

Traditional range free algorithms mainly used in wireless sensor networks (WSN) have been implemented straightforward for VLC networks. These algorithms are Cell ID [KVAS16], convex position estimation (CPE) [SGY+16] and centroid algorithm [SKS+16].

Cell ID

Cell ID, also known as cell of origin (COO), is the simplest range free positioning method. This algorithm uses the fact that every anchor node is sending out an unique ID (address) combined with different parameters. Basically, the mobile node that receives the ID from the base station is assumed to be placed somewhere within the anchor node's coverage radius. This method suffers from low accuracy. Hence, it is mostly used to provide room-level accuracy positioning systems.

Centroid

The Centroid scheme was proposed by Bulusu et al. in [BHE00]. This localization scheme assumes that a set of M connected LED anchor nodes, with overlapping regions of coverage, exist in the deployment area of the VLC network. The main idea is to treat the VLC nodes, located at (x_j, y_j), as point masses. In the most general form, the "mass" of each anchor node is considered to be equal and the estimated mobile node's position is obtained as follows.

$$(\hat{x}, \hat{y}) = \left(\frac{1}{M} \sum_{1}^{M} x_j, \frac{1}{M} \sum_{1}^{M} y_j \right) \tag{4.10}$$

As it can be seen, this method does not requires any ranging estimation and depends fully on network connectivity. Moreover, coordination between the unknown node and anchor node is not required. Implementation of centroid algorithm is relatively simple. The main disadvantage of the centroid localization algorithm is that the positioning accuracy depends on the density of the anchor node [LDY15].

Convex position estimation

Traditional CPE algorithm proposed by by Doherty et al. [DPE01] identify the feasible zone in which the mobile node could be located. This feasible zone is represented by the minimum bounding rectangle of a connection-based set which is depicted with a dashed line in Figure 4.11.

This minimum rectangle, also called bounding box, is found by solving iteratively a linear optimization problem with connectivity constraints. The bounding box is a convex set in $\mathbb{R}^2$, since the rectangle is the intersection of four halfspaces, hence is a convex set in $\mathbb{R}^2$ [BV04].

The CPE optimization problem is state as follows

$$\begin{array}{ll} \underset{\hat{\mathbf{x}} \in \mathbb{R}^2}{\text{minimize}} & \mathbf{D}^T \hat{\mathbf{x}} \\ \text{subject to} & \|\hat{\mathbf{x}} - \mathbf{C}_j\| \leq R_j \end{array} \tag{4.11}$$

where $\mathbf{D} \in \mathbb{R}^2$ is the vector which takes the values $\mathbf{D} = [1\ 0]$, $\mathbf{D} = [-1\ 0]$, $\mathbf{D} = [0\ 1]$ and $\mathbf{D} = [0\ -1]$ in order to find the minimum and maximum of the bounding box and, $\mathbf{C}_j = (x_j, y_j)$ is the vector that contains the jth LED position.

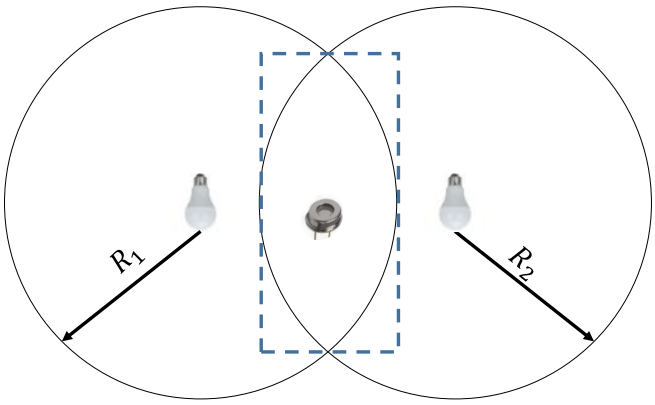

Figure 4.11: Convex position estimation

The restriction of CPE positioning problem of Equation 6.3 states that a feasible estimated localization point $\hat{\mathbf{x}} = (x_i, y_i)$ must lie inside the connectivity area.

As it can be seen from equations (3.16) the connectivity area of the jth transmitter strongly depends on the angle of incidence and receiver's FOV. Whilst the FOV of the receiver is a fixed parameter the angle of incidence depends on the relative position between the transmitter and receiver and, for the same position in the X-Y plane different angles can be obtained when the receiver is positioned at different a height. Therefore, the coverage radius of a single VLC spot depends on the variable Δh_{ji} as follows.

$$R_j = \Delta h_{ji} \tan(\Psi_{l/2}) \tag{4.12}$$

This special property of VLC networks has been named as *Inherent spatial diversity* [GPR12]. It is important to notice that VLC network's property will be use in further sections in order to derive our novel positioning method.

The main drawback of this method is that only low accuracy 2-D positioning can be delivered. In addition to this, the difference height must be known beforehand.

4.3.3 Fingerprinting (FP)

Fingerprinting (FP), also known as scene analysis, estimates the position of mobile node by comparing the characteristics of the received signal with a previously collected fingerprint map. This algorithm requires two phases: First, an offline phase during where scene information is collected and, second, an online phase where receiver seeks the best match with the offline measurement in order to estimate its position.

Finding the best match can be carried out through probabilistic inference, or classification algorithms such as k-nearest neighbors, support vector machine, Naives-Bayes classifier, and artificial neural networks [LDBL07]. Fingerprinting method does not require LOS from different sources, unlike range based solutions.

VLP domain, fingerprinting has been used both in simulation and experimental studies. In general, VLP systems based in FP use a type of RSS measurement to estimate mobile node's position. This measurement could be the signal impulse response [LPC+14], and power spectral density (extracted power of each modulated frequency) of LED lights (with unique frequency modulation) [VCZM12] just to name a few.

Table 4.3: Summary of range based, range free and fingerprinting positioning methods (Table adapted from [AIA+17])

Localization category	**Signal perturbation**		**Link configuration**		**Hardware dependency**
	Noise	**Multipath**	**LOS**	**non-LOS**	**Infrastucture**
Range based	Suceptible	Suceptible	Supported	Non supported	Highly infrastucture dependent
Range free	Robust	Robust	Supported	Supported	Low infrastucture dependency
Fingerprint	Robust	Robust	Supported	Supported	Highly infrastucture dependent

FP methods does not require to receive information from several beacon LED nodes unlike range-based techniques. However, constructing the required database in the offline phase, as well as, updating the map as the configuration of the environment changes is a major challenge for this type of methods. The requirement of updated fingerprint maps increases the cost of maintenance. Moreover, FP methods performance could be affected by the blockage from bodies or new objects in the scene [LPC+14, LDBL07]. To address this problem, in Kail et al. [KMPB14] a Bayesian signal model that considers the possibility of obstructions is proposed. The authors of this article have stated that their proposed model is robust to light signal blockage, considering the sparsity in detecting the simultaneous visible lights.

4.4 Robustness and characteristics analysis of VLP methods

As mentioned before, range based, range free and fingerprint positioning methods have different properties. In Table 4.3 the main characteristics of each type of localization approach are summarized.

When using range based methods for localization in underground mines tunnels tilt transmitters and receivers, multipath effects, low anchor node's density and diffuse link has to be considered as shown in Figure 3.4 (a). Moreover, machinery inside the mine can cause shadowing as shown in Figure 3.4 (d). Due to this, the signal received by workers inside the mine will be provided by the light reflections inside the tunnel (diffuse link).

RSS, TOA, TDOA and AOA based methods suffer detrimental effects when noise, multipath, shadowing and diffuse link are considered. Tilt receivers have to be considered since workers will be performing labours inside the tunnel. Finally, inside the tunnel low anchor node's density exists. In general, range based methods will not provide position estimation when fewer than 2 or 3 LED sources are perceived.

Range free algorithms are robust to noise, multipath effect, diffuse link and shadowing conditions. Moreover, they support positioning systems when tilt transmitters or receivers are considered. Nevertheless, they suffer from low accuracy. This issue is solved traditionally by increasing the number of LED lights. In underground mines an accuracy of $60.96(m)$ is established by regulation. Due to this, a high accuracy positioning system is not required in underground mine's tunnels.

We use this analysis in order to propose a robust VLP system for underground mines which will be developed by using a range free approach. Our proposed method is detailed and evaluated in Chapter 6.

Chapter 5

Design and implementation of a low-cost/large-scale visible light positioning system

Sommaire

5.1 Introduction 68
5.2 Uplink for remote positioning 68
5.3 Visible light communications downlink 70
5.4 Visible light communications receiver 71

5.1 Introduction

In this section we provide the design and the hardware implementation of a low cost/large scale visible light positioning system. As a result of this design, a VLP testing platform has been implemented at the Center for research in automatic at Nancy (CRAN) of the Université de Lorraine. This hardware implementation is used to deliver different positioning techniques from PD to camera based positioning methods. In addition to this, the design will be done in order to support different multiplexing techniques and data rates of up to 20 Kbps. As detailed in previous sections, the proposed VLP system must provide indirect remote positioning topology. In addition to this, it must be scalable and have a low cost on its implementation. This chapter is organized as follows: First the uplink technology use for remote positioning capabilities as detailed in table 4.2 is presented, a coverage analysis is done by measuring the package success ratio. Further on, the VLC transmitter hardware architecture is presented. Finally, the receiver is detailed and real data obtained from the implemented platform is delivered.

5.2 Uplink for remote positioning

As depicted in Table 4.2 VLC technology requires to be hybridized in order to support remote positioning technologies. Among all wireless communications technologies RF and IR are used to support uplink communication. IR communications have a short range of coverage (about 10 m). On the other hand RF has shown to cover a large area inside tunnels. Different RF bands

have been studied inside tunnels. Channel modelling and signal propagation characteristics of RF in underground mines can be found in literature [SA10, HKJ14, FBMN13].

In Emslie et al. the propagation of RF signals between 500-1000 MHz was studied. The experimental study shown that attenuation of signals in this frequencies is relatively low in straight mine entries [ELS75]. on the other hand, practical tests have revealed that the MFband (300 kHz-3 MHz) has more coverage and less attenuation compared to UHF-band in both coal and metal/non-metal mines [HKJ14].

Higher frequencies such as VHF, UHF and SHF propagate in LOS and 300 m down a mine entry. As a result, considering practical tests, and theoretical and experimental results, although high frequencies (UHF band higher) may offer a larger coverage area in straight and unobstructed tunnels, better coverage may be achievable by frequencies lower than UHF (MF-VHF) [SA10] when corners, crossings and obstacles exist. Regardless, UHF based technologies are more appealing to the mining industry because low cost, small form factor, scalable and easy to use applications are available off-the-shelf. In addition, their coverage and other propagation issues (e.g., requiring line-of-sight between Tx and Rx) can be resolved by appropriate antenna and wireless network designs.

Taking into account this analysis on RF signal propagation inside mine tunnels we choose a technology capable of providing communication in UHF band (300 MHz to 3 GHz). Different low cost devices are capable to provide wireless communications using this frequency band. In particular we have chosen a low cost wireless device nRF905 transceiver which is a single chip communication device that can work at frequencies of 433, 868 and 915 MHz. It has an adjustable output power up to 10 dBm and low current consumption on transmit mode (9 mA) and receive mode (12 mA). In Fig. 5.1 the transceiver is shown. More details about the transceiver can be found in [sem].

Figure 5.1: Single chip transceiver nRF905

This device does not provide online channel gain measurement. Due to this, the performance of the technology is obtained by measuring the package error rates. We send 1000 communications packages with fixed data to different distances between transmitter and receiver in a straight hall located at Universidad de Santiago de Chile. In Figure 5.2 the packet error rate for different

distances is shown.

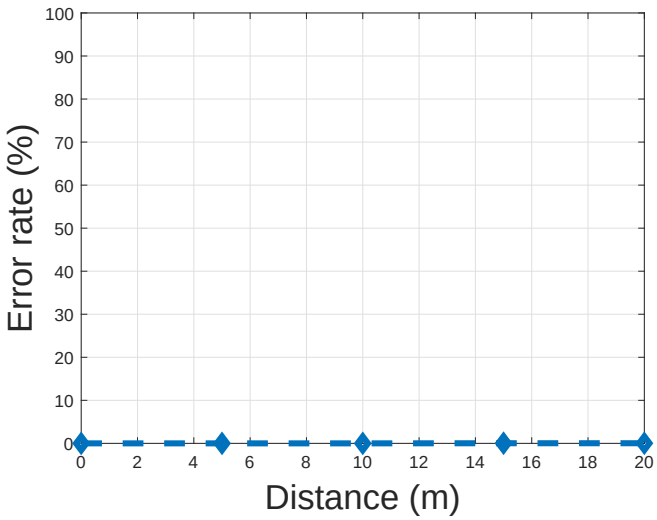

Figure 5.2: Packet error rate versus distance for nRF905

As it can be seen, this device achieves a packet error rate near to 0 % for a distance of up t0 20 m. Due to this, we consider that this technology feasible for underground mine communications and for enabling remote positioning.

5.3 Visible light communications downlink

In this section design of the low cost device used for visible light communications is delivered. In order to provide a wide range of communication possibilities, we design the device to support TDM and FDM access methods. The used modulation for this purpose is on-off-keying (OOK). Each VLC spot must be reconfigurable and must have a low cost. Due to this, we use low general purpose microcontrollers to configure our system and provide the wireless link. In Fig. 5.4 the transmitter design schematics is shown.

In order to evaluate the scenario proposed in Fig. 6.1 a real platform using 9 LED light transmitters. In Fig. 5.4 detailed photos of the proposed hardware are delivered. The microcontroller used for signal modulation is an Arduino Uno which cab be connected to a backbone network trough serial or ethernet. In addition to this, stand-alone operation is supported by saving the beacon packet in the microcontroller permanent memory.

As mentioned before, two different access methods are supported by our hardware design. The first method is randomly allocated time division multiplexing. An emitter with a data rate of 10 Kbps is used in order to transmit the message. The VLC beacon is randomly allocated in a time slot. The general structure of this protocol is shown in Fig. 5.5.

As it can be seen out frequency is used in order to differentiate idle stated from transmission states. Collision between two emitters who transmits the beacon at the same time slot is avoided by multiple observations. This method has been studied previously in Li et al. [LZZ+14] were a which uses a BFSA-based random access scheme first proposed in Zhang et al [ZCK14].

In addition to the random access scheme detailed above a frequency division multiplexing access is implemented in the platform. In Fig. 5.6 the general structure of this access method is shown.

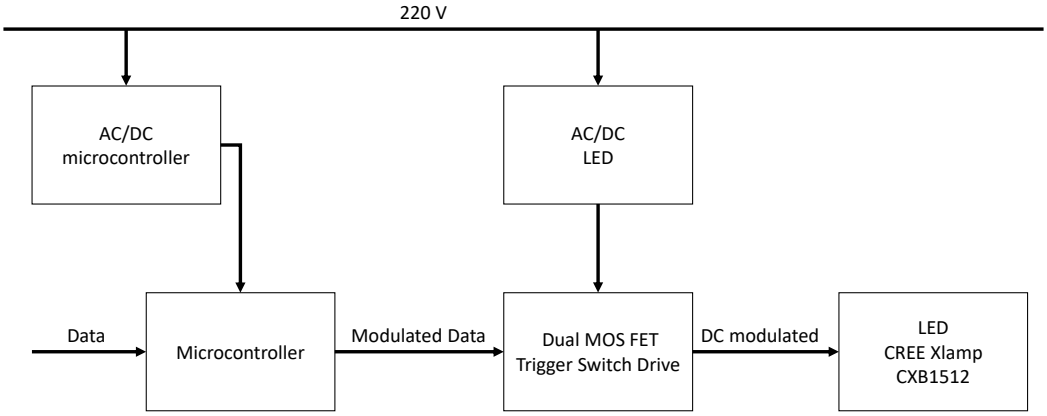

Figure 5.3: Transmitter design schematic

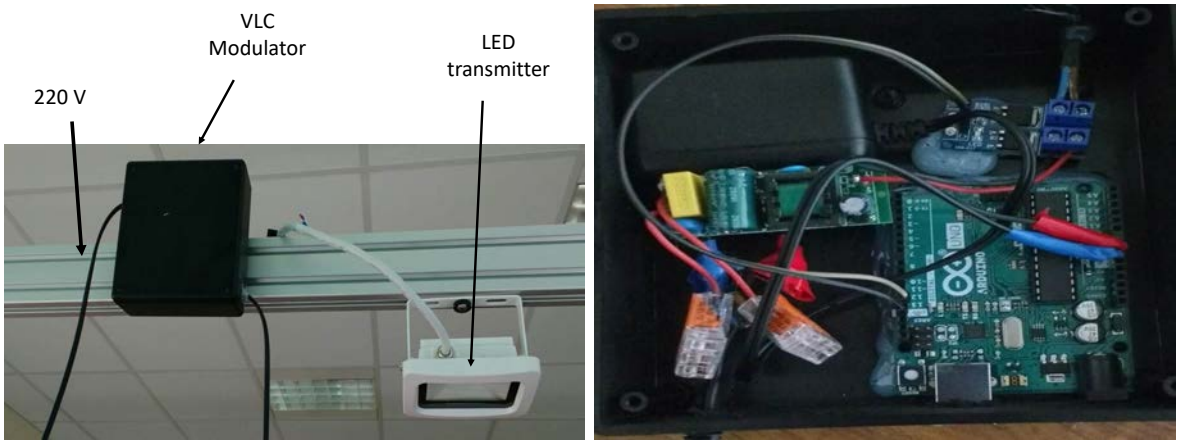

(a) (b)

Figure 5.4: Real implementation of VLC transmitter (a) general overview and (b) modulator in detail

Contrary to TDM method, in FDM systems there is no need for random allocation in a time slot since different VLC cells are not competing for the same resource (time slot) instead, they use separated channel that can be transmitted simultaneously and recognized at receiver side. In order to separate different sources band pass filters are implemented at receiver side.

5.4 Visible light communications receiver

As detailed in Chapter 3, section 3.3.3 in order to detect the wireless communications signal photodetectors are used to transform the modulated optical signal into an electrical one. In particular in this thesis, a PDA36A2 thorlabs photodetector shown in Fig. 5.7 is used. This Si

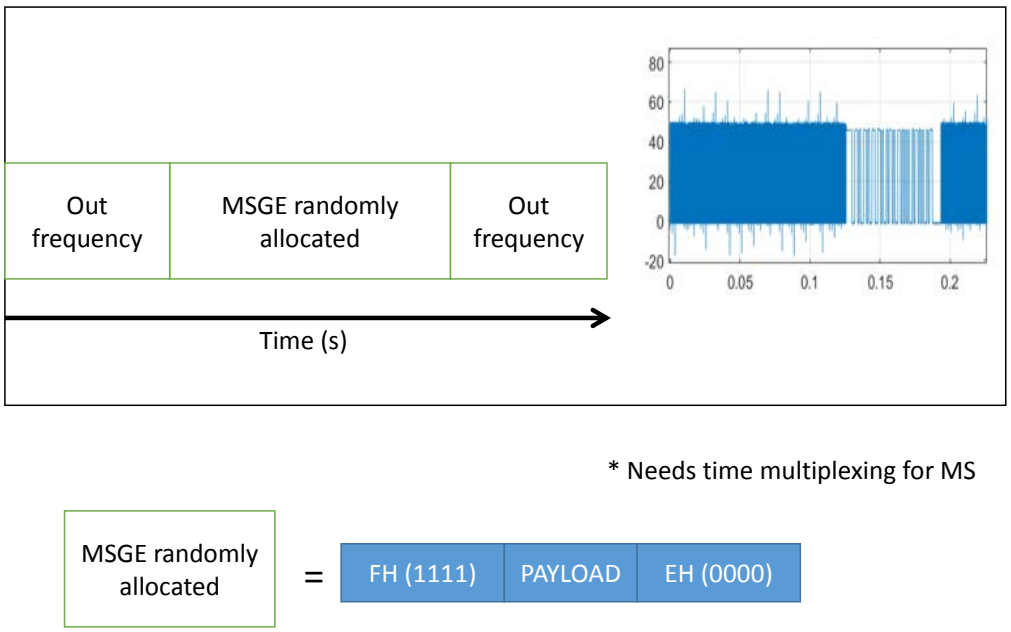

Figure 5.5: Random time slot access schematic

free space amplified PD has wavelength range within 200 to 1100 nm and a bandwidth from DC up to 12 MHz.

In order to process the received signal, analog to digital converter (ADC) is attached to the output of this PD. In particular we use an KEYSIGHT InfiniiVision 2000 X-Series Oscilloscope shown in Fig. 5.8. It is important to notice that the bandwidth of this converter is larger than the bandwidth of the PD used. In order to process the digitalized signal a MATLAB interface between the computer and the oscilloscope is created in order to retrieve the received data.

The receiver scheme is shown in Fig. 5.9. The message and the positioning algorithms are processed using an Acer aspire5 with an i5 processor of 1.60 GHz and 4GB RAM.

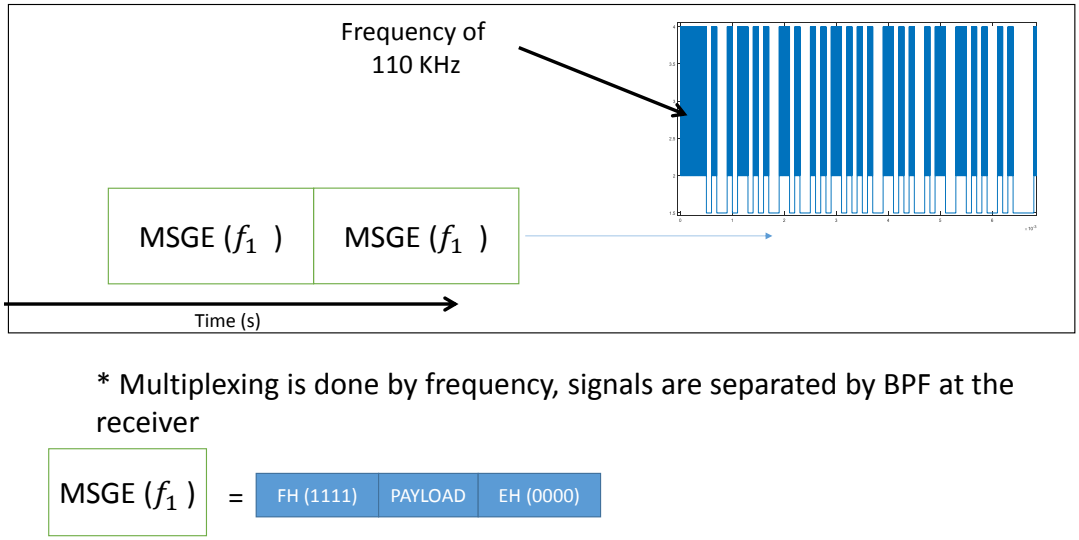

Figure 5.6: Frequency access schematic

Figure 5.7: PDA36A2 photodetector

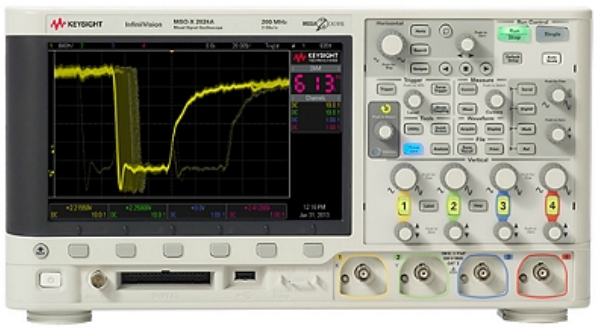

Figure 5.8: Oscilloscope used as digital to analog converter

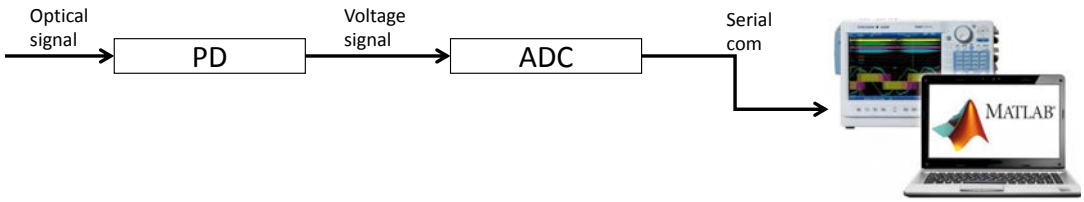

Figure 5.9: Proposed receiver architecture

Chapter 6

Design and implementation of a novel range free positioning method for robust visible light positioning in underground mines

Sommaire

6.1 Introduction **75**

6.2 System description **76**

6.3 Network architecture based positioning method: Convex polygon positioning (CPP) **77**

6.4 Enhance of position accuracy using imaging receivers (IR-CPP) . . **83**

6.5 Simulation results **85**

6.5.1 Square room 86

6.5.2 Tunnel section 92

6.6 Real implementation of CPP method using VLP testing platform . **94**

6.1 Introduction

As it was detailed in precious chapters VLP system have its merits to be implemented in underground mines for monitoring of personnel inside the tunnel. In chapter 5 a low cost/large scale hardware VLP system was detailed. This design and implementation hybridize VLC technology with a low cost-large coverage RF hardware in order to enable remote positioning which solves the problem enunciated in Chapter 2.

In Chapter 4 different VLP methods were evaluated in terms of their robustness. As a consequence range free positioning methods has been chosen due to their merits in terms of robustness against: signal perturbations, link configuration and hardware dependency. Nowadays, most of the range VLP free methods that can be found in literature are used straightforward from RF based solutions. In this chapter, we introduce a novel range free positioning method that uses intersect characteristics of VLC networks in order to increase the robustness and accuracy.

This chapter is organized as follows: In Section 2 the system description in which the proposed algorithm performance will be evaluated is presented. Next, the procedure of our range free method is detailed. Results in terms of accuracy and robustness are displayed in Section 4. Finally, the main conclusions are delivered.

6.2 System description

The spatial deployment of VLC network has an important impact in performance of the communication as well as accuracy of the positioning methods. Many authors have proposed the optimization of the diffusion spots of VLC networks as an important parameter in order to ensure fast and reliable communication between transmitter and receiver [EMGO18, LLZ14, WC05]. In particular, in [LLZ14] two lighting arrangements were tested for VLC networks, these are, Lattice and tunnel structure shown in Figure 6.1.

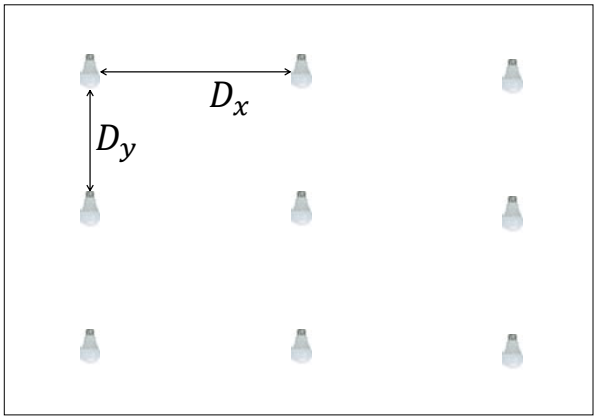

(a)

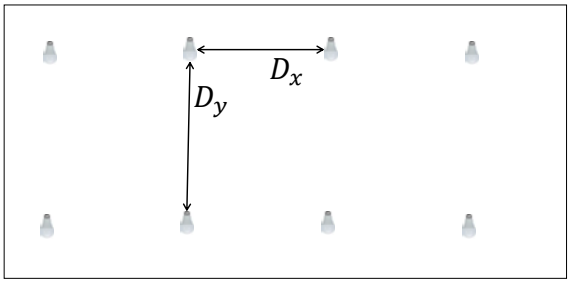

(b)

Figure 6.1: Different LED arrangements for VLC networks (a) Lattice architecture and (b) Tunnel architecture

The two proposed LED architectures are presented an square room. In Lattice structure the distance between LED lights in the X and Y axes are the same for all the LED lights sharing a common column or row whilst in Tunnel structure there is a maximum of two LED lights in the same column.

These structures are used due to the illuminations constraints, which means that VLC networks are mostly deployed as homogeneous networks to reach minimum luminosity levels. Dif-

ferent spatial deployments of LEDs will provide different coverage pattern, inter-cell interference, signal to noise ratio and illumination distribution due to the characteristics of VLC channel.

6.3 Network architecture based positioning method: Convex polygon positioning (CPP)

The channel gain on the receiver side for the n-LOS component depends on the FOV and orientation of the photodetector. Due to this, the equation (3.16) is expressed as

$$h_{nlos} = \begin{cases} \text{Eq. (3.23)} & 0 \leq \psi_{mi} \leq \Psi_l \\ 0 & \text{elsewhere} \end{cases} \tag{6.1}$$

as it can be seen from equation (6.1) the coverage radius of the transmitter j strongly depends on the angle of incidence and the receiver's FOV. While the FOV is a fixed parameter, the angle of incidence depends on the relative position between the transmitter and receiver and, for the same position in the X-Y plane different angles can be obtained when the receiver is positioned at different height as shown in Figure 6.2

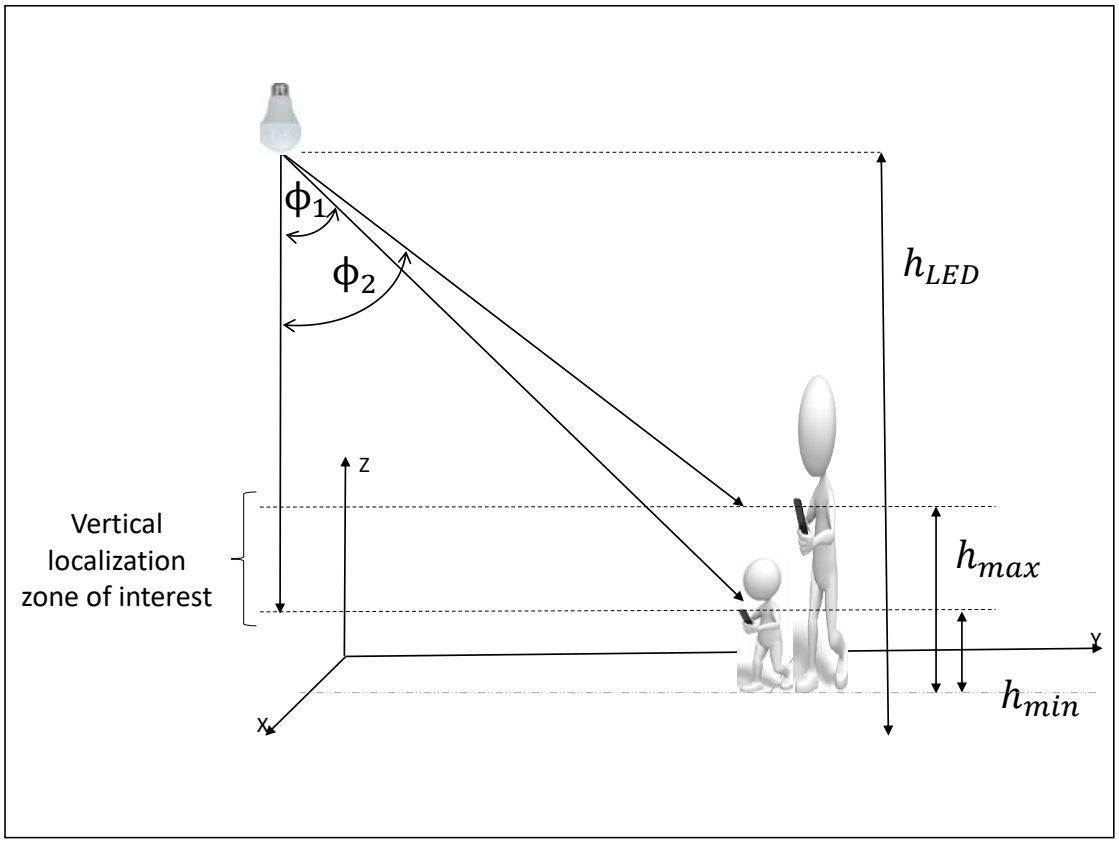

Figure 6.2: Sample graph with blue (dotted), green solid) and red (dashed) lines

since the coverage radius of a single VLC spot depends on the variable Δh we define Δh_{min} as the minimum height difference between transmitter and receiver and Δh_{max} as the maximum

difference. The maximum coverage radius for a single VLC spot using LOS signal can be derived from equation (3.16) considering $\max\psi_{ji} = \Psi_l$ and a given height difference Δh as follows

$$R_{max} = \Delta h \tan(\Psi_l) \tag{6.2}$$

it can be seen that the maximum coverage radius of the diffusion spot is proportional to the height difference Δh.

In order to estimate the maximum coverage radius, CPP method requires previous knowledge of receiver height in order to compute the height difference Δh. The height of the LED transmitter, h_j, is obtained by decoding data transmitted by a VLC beacon in Figure 6.4. On the other hand, the receiver height must be determined by using additional 1-D ranging sensors. In particular, two different low cost technologies are proposed in order to measure receiver's height, these are the ultrasound range sensor HC-SR04 and the Time-of-Flight optical ranging sensor VL53L0X.

Since ranging information is not always precise, the algorithm will be affected by the mismatch between real and measured height. In Figure 6.3 (a) real measurements of receiver's height performed by the two proposed ranging sensors for a $h_i = 0.7(m)$ are shown. As it can be seen, measurements done by the sensor are not perfect. In addition to this, outliers are present when HC-SR04 is used. In order to overcome this problem, a median filter is commonly use for outlier elimination as shown in Figure 6.3 (b). We use the ultrasonic technology instead the optical sensor since measurements done by VL53L0X have an offset larger than 10 centimetres. In this figure, outliers are eliminated from signal. Moreover, errors in receiver's height measurement smaller than 4 centimetres are obtained.

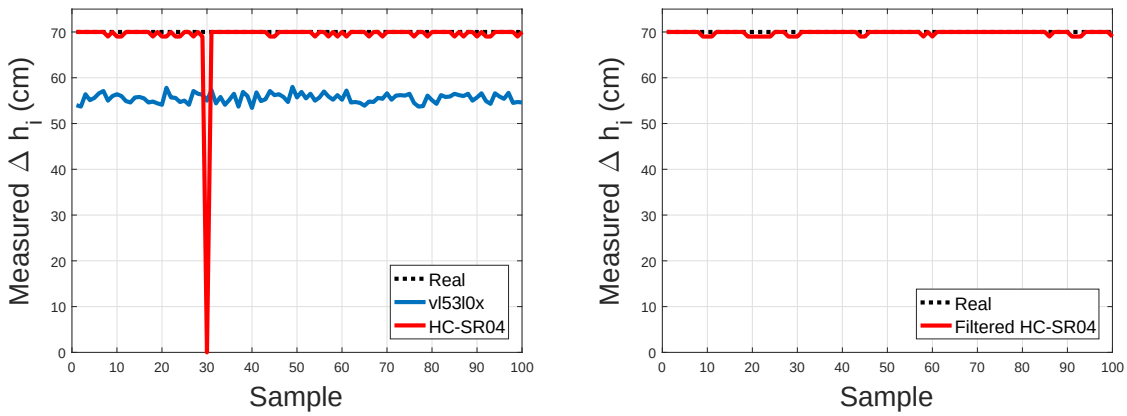

(a) (b)

Figure 6.3: Difference height distance measurements (a) raw measurements and (b) filtered measurements

The standard deviation of the filtered difference height measurement $\sigma_{\Delta h_{ij}} = 0.0064$ (m).

In this section we will show how the proposed method uses the architecture information of the nearest VLC diffusion spots in order to increase the accuracy and robustness of position estimation. As a practical example we consider, without losing generality, a small square room with a lattice LED deployment of 4 lights.

Each VLC spot sends periodically information its unique ID number as well as its own position and the coordinates of its nearest neighbours as shown in Figure 6.4. In order to receive

information from multiple sources the algorithm requires the usage of a multiple access technique such as frequency division multiplexing (FDM), time division multiplexing (TDM) code division multiplexing (CDM) or other [PL18]. The low cost7large scale platform presented in Section 5 support both, TDM and FDM.

For this example we consider that the mobile node is connected to three LED lights as shown in Figure 6.5. It receives simultaneously the VLC beacon shown in 6.4 from each connected light.

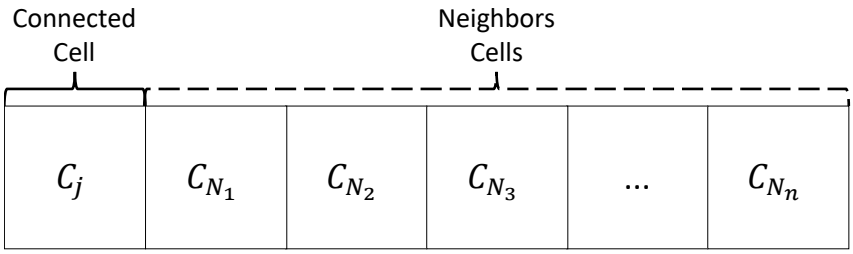

$$C_j = [Cell\ ID, x_j, y_j, z_j]$$
$$C_{N_k} = [Cell\ ID, x_{N_k}, y_{N_k}, z_{N_k}]$$

Figure 6.4: Broadcast VLC Packet

As it can be seen the mobile node receives position information from the connected node and, additionally, its neighbours. The proposed method uses both, connected and non-connected cells to perform localization of the unknown node.

First, connected cells are used by using the traditional CPE algorithm. The feasible zone in which the MN could be located is represented by the minimum bounding rectangle of the feasible connection-based set. This minimum rectangle, also called bounding box, is found by solving iteratively a linear optimization problem with connectivity constraints. The bounding box is a convex set in $\mathbb{R}^2$, since the rectangle is the intersection of four half-spaces, hence is a convex set in $\mathbb{R}^2$ [BV04].

The CPE optimization problem is state as follows

$$\begin{aligned} \underset{\mathbf{x} \in \mathbb{R}^2}{\text{minimize}} \quad & \mathbf{D}^T \mathbf{x} \\ \text{subject to} \quad & \|\mathbf{x} - \mathbf{C}_j\| \leq R_j \end{aligned} \tag{6.3}$$

where $\mathbf{D} \in \mathbb{R}^2$ is the vector which takes the values $\mathbf{D} = [1\ 0]$, $\mathbf{D} = [-1\ 0]$, $\mathbf{D} = [0\ 1]$ and $\mathbf{D} = [0\ -1]$ in order to find the minimum and maximum of the bounding box. The restriction of the problem states that the feasible point $\mathbf{x}$ must lie in the connectivity area. CPE method estimates position of the MN as the bounding box centroid as shown in Figure 6.5. Our proposed method uses this bound box as the first step of the procedure.

For the second step, neighbour cells overlapped with the bounding box are found. Since the coverage radius and the central position of each neighbour cell is known by the MN it can perform an overlapping condition testing algorithm. The overlapped condition state next is tested for each known neighbour and the bounding box set already found in the first step.

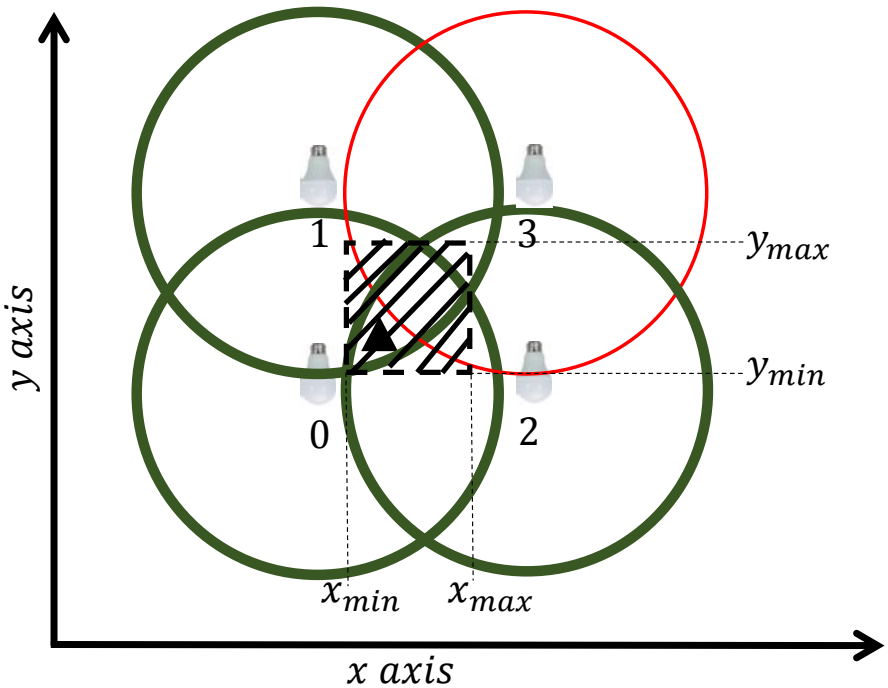

Figure 6.5: Convex bounding box for the mobile node position

Definition 1 *Overlapping condition: A bounding box set $\mathbb{BB}$ and an optical cell coverage area set $\mathbb{A}_j$ are considered to be overlapped if the inferior value of the distance between a point $\boldsymbol{x}$ in the bounding box set, $\boldsymbol{x} \in \mathbb{BB}$ and the central point of the coverage area set of the mth LED $\boldsymbol{C}_m$ is inferior to the coverage radius of the mth cell R_m. Mathematically this can be expressed as*

$$\mathbb{BB} \cap \mathbb{A}_m \neq \phi \Leftrightarrow \inf_{\boldsymbol{x} \in \mathbb{BB}} \|\boldsymbol{x} - \boldsymbol{C}_m\|_2 \leq R_m \tag{6.4}$$

Where ϕ is the empty set and $\|.\|_2$ is the euclidean norm in $\mathbb{R}^2$.

The before mentioned overlapping condition can be expressed as convex optimization problem since $\inf_{\mathbf{x} \in \mathbb{BB}} \|\mathbf{x} - \mathbf{C}_m\|_2$ is the minimization of the distance between a convex set and a fixed point in $\mathbb{R}^2$, i.e., the minimization of the distance between the bounding box set and the center of the coverage area set of the mth which is a neighbor cell defined as

$$\begin{aligned} \underset{\mathbf{x} \in \mathbb{R}^2}{\text{minimize}} \quad & \|\mathbf{x} - \mathbf{C}_m\|_2 - R_m \\ \text{subject to} \quad & \mathbf{x} \preceq \mathbf{x}_{max}, \\ & -\mathbf{x} \preceq -\mathbf{x}_{min} \end{aligned} \tag{6.5}$$

Where the constraints $\mathbf{x}_{min}$ and $\mathbf{x}_{max} \in \mathbb{R}^2$ are the minimum and maximum values of the bounding box set, $\preceq$ is an element-wise comparator and R_m is the coverage radius of the cell. When the fitness function of the optimization problem in (6.5) is strictly negative means that the cell m is and overlapped cell of the bounding box. Otherwise the cell is not an overlapping

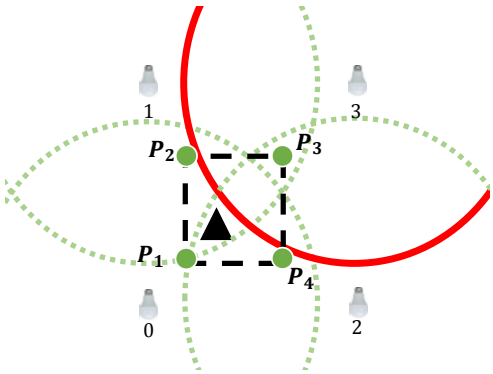

Figure 6.6: Overlapped cell to bounding box with binary indicator of Equation (6.6) equals to one

x_{min} x_{max}

cell. We use an overlapping binary function indicator defined as

$$Overlapping = \begin{cases} 1 & \text{if } \|\mathbf{x}^* - \mathbf{C}_m\|_2 - R_m < 0 \\ 0 & \text{if } \|\mathbf{x}^* - \mathbf{C}_m\|_2 - R_m \geq 0 \end{cases} \tag{6.6}$$

where $\mathbf{x}^*$ is the minimum of the convex optimization problem stated in (6.5).

Once the overlapping condition is check, only overlapped cells are considered in the reduction process as shown in Figure 6.6. In particular, for this example coverage area of cell 3 (depicted in red) is overlapped with the bounding box. For this reason, the VLC cell 3 is used to reduce the feasible localization set delimited by vertices points of the bounding box, i.e., $\mathbb{P}_{BB} = \{\mathbf{p}_1, \mathbf{p}_2, \mathbf{p}_3, \mathbf{p}_4\}$ as shown in Figure 6.6.

In order to find the new feasible localization set, a feasibility check is implemented using the non connectivity constraints, i.e., the possible intersection points that does not satisfy the non-connectivity condition are discarded. As it can be seen in Figure 6.7 the vertex point $\mathbf{p}_3 = (x_{max}, y_{max})$ is inside the coverage area of the non-connected cell 3, i.e., $\mathbf{p}_3 \in \mathbb{A}_3$ where $\mathbb{A}_3$ is the coverage area set of LED 3. Since the mobile node is not connected to the VLC spot with ID 3 we can conclude that the $\mathbf{p}_3$ vertex is not a feasible point for the positioning method. Due to this, $\mathbf{p}_3$ is removed from the positioning polygon set. We named this provisional set as $\mathbb{P}_{CP1} = \{\mathbf{p}_1, \mathbf{p}_2, \mathbf{p}_4\}$.

Once the point feasibility check is done, intersection points between the overlapped cells and the original bounding box are found as shown in Figure 6.8. At this point, new vertices $\mathbf{p}'_1$ and $\mathbf{p}'_2$ will be use to provide a convex approximation for the non-convex constraint $\|\mathbf{x} - \mathbf{C}_j\| > R_j$. We named this provisional set as $\mathbb{P}_{CP2} = \{\mathbf{p}'_1, \mathbf{p}'_2\}$

Once the new set of feasible set $\mathbb{P}_{CP2}$ is found, it is merged with the provisional vertices set $\mathbb{P}_{CP1}$ as $\mathbb{P}_{CP} = \mathbb{P}_{CP1} \cup \mathbb{P}_{CP1}$ shown in Figure 6.9.

Finally, a convex polygon is formed using the points of the set $\mathbb{P}_{CP} = \{\mathbf{p}_1, \mathbf{p}_2, \mathbf{p}_4, \mathbf{p}'_1, \mathbf{p}'_2\}$ as the vertices of the polygon.

In order to create this convex polygon, the smallest convex set that contains $\mathbb{P}_{CP}$ is must be found. This set has been named as the convex hull of the feasible vertices set $\mathbb{P}_{CP}$ denoted as $\mathcal{CH}(\mathbb{P}_{CP})$ shown in Figure 6.10. In this practical example the convex polygon $\mathcal{CH}(\mathbb{P}_{CP}) = \{\mathbf{p}_1, \mathbf{p}_2, \mathbf{p}'_1, \mathbf{p}'_2, \mathbf{p}_4\}$

The estimated position on the mobile node will be computed as the centroid of the convex hull shown in Figure 6.10. Since the convex hull in $\mathbb{R}^2$ is a convex close polygon, its centroid can obtained by

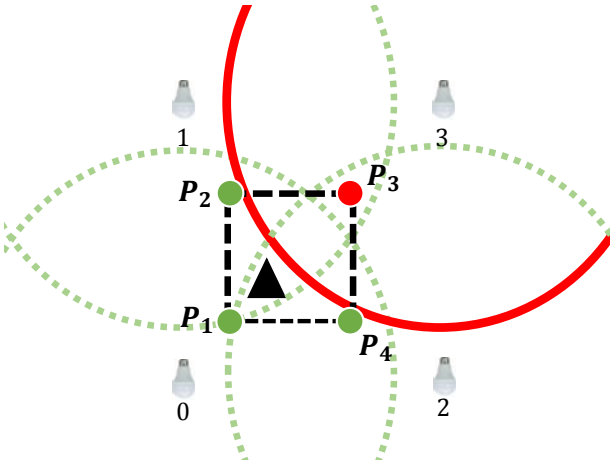

Figure 6.7: Unfeasible point elimination based on connectivity feasibility check

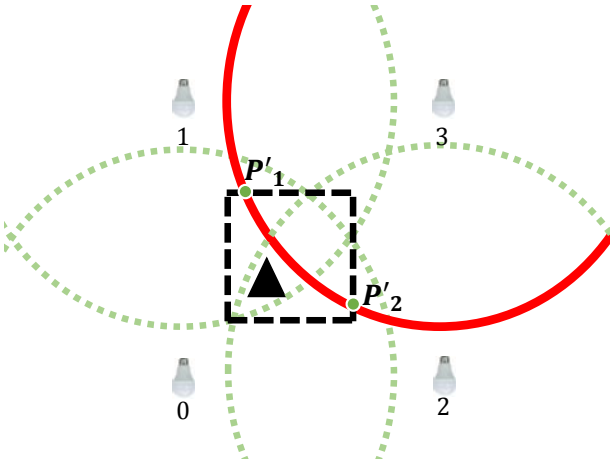

Figure 6.8: New feasible vertices using overlapped non-connected cells

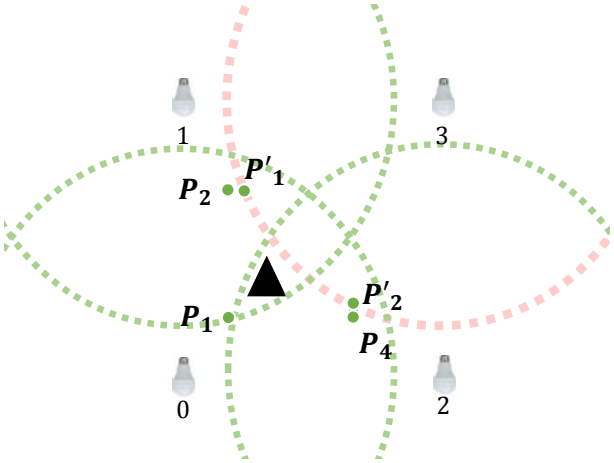

Figure 6.9: Set of vertices found by using connectivity and infrastructure information

x_{min} x_{max}

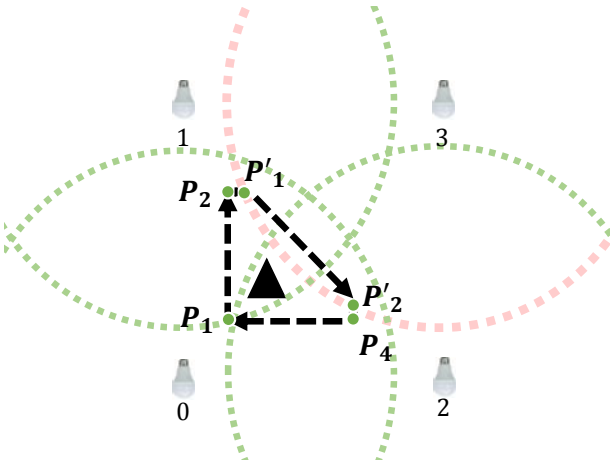

Figure 6.10: Convex polygon for feasible positioning area

$$\hat{x}_{MN} = \left(\frac{1}{6A_p} \sum_{j=1}^{K} \overbrace{(x_j + x_{j+1})}^{x_{min}} \overbrace{(x_j y_{j+1} - x_{j+1} x_j)}^{x_{max}} \right)$$

$$\hat{y}_{MN} = \left(\frac{1}{6A_p} \sum_{j=1}^{K} (y_j + y_{j+1})(x_j y_{j+1} - x_{j+1} x_j) \right) \tag{6.7}$$

where K is the total number of points in the convex hull set $\mathcal{CH}(\mathbb{P}_{CP})$, (x_j, y_j) are the components in the X and Y axis. Finally, $\mathbb{A}_{CP}$ is the area of our convex polygon calculated by:

$$A_p = \frac{1}{2} \sum_{j=1}^{K} (x_j y_{j+1} - x_{j+1} y_j) \tag{6.8}$$

Since the final feasible are of positioning is described by a convex polygon, we refer to the proposed method as convex polygon positioning (CPP).

6.4 Enhance of position accuracy using imaging receivers (IR-CPP)

Imaging receivers [GC18] allow multiple-input-multiple-output (MIMO) capacity for indoor VLC. Imaging receivers consist on the usage of various PDs at the receiver side. In this work, we consider the usage of imaging detectors composed by two or four vertically oriented PDs with different FOV angles. Single PD and imaging receiver architectures are shown in Figure 6.11.

Our method uses the imaging receivers to reduce the feasible localization area and increase the accuracy of position estimation. These type of algorithms assume a fixed coverage radius R_j. As detailed previously, the maximum coverage area strongly depends on detector's FOV and height difference.

In Figure 6.12 intersection patterns of maximum coverage area of each VLC source are displayed for single PD detector and imaging receiver composed by 2 PDs.

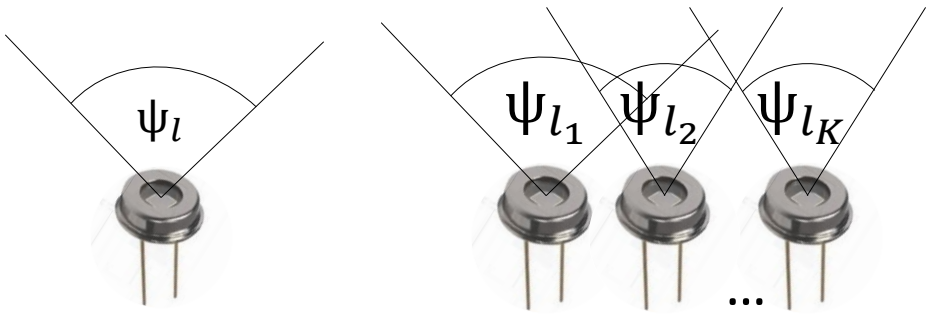

(a) (b)

Figure 6.11: Detector architectures: (a) single photodetector and (b) imaging receiver

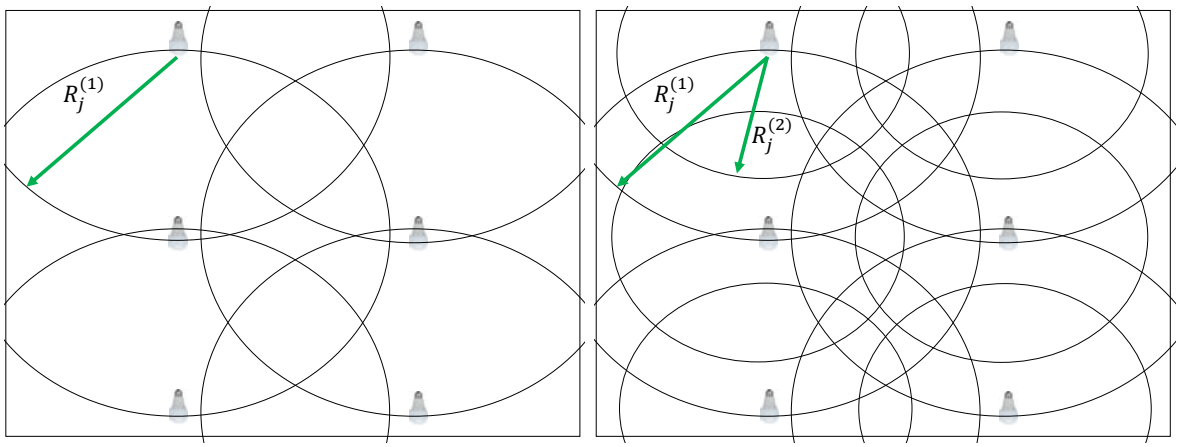

(a) (b)

Figure 6.12: Intersection pattern of feasible localization area based on (a) single PD and (b) imaging receiver

As it can be seen, the usage of two PDs with different FOV angles creates a more dense intersection pattern. Due to this, the complete area of the considered room is divided into smaller feasible regions.

Since imaging receivers are used in our method, the constraints of original CPE algorithm proposed in [DPE01] have been modified in order to take into account multiple detectors as

detailed in Eq. (6.9)

$$\begin{aligned} \underset{\mathbf{x} \in \mathbb{R}^2}{\text{minimize}} \quad & \mathbf{D}^T\mathbf{x} \\ \text{subject to} \quad & \|\mathbf{x} - \mathbf{C}_1\|_2 \leq R_1^{(1)}, \\ & \|\mathbf{x} - \mathbf{C}_1\|_2 \leq R_1^{(2)}, \\ & ..., \\ & \|\mathbf{x} - \mathbf{C}_1\|_2 \leq R_1^{(K)}, \\ & \|\mathbf{x} - \mathbf{C}_2\|_2 \leq R_2^{(1)}, \\ & \|\mathbf{x} - \mathbf{C}_2\|_2 \leq R_2^{(2)}, \\ & ..., \\ & \|\mathbf{x} - \mathbf{C}_j\|_2 \leq R_J^{(K)} \end{aligned} \tag{6.9}$$

similarly to traditional CPE method, $\mathbf{D}$ is a two dimensional vector which takes the values $\mathbf{D} = [1\ 0]$, $\mathbf{D} = [-1\ 0]$, $\mathbf{D} = [0\ 1]$ and $\mathbf{D} = [0\ \ -1]$. Position of the connected cell in X and Y axis, $\mathbf{C}_j$, and maximum coverage radius of connected cells for each detector $R_j^{(k)}$ are considered as constraints of the optimization problem. The number of constraints in the optimization problem is directly related to the total number of PDs (K) at the receiver side and the number of connected cells.

The step by step procedure of imaging receiver convex polygon positioning (IR-CPP) is similar to the single PD method detailed in the previous section. The main difference is that the usage of imaging receivers, increase the number of constraints and feasibility checks and, consequently, reduces the feasible positioning area and increases the accuracy.

6.5 Simulation results

To solve problem convex optimization problems we use CVX, a package for specifying and solving convex programs in MATLAB [GB08]. In order to find the final convex hull, rapid-hull algorithm proposed in [BDH96] is used.

The LED deployment shown in Figure 6.1(a) and (b) are used to evaluate the performance of our proposed algorithm. Parameters used for simulation are delivered in Table 6.1. Seven different receiver architectures are detailed in the table below, these are, PD(s_1), PD(s_2), PD(s_3), PD(IR_1), PD(IR_2), PD(IR_3) and PD(IR_4). These architectures are used in order to measure the effect of using different FOV combinations at the receiver side and, the impact of using imaging receivers instead traditional single detector approach.

The accuracy of our method is analysed based on two different heights Δh_{ij}. Numerical results were obtained using a square grid with a separation of 0.1 meters between each testing point.

In order to measure the impact of tilting and rotation angles, an horizontal tilting angle β is assumed to be in the range of $\pm 2°$. Furthermore, a rotation angle $\alpha \in [0°, 360°]$ is considered.

Results must be evaluated separately for each proposed scenario, i.e., Square room with lattice arranged beacon nodes and, tunnel network architecture.

Parameter	Value	Parameter	Value
$\Phi/2$	70°	m_l	0.6461
P_j	10W	A	10^{-4} m^2
T_s	1	Simulation grid	0.1× 0.1 m
Δh_{max}	2 m	Δh_{min}	1.5 m
Room size	3×3 ×3m	Number of LEDs	9
ρ	0.8	Mismatch	±0.04 m
Tunnel size	6×3 ×3m	FOV PD(s_1)	60
FOV PD(s_2)	80	FOV PD(s_3)	100°
FOV PD(IR_1)	60 and 80°	FOV PD(IR_2)	60 and 100°
FOV PD(IR_3)	40, 60, 80 and 100°	FOV PD (IR_4)	60, 80, 100 and 120°
$\lvert\beta_{tilt1}\rvert$	1°	$\lvert\beta_{tilt2}\rvert$	2°
α_{rot1}	0°	α_{rot2}	90°
α_{rot3}	180°	α_{rot4}	270°

Table 6.1: Parameters for computational simulation

6.5.1 Square room

In this section performance of the proposed method for the scenario described in Figure 6.1 (a) is analysed. First, a comparison between different FOVs is done by assuming a a single PD at receiver's side. Then, imaging receivers CPP is evaluated under the same conditions using four different imaging receiver's architectures. Next, a coverage analysis between range free and range based VLP is performed. Finally, effects of multipath reflections, tilt and rotation angles and height mismatch measurements in position estimation are studied.

Method performance: Single PD versus imaging receiver

System parameters of the VLC network such as: testing grid, room dimensions, receiver's FOV and height difference are delivered in Table 6.1. In this section performance of CPP method using single PD and imaging receivers with different FOVs is obtained through computational simulation.

In Figure 6.13 the CDF of positioning errors using CPP method is delivered for two difference heights, i.e., $\Delta h_{ji} = 2$ m and $\Delta h_{ji} = 1.5$ m. As it can be seen the proposed method is highly robust to changes in the receiver's FOV considering an interval of angles from 60° to 100°.

The detrimental effect on the accuracy suffered by $CPP(s_3)$ can be explained due to the increment of coverage area from each VLC cell. Since the method uses architecture information and overlapping conditions to reduce the feasible positioning area, it becomes less effective when the coverage area of each cell $\mathbb{A}_j$ becomes relatively big compared to the room dimensions and the network is not enough densely deployed. This effect is more pronounced for larger difference heights since the coverage radius increases along with Δh_{ji}. The most accurate position estimation is obtained by using a FOV=60° at receiver's side.

Different combinations of FOV angles provide variety of intersection patterns (see Figure 6.12). Due to this, measuring the effect of multiple coverage radius $R_j^{(k)}$ is important. Four different FOV combinations detailed in Table 6.1 are proposed. In Figure 6.14 the cumulative distribution function (CDF) of errors is displayed for $\Delta h_{ij} = 1.5$ and $\Delta h_{ij} = 2$ meters using the four proposed detector architectures. The acronym of algorithm along with the receiver architecture is used as abbreviation to simplify the performance analysis. For instance, $CPP(IR_1)$

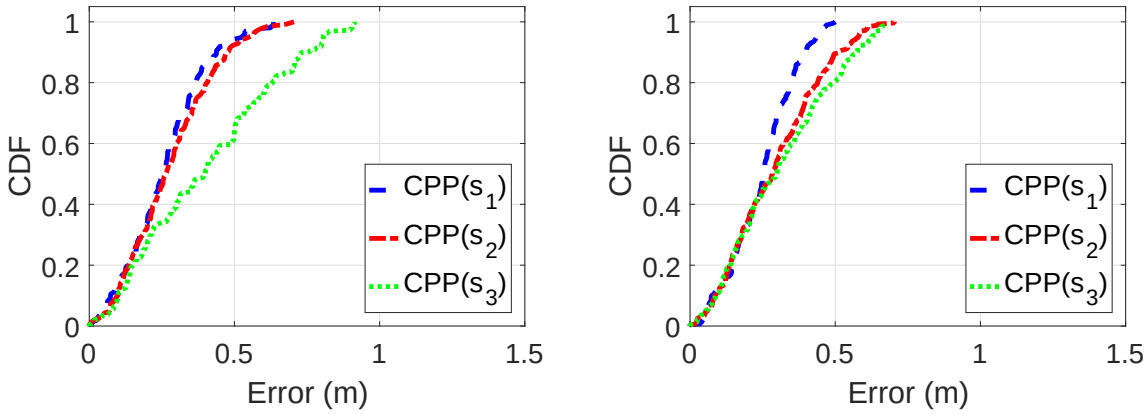

(a) (b)

Figure 6.13: CPP performance using a single PD for (a) Δh_{ji}=2 m and (b) Δh_{ji}=1.5 m

stands for the performance of CPP algorithm using the receiver architecture PD(IR_1) of Table 6.1.

As it can be seen, the combination of CPP method and imaging receiver overcomes increases the accuracy of position estimation. The best performance is achieved when a large variety of FOV angles are used as detectors. In this thesis a maximum number of four PDs is used.

Changes in receiver's height have small impact on IR-CPP performance. IR-CPP method shows also to be robust to changes on the FOV combination. For instance, IR-CPP performance is similar for PD(IE_3) and PD(IR_4) architectures in both proposed scenarios. We can infer that the robustness of the method to changes in the FOV increases along with the number of PDs used at receiver's side.

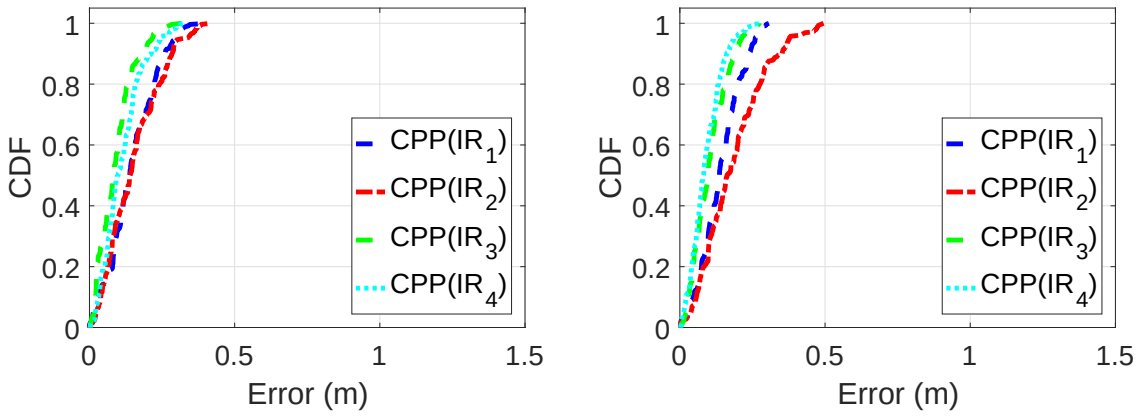

(a) (b)

Figure 6.14: CPP performance using a imaging receiver for (a) Δh_{ji}=2 m and (b) Δh_{ji}=1.5 m

As the receiver height difference increases to from $\Delta h_{ij} = 1.5(m)$ to $\Delta h_{ij} = 2(m)$, mean accuracy of CPP method changes. The overall performance of PD(IR_3) architecture overcomes slightly PD(IR_4), which shows to be a bit more sensitive to changes in receiver's height.

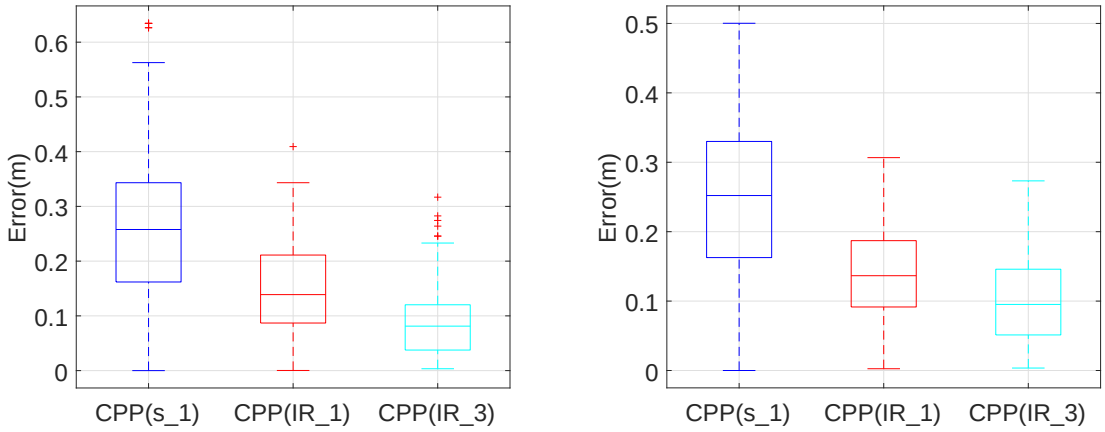

(a) (b)

Figure 6.15: Comparison of best PD architectures for (a) Δh_{ji}=2 m and (b) Δh_{ji}=1.5 m

Coverage analysis: Range based vs range free approach

Whilst range based method uses signal characteristics in order to estimate the mobile's node position range free methods use only connectivity information as detailed in Chapter 4.

Another important drawback of range based positioning method is that they required at least two or three connected nodes in order to perform localization. In general, for low cost positioning using off-the-shelf devices, RSS based range free positioning is preferred.

In Figure 6.16 a two dimensional representation of coverage distribution for range based and range free positioning approaches is presented. A receiver's FOVs of $\Psi_l = 60°$, $\Psi_l = 80°$ and $\Psi_l = 100°$ are used to measure the coverage of VLC cells.

It can be seen that RSS range based method is not capable to cover completely the proposed scenario when a receiver FOV of 60° is used. In order to compute RSS-based method, the mobile node requires the reception of least three VLC cells to estimate its position. The RSS-based algorithm has a coverage area percentage of 51.8813% whilst, under the same FOV conditions, our range free method is capable to cover the 100% of proposed scenario.

Effect of multipath reflections: boundary conditions

In this section the effect of multipath reflection in underground mine walls is analysed. Traditional VLP systems use high accuracy range based method. As mentioned before, RSS based positioning is preferred due to its low cost and off-the shelf device usage. Nevertheless, this method is highly sensitive to multipath reflections and noise.

In Figure 6.17 the error of RSS based trilateration and our proposed method in a surface plot is presented. The overlapped area reduction proposed by CPP algorithm improves the performance by reducing the error variability over the considered area. Errors near to walls and boundaries present in VLP systems due to lack of connectivity and reflections is reduced by using disconnected cells in the localization process. Since CPP is a range free method, its performance in terms of accuracy is enhanced as the density of network increases. Due to this, the central zone of the proposed scenario shows a higher accuracy compared with the border in both proposed network methods. On the other hand, RSS based method suffers from the effect

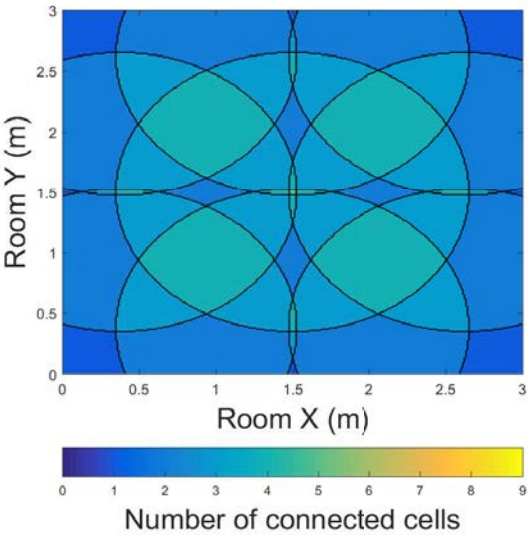

(a)

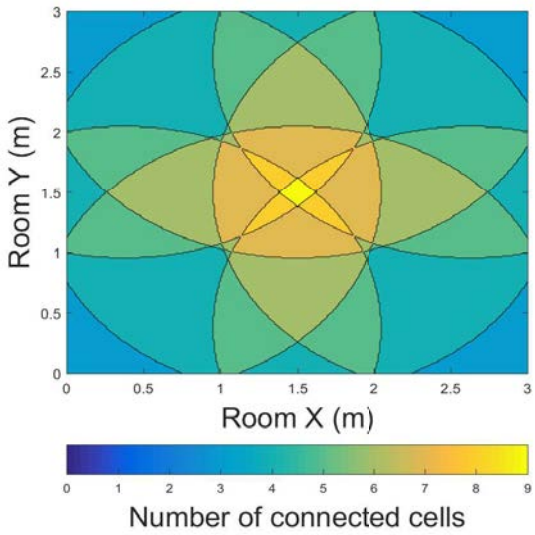

(b)

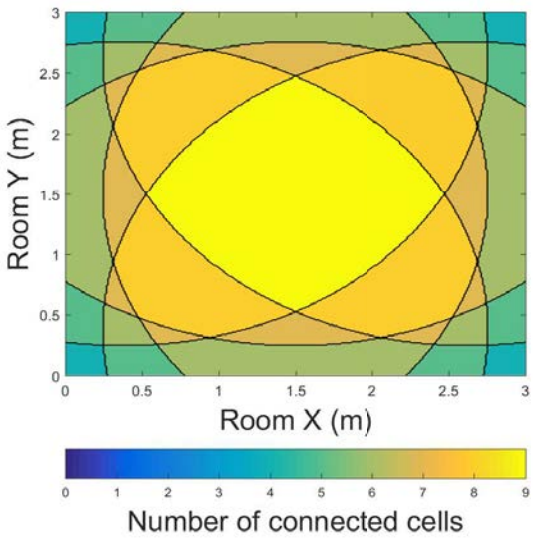

(c)

Figure 6.16: Two dimensional coverage representation for Δh_{ji}=2 m (a) FOV=60°, (b) FOV=80° and (c) FOV=100°

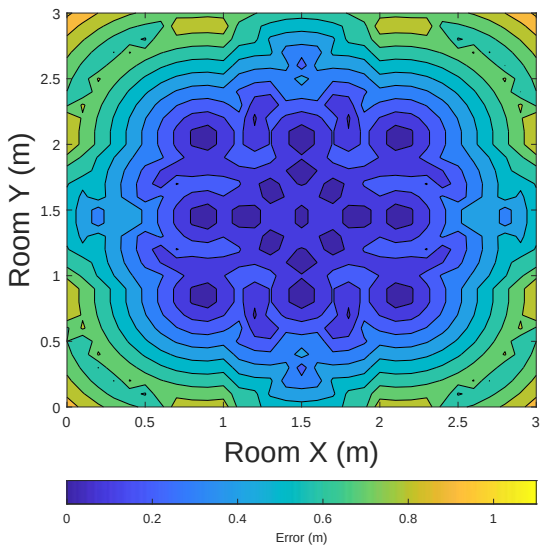

(a)

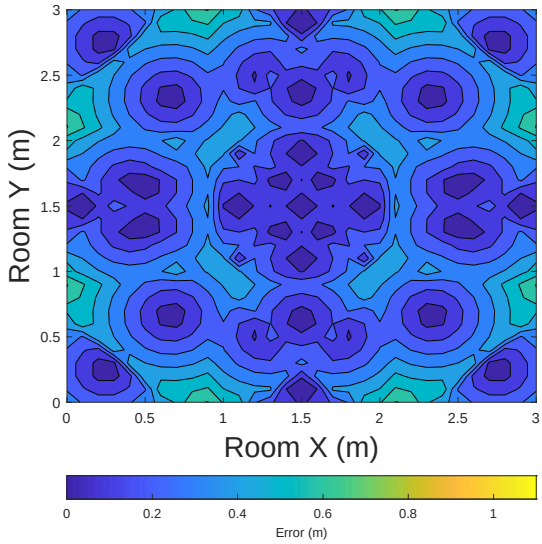

(b)

Figure 6.17: Method performance using an 80° FOV detector for (a) RSS trilateration and (b) CPP

of multipath reflections. It can be seen in Figure 6.17 (a) the RSS based method suffers a high impact from boundary conditions.

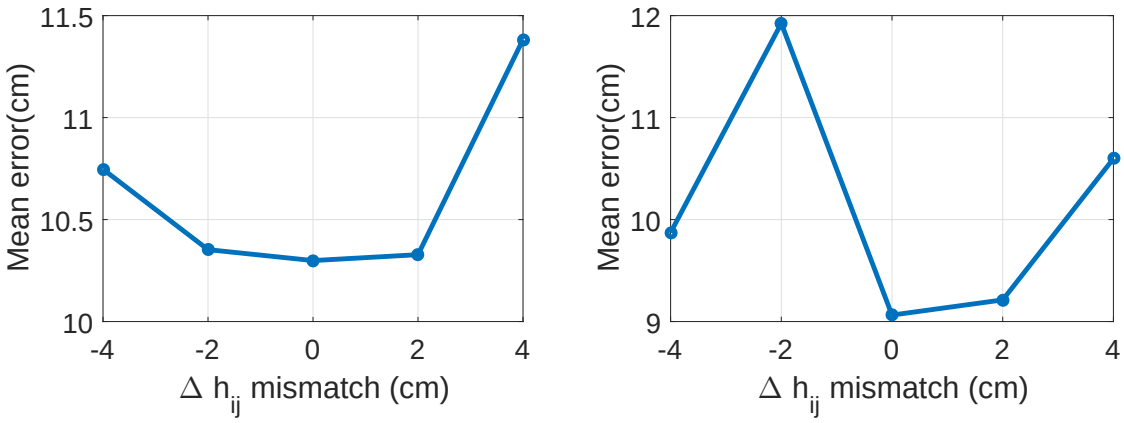

(a) (b)

Figure 6.18: Impact of mismatch measurements on receiver's heigth using PD(IR_3) architecture for (a)$\Delta h_{ij} = 1.5$ meters and (b)$\Delta h_{ij} = 2$ meters

Effect of mismatch receiver's height measurements

In Figure 6.18 the effect of mismatch measurements of receiver's height is shown. The performance of the method to mismatch estimations in an interval between ±4 cm is simulated. This interval is proposed based on the measurements obtained in Figure 6.3 (b). CPP method using PD(c) architecture at receiver side is used to analyse the effect of mismatch measurements.

As it can be seen in Figure 6.18, the impact of a mismatch in the estimation of height difference in the range of ±4 cm increases the mean error in less than 1 cm when PD(IR_3) architecture is used, for a height difference $\Delta h_{ij} = 1.5$ m. In addition to this, negative mismatch produces lower error than positive mismatch.

On the other hand, for $\Delta h_{ij} = 2$ m, mismatches in measurement have higher impact, increasing the mean error from less than 10 cm to approximately 12 cm as shown in Figure 6.18 (b). The impact of mismatch measurements on method performance increases along with the difference height between the source and receiver.

Impact of tilting and rotation angles

In order to perform localization, CPP method uses an initial estimation of the maximum coverage radius based on the FOV of receiver. Since receivers and transmitter are not always parallel, the maximum coverage range may vary based on the tilting angle of the receiver. In Figure 6.19 the effect of tilting and rotation angles on method performance are shown. Mean error of the algorithm is obtained by computational simulation for tilting angles of $\beta = 1°$ and $\beta = 2°$ as proposed in Table 6.1. Furthermore, four discrete values of rotation angle α are analysed.

As it can be seen the rotation angle α has low impact in method performance for a difference height $\Delta h_{ij} = 1.5$ m. On the other hand, as tilting angle β increases, accuracy of the proposed method decreases. The impact of tilting angle β in CPP accuracy is stronger when $\Delta h_{ij} = 2$ m. In addition to this, rotation angles between 180° and 270° also significantly increase the error in this scenario.

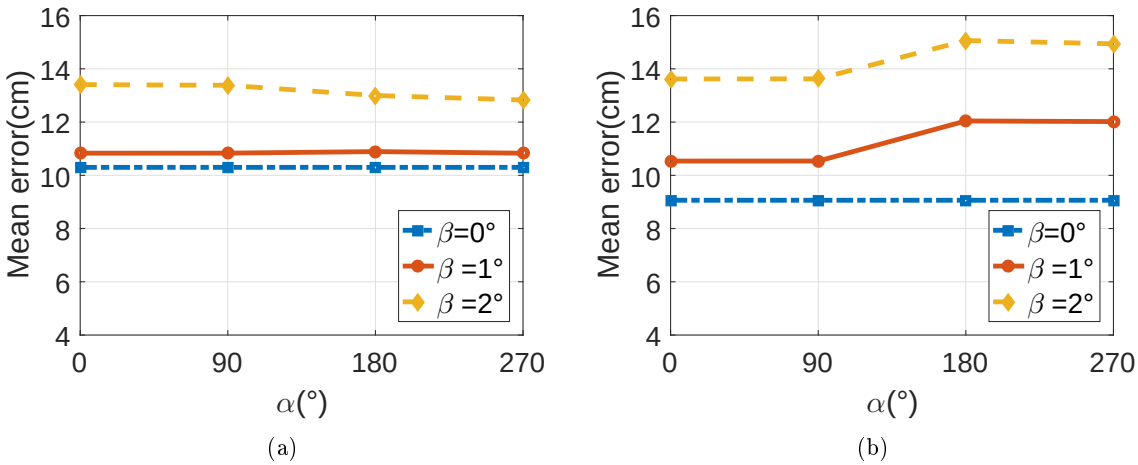

Figure 6.19: Impact of tilting and rotation angles using PD(IR_3) architecture for (a) $\Delta h_{ij} = 1.5$ meters and (b)$\Delta h_{ij} = 2$ meters

6.5.2 Tunnel section

In this section performance of the proposed method for the scenario described in Figure 6.1 (b) is analysed. First, a comparison between different FOVs is done by assuming a a single PD at receiver's side. Then, imaging receivers CPP is evaluated under the same conditions using four different imaging receiver's architectures. Next, a coverage analysis between range free and range based VLP is performed. Finally, effects of multipath reflections, tilt and rotation angles and height mismatch measurements in position estimation are studied.

Method performance: Single PD versus imaging receiver

System parameters of the VLC network such as: testing grid, tunnel dimensions, receiver's FOV and height difference are delivered in Table 6.1. In this section performance of CPP method using single PD and imaging receivers with different FOVs is obtained through computational simulation.

In Figure 6.20 the CDF of positioning errors using CPP method is delivered for two difference heights, i.e., $\Delta h_{ji} = 2$ m and $\Delta h_{ji} = 1.5$ m. As it can be seen the proposed method is suffers changes in accuracy when the receiver's FOV varies.

The detrimental effect on the accuracy suffered by $CPP(s_1)$ can be explained due to the lack of sufficient infrastructure and VLC cell coverage area. Since the method uses architecture information and overlapping conditions to reduce the feasible positioning area, it becomes less effective when the coverage area of each cell $\mathbb{A}_j$ becomes relatively big compared to the tunnel dimensions and the network is not enough densely deployed. Notice that a the number of LED spots used in tunnel scenario is eight. Due to this, density of the network is lower compared to the room scenario. Moreover the proposed tunnel section has an area of 18 m^2 whilst the area of the square room scenario is 9 m^2. This effect is more pronounced for larger difference heights since the coverage radius increases along with Δh_{ji}. The most accurate position estimation is obtained by using a FOV=80° ($CPP(s_2)$) at receiver's side.

Different combinations of FOV angles provide variety of intersection patterns (see Figure 6.12). Due to this, measuring the effect of multiple coverage radius $R_j^{(k)}$ is important. Four

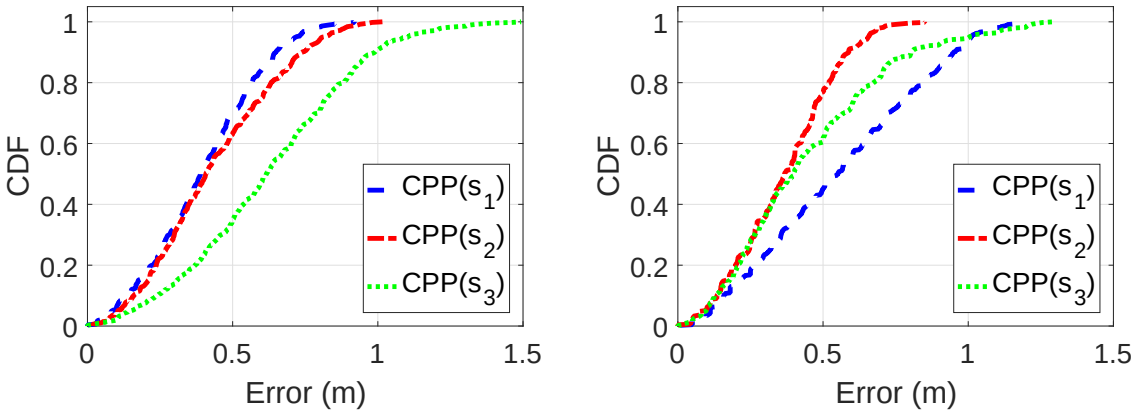

(a) (b)

Figure 6.20: CPP performance using a single PD in tunnel scenario for (a) Δh_{ji}=2 m and (b) Δh_{ji}=1.5 m

different FOV combinations detailed in Table 6.1 are proposed. In Figure 6.21 the cumulative distribution function (CDF) of errors is displayed for $\Delta h_{ij} = 1.5$ and $\Delta h_{ij} = 2$ meters using the four proposed detector architectures.

As it can be seen, the combination of CPP method and imaging receiver increases the accuracy of position estimation. The best performance is achieved when a large variety of FOV angles are used as detectors. In this thesis a maximum number of four PDs is used.

Changes in receiver's height have small impact on IR-CPP performance. Proposed detectors PD(IR_2) and PD(IR_4) are more robust to changes in height difference compared to PD(IR_1) and PD(IR_3) architectures. We can conclude that when there exist a low density of VLC spots in the positioning scenario (VLC spots per square meter), wider FOV angles provide more accurate and robust position estimation.

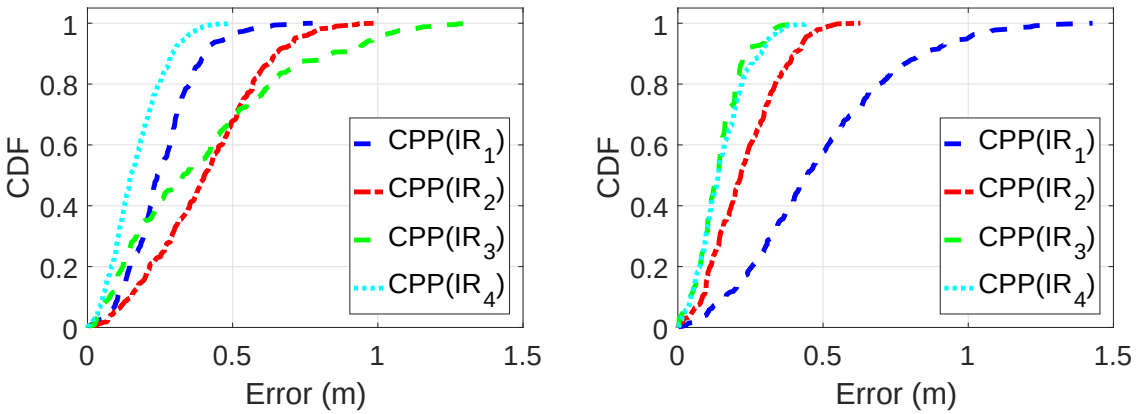

(a) (b)

Figure 6.21: CPP performance using a imaging receiver in tunnel scenario for (a) Δh_{ji}=2 m and (b) Δh_{ji}=1.5 m

As the receiver height difference increases to from $\Delta h_{ij} = 1.5(m)$ to $\Delta h_{ij} = 2(m)$, mean accuracy of CPP method changes. The overall performance of PD(IR_4) architecture overcomes all other proposed detector architectures.

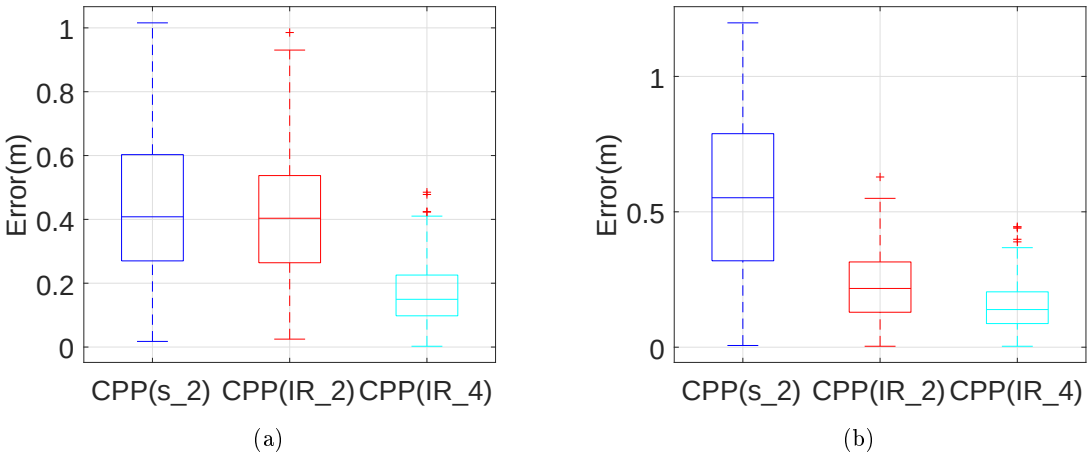

Figure 6.22: Comparison of best PD architectures for (a) Δh_{ji}=2 m and (b) Δh_{ji}=1.5 m

Coverage analysis: Range based vs range free approach

Similarly to the analysis conducted in previous sections we analyse the coverage distribution of VLC spots in tunnel scenario. In Figure 6.23 a two dimensional representation of coverage distribution for range based and range free positioning approaches is presented. A receiver's FOVs of $\Psi_l = 60°$, $\Psi_l = 80°$ and $\Psi_l = 100°$ are used to measure the coverage of VLC cells.

It can be seen that RSS range based method is not capable to cover completely the proposed scenario when a receiver FOV of 60° is used. In order to compute RSS-based method, the mobile node requires the reception of least three VLC cells to estimate its position. The RSS-based algorithm has a coverage area percentage of 3.2786% whilst, under the same FOV conditions, our range free method is capable to cover the 100% of proposed scenario. Moreover, for an 80° PD FOV at receiver side the range based RSS method reach an coverage area of 48.5929% compared again, to the 100% reached by the range free architecture based method.

We can conclude that our proposed range free method is more robust to low infrastructure deployment, whilst range free methods left blind areas with no coverage in underground mine's tunnels.

6.6 Real implementation of CPP method using VLP testing platform

In order to measure the performance of CPP method in a real scenario we use the platform architecture proposed in Chapter 5. In particular, an square room platform of 3x3x3 m of dimensions with 9 LED VLC beacon transmitters is implemented as shown in Figure 6.24. In order to transmit simultaneously position information of VLC beacon nodes FDM is used. Each VLC spot has a unique transmission frequency detailed in Table 6.2.

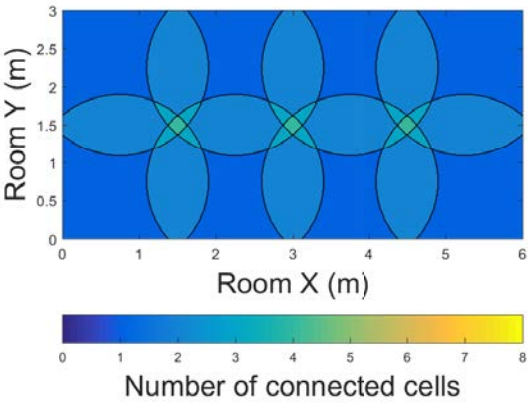

(a)

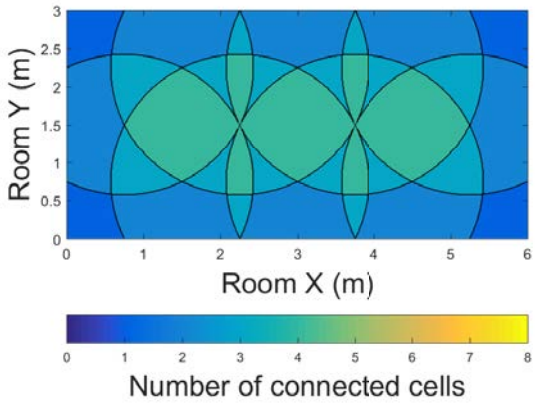

(b)

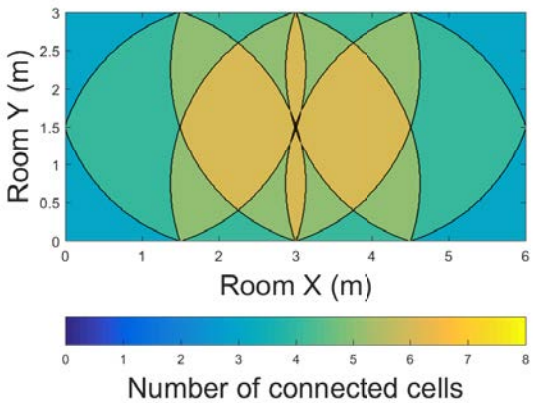

(c)

Figure 6.23: Two dimensional coverage representation in tunnel scenario for Δh_{ji}=2 m (a) FOV=60°, (b) FOV=80° and (c) FOV=100°

Frequency (KHz)	**110**	**130**	**150**	**170**	**190**	**210**	**230**	**250**	**270**
ID number	ID1	ID2	ID3	ID4	ID5	ID5	ID7	ID8	ID9

Table 6.2: Frequencies of VLC beacon nodes

Figure 6.24: Real square room VLC platform for VLP testing

The proposed platform transmits data using OOK modulation with a data rate of 10 Kbps. Dara rate can be incremented easily by software configuration. At receiver side, PD is connected to computer as shown in Figure 5.9. In order to verify our proposed method testing grid shown in Figure 6.25 is used. Each testing grid point is separated by 25 cm. The distance between transmitter and receiver Δh_{ji}=2.25 m. The receiver's FOV is approximately 60°, which means that the coverage radius R_j= 1.3 m. We use these parameters in order to test the method performance in real scenario.

In Figure 6.26 a two dimensional representation of the received power from two simultaneous VLC sources is displayed. In particular ID1 and ID2 sources are represented in these figured. Real power measurements were obtained by using a 0.25x0.25 testing grid. As it can be seen the coverage radius of each VLC spot is larger than 1 m. The power of each source is obtained by passing the received signal through a bandpass filter. Each bandpass filter has a central frequency that correspond with one of the sources detailed in Table 6.2.

In Figure 6.27 the 3-D error distribution of our CPP method is shown. As it can be seen the algorithm shows an accuracy below 1 meter. In addition to this, boundary effects are reduced due to the usage of non-connectivity constraints in the position estimation. In this test only static point by point localization is considered.

Figure 6.25: Photodetector receiver in the testing grid for CPP VLP method validation

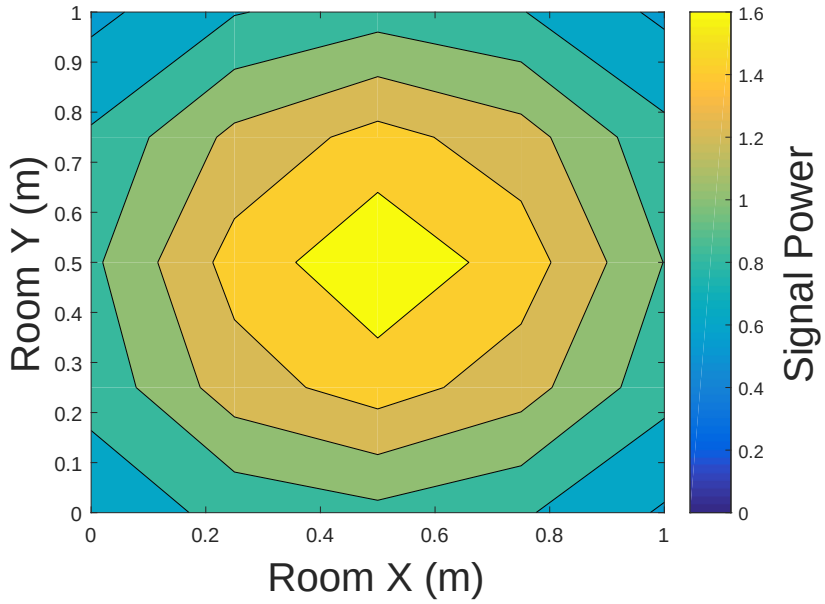

(a)

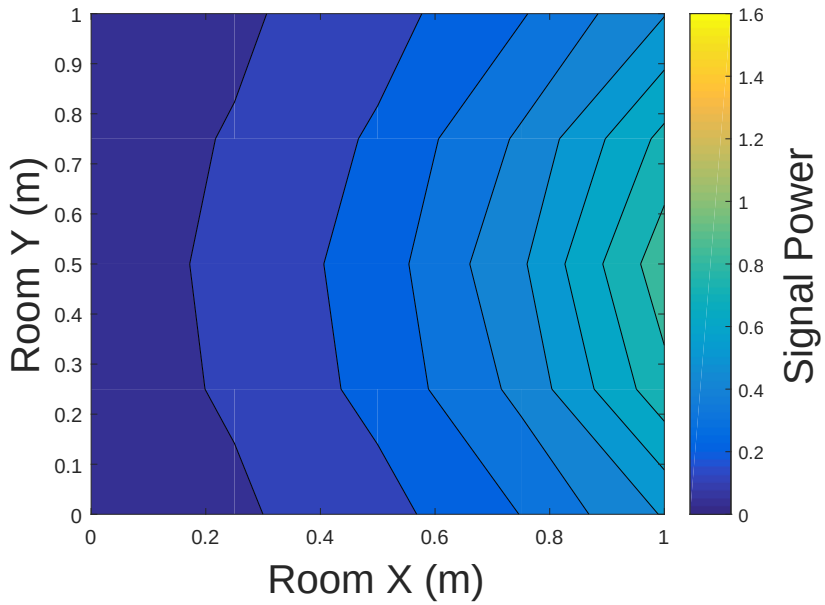

(b)

Figure 6.26: Two dimensional received power representation in testing platform for Δh_{ji}=2.25 m and FOV=60° (a) ID1 VLC beacon and (b) ID2 VLC beacon

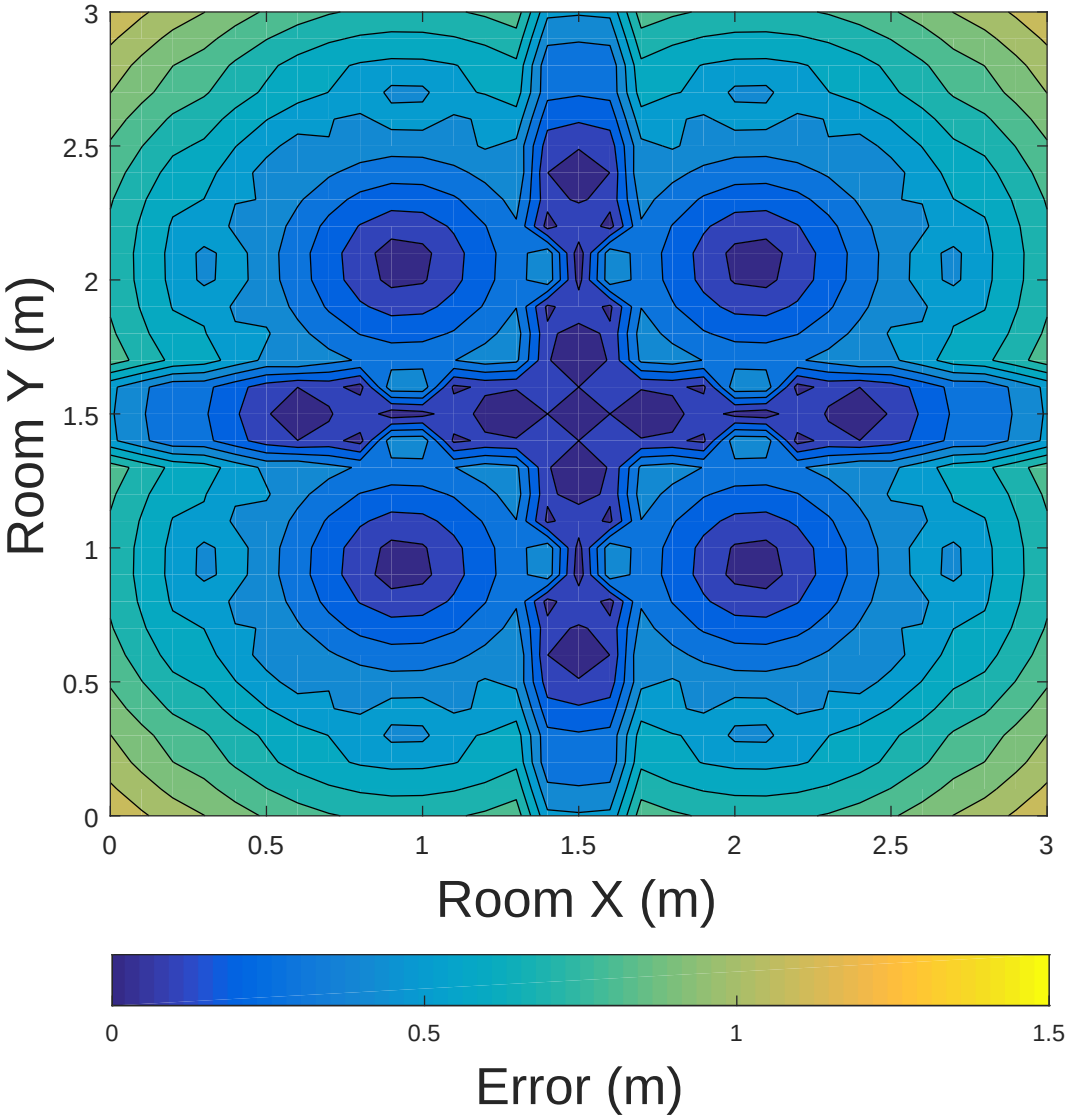

Figure 6.27: Performance of CPP method using the testing VLP platform

Chapter 7

Conclusions and perspectives

Sommaire

7.1 Conclusion **100**
7.2 Perspectives **101**
7.2.1 Reduce the size of proposed receiver 101
7.2.2 Energy efficiency 102
7.2.3 Mobility and Tracking 102

7.1 Conclusion

Visible Light Communication (VLC) has gained the interest as a feasible future wireless communications technology due to its merits in terms of data rate, confidentiality and safety. As a consequence, visible light positioning methods have emerged in the recent years as a technology that uses lighting communication infrastructure to provide high accuracy and low cost position information. In literature, most of the VLP methods have been proposed for low-complexity and safe indoor scenarios such as interior buildings, offices, parkings, etc. However, in some hazardous industrial scenarios most of these scenario conditions are not satisfied as described in Chapter 1 and 2. Due to this, a complete analysis of current positioning technologies and visible light communication link under extreme environmental conditions in indoor environments is required.

Different parameters must be considered when designing a positioning system. Nowadays, different positioning solutions for underground mines exist in the market. These solutions use a wide range of technologies from acoustic to radio-frequency in order to localize workers inside a mine tunnel. Each of them suffers from critical drawbacks in terms of accuracy, scalability, cost and deployment.

Specifically, in Chapter 2 we analyze the already existent positioning methods for underground mines. An extensive discussion and study of this technologies identifies the main strengths and weaknesses of each proposed technology. The main drawbacks of the already proposed technologies are, as mentioned before, their accuracy, scalability and cost. Accuracy of the system established in the MINER act. [10906] is used in order to select a feasible method. As underground tunnel expands, also the positioning system must cover a larger area and, as a consequence, the cost of this localization will increase. Due to this, the system must be scalable and have a low cost of implementation. Underground mines must be illuminated using artificial lights

due to safety and health regulation. Due to this fact, two main question arises: *"Is it possible to provide a positioning system by using the already deployed lighting infrastructure?"* and *"Is this system capable to fulfil the user requirements established by law?"*. These questions are addressed throughout the thesis.

In order to answer these questions first we study the channel propagation characteristics of light inside the tunnel. Different perturbations are taken into account in order to deliver the nearest real-conditions model. We use this model to validate our positioning method and to compare it with traditional VLP algorithms. Our model shows that underground mines are quite unique scenario and three main perturbation can be identified as potential challenges to our proposal, these are: tilted and rotated transmitters, limited deployed lighting infrastructure and presence of dust.

In the following chapter, we analyse these challenges and its effect to visible light positioning methods. As a result of this, we determine that a range free positioning method is more suitable to meet the challenges of underground mines since they are robust to lack of infrastructure and signal propagation characteristics.

Based on the insights provided by previous chapters we design a low cost/large scale visible light positioning hardware in order to test our localization methods. In order to tackle the deficiency of VLC systems to provide uplink communication an hybrid VLC/RF link is proposed as the solution. We exploit the large coverage of UHF band to enable visible light remote positioning and fulfil the requirements of MINER act. [10906]. We design a low cost hardware that supports PD-based and camera based VLP. In addition to this, the proposed architecture support different multiple access methods such as, FDM and TDM.

In Chapter 6 we provide a novel range free algorithm. as established in Chapter 3, range free methods are more robust to the specific characteristics of underground mines. Nevertheless, in order to provide range free and, in general, low cost position estimation previous knowledge of receiver height is required. In order to meet this challenge, two different ranging technologies were studied, these are: IR optical and acoustic ranging. The latter showed better results in terms od accuracy and precision. This technology was used for practical implementation. In general, range free method have high robustness but they suffer from low accuracy. This problem is combated by creating a novel range free algorithm that uses network architecture information in order to provide a convex solution for position estimation. We named this methods convex polygon positioning (CPP). In order to increase the accuracy of our proposed method, we exploit the angular diversity of novel receiver's design. The usage of this type of receivers (image receivers) increase the robustness and accuracy of the proposed method. Finally, the performance of our method is delivered by computational simulations and real implementation on a testing platform.

7.2 Perspectives

7.2.1 Reduce the size of proposed receiver

As described in Chapter 5 the proposed receiver is based on commercially available laboratory instrumentation such as Thorlabs photodetector, oscilloscope and Matlab software. In order to reach mobility, size of proposed method must be reduced. In order to do that, a helmet suitable size transceiver should be designed. Mobility issued will lead to different challenges such as : computational capacity, size, weight and physical robustness among others. An immediate or short-term alternative is to use an small single board computer such as Raspberry Pi zero which is compatible with CVX package for Python. In Figure 7.1 a draft of the proposed portable

device is shown. As it can be seen, the mobile device is capable to support Hybrid VLC and RF communications for downlink and uplink correspondingly.

Figure 7.1: Portable helmet mounted device for VLP in underground mines

7.2.2 Energy efficiency

One of the most important drawbacks of user mobility is the lifespan of mobile devices. Whilst most of the RF based solutions use low energy transceivers, VLC use light detectors. The optical signal retrieve with this type of devices is transformed into a current signal which is amplified and converted into a voltage signal. Energy efficiency of this amplifier must be optimized in order to provide a larger battery lifespan of VLC devices.

Another important aspect to be considered is that the usage of light detectors is similar to the principle use by Photovoltaics (PV) cell. PVs convert light into electricity using semiconducting materials. The electricity produced by the PV device can be used to power the mobile device and, simultaneously, detect the optical VLC signal.

In literature there exist few proposals that use PVs to power the VLC transceiver and detect the optical signal [WCL+17]. In particular, a zero energy visible light communication receiver is proposed in Prabhakar et al. [TSM+18]. Here, optical communication signal is detected while harvesting energy from the same transmission source. In Figure 7.2 the zero energy VLC device scheme is shown.

7.2.3 Mobility and Tracking

Throughout this thesis, the performance of range free visible light positioning methods has been obtained through static computational simulation and real implementation. Due to this, effect of mobility has not been studied.

Typically, mobility has a detrimental effect on positioning accuracy. Due to this, instead using current information to compute position estimation previous estimations are used in order to improve the performance of localization process. The main difference between positioning and tracking is that the first computes current position whereas the latter records a position history.

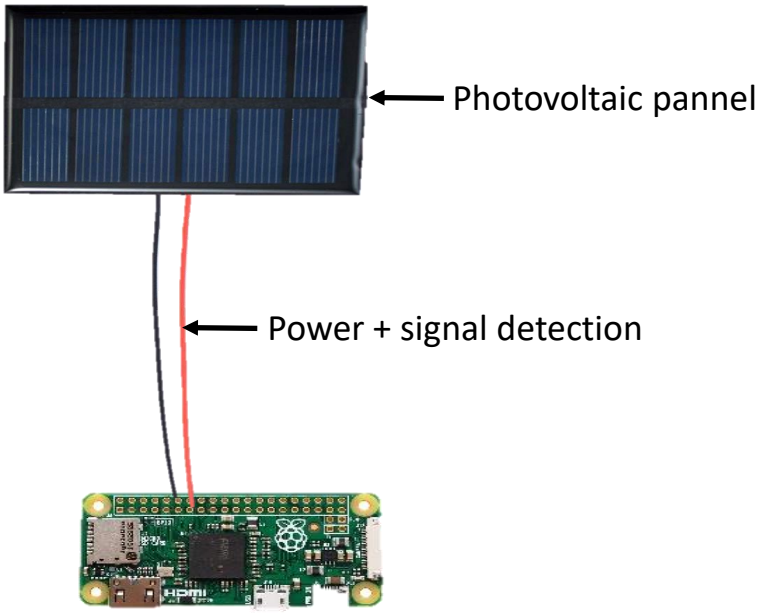

Figure 7.2: Zero energy mobile VLC receiver

Different methods can be found in literature to provide tracking capabilities for VLP systems. Among them, particle filters and extended Kalman filter are the most used methods [GZK14]. Most of the accuracy enhancement techniques have been applied to range based positioning methods.

Further developments on trajectory filtering using mobility and tracking techniques can be hybridized with range free positioning methods in order to increase the robustness of position estimation.

Bibliography

[10906] 109th Congress. Mine Improvement and New Emergency Response, 2006.

[AA14] Abdulsalam Ghalib Alkholidi and Khaleel Saeed Altowij. Free Space Optical Communications — Theory and Practices. In *Contemporary Issues in Wireless Communications*. InTech, nov 2014.

[AIA+17] Ammar M. A. Abu Znaid, Mohd. Yamani Idna Idris, Ainuddin Wahid Abdul Wahab, Liana Khamis Qabajeh, and Omar Adil Mahdi. Sequential Monte Carlo Localization Methods in Mobile Wireless Sensor Networks: A Review. *Journal of Sensors*, 2017:1–19, apr 2017.

[AJ19] Milad Afzalan and Farrokh Jazizadeh. Indoor Positioning Based on Visible Light Communication. *ACM Computing Surveys*, 52(2):1–36, may 2019.

[ASN13] Jean Armstrong, Y. Sekercioglu, and Adrian Neild. Visible light positioning: a roadmap for international standardization. *IEEE Communications Magazine*, 51(12):68–73, dec 2013.

[AXMT16] Traian E. Abrudan, Zhuoling Xiao, Andrew Markham, and Niki Trigoni. Underground Incrementally Deployed Magneto-Inductive 3-D Positioning Network. *IEEE Transactions on Geoscience and Remote Sensing*, 54(8):4376–4391, 2016.

[Bar12] John R. Barry. *Wireless Infrared Communications*. Springer Science & Business Media, Boston, MA, 2012.

[BCS+17] Behlouli, P. Combeau, S. Sahuguede, A. Julien-Vergonjanne, C. Le Bas, and L. Aveneau. Impact of physical and geometrical parameters on visible light communication links. In *2017 Advances in Wireless and Optical Communications (RTUWO)*, pages 73–76. IEEE, nov 2017.

[BDH96] C. Bradford Barber, David P. Dobkin, and Hannu Huhdanpaa. The quickhull algorithm for convex hulls. *ACM Transactions on Mathematical Software*, 22(4):469–483, dec 1996.

[BHE00] N. Bulusu, J. Heidemann, and D. Estrin. GPS-less low-cost outdoor localization for very small devices. *IEEE Personal Communications*, 7(5):28–34, 2000.

[BL05] Dioén Biosca Rojas and Jorge Luís López Presmanes. Generalización del algoritmo de trazado de rayos de Monte Carlo modificado para el cálculo de la respuesta al impulso de canales ópticos infrarrojos en interiores. *Universidad, Ciencia y Tecnología*, 9(33):17–25, 2005.

[BMC10] L. K. Bandyopadhyay, P. K. Mishra, and S. K. Chaulya. *Wireless Communication in Underground Mines*. Springer US, New York, NY, 1 edition, 2010.

[Bus15] BusinessWire. Retail Indoor Location Market Breaks US$10 Billion in 2020, Says ABI Research, 2015.

[BV04] Stephen P. Boyd and Lieven. Vandenberghe. *Convex optimization*. Cambridge University Press, New York, USA, 2004.

[CBH16] Cheng Chen, Dushyantha A. Basnayaka, and Harald Haas. Downlink performance of optical attocell networks. *Journal of Lightwave Technology*, 34(1):137–156, 2016.

[CFT12] Abdellah Chehri, Paul Fortier, and Pierre Martin Tardif. Characterization of the Ultra-Wideband Channel in Confined Environments with Diffracting Rough Surfaces. *Wireless Personal Communications*, 62(4):859–877, feb 2012.

[CLB15] Francisco Chueco, Fernando L??pez, and Miguel Bobadilla. Technical and economic evaluation of fluorescent and LED luminaires in underground mining. A case study: New mine level of El Teniente. *Energy and Buildings*, 93(August):16–22, 2015.

[Com] Safety in Mines Research Advisory Committee. Final Project Report, Assessment of World-wide Illumination and Visibility Standards in Coal Mines ,COL 451.

[CZHG15] Petr Chvojka, Stanislav Zvanovec, Paul Anthony Haigh, and Zabih Ghassemlooy. Channel Characteristics of Visible Light Communications Within Dynamic Indoor Environment. *Journal of Lightwave Technology*, 33(9):1719–1725, may 2015.

[DAMG15] Edith Deretey, Mirza Tahir Ahmed, Joshua A. Marshall, and Michael Greenspan. Visual indoor positioning with a single camera using PnP. In *2015 International Conference on Indoor Positioning and Indoor Navigation, IPIN 2015*. Institute of Electrical and Electronics Engineers Inc., dec 2015.

[Des15] Product Description. Cree ® XLamp ® CXB1512 LED Datasheet, 2015.

[DMS98] C. Drane, M. Macnaughtan, and C. Scott. Positioning GSM telephones. *IEEE Communications Magazine*, 36(4):46–54, 59, apr 1998.

[DPE01] L. Doherty, K.S.J. Pister, and L. El Ghaoui. Convex position estimation in wireless sensor networks. In *Proceedings IEEE INFOCOM 2001. Conference on Computer Communications. Twentieth Annual Joint Conference of the IEEE Computer and Communications Society (Cat. No.01CH37213)*, volume 3, pages 1655–1663, Anchorage, USA, 2001. IEEE.

[DY16] Trong-Hop Do and Myungsik Yoo. An in-Depth Survey of Visible Light Communication Based Positioning Systems. *Sensors*, 16(5):678, 2016.

[EFA16] Maged Abdullah Esmail, Habib Fathallah, and Mohamed-Slim Alouini. An Experimental Study of FSO Link Performance in Desert Environment. *IEEE Communications Letters*, 20(9):1888–1891, sep 2016.

[ELS75] Alfred G. Emslie, Robert L. Lagace, and Peter F. Strong. Theory of the Propagation of UHF Radio Waves in Coal Mine Tunnels. *IEEE Transactions on Antennas and Propagation*, 23(2):192–205, 1975.

[EMGO18] Mahmoud W Eltokhey, Korany R Mahmoud, Zabih Ghassemlooy, and Salah S A Obayya. Optimization of intensities and locations of diffuse spots in indoor optical wireless communications. *Optics Communications*, 410(May):1–7, 2018.

[ER02] Ahmed. El-Rabbany. *Introduction to GPS : the Global Positioning System*. Artech House, 2002.

[FBMN13] Arghavan Emami Forooshani, Shahzad Bashir, David G. Michelson, and Sima Noghanian. A survey of wireless communications and propagation modeling in underground mines. *IEEE Communications Surveys and Tutorials*, 15(4):1524–1545, 2013.

[FFCM17] Andre Ferreira, Duarte Fernandes, Andre Catarino, and Joao Monteiro. Localization and Positioning Systems for Emergency Responders: a Survey. *IEEE Communications Surveys & Tutorials*, pages 1–1, 2017.

[GB79a] F.R. Gfeller and U. Bapst. Wireless in-house data communication via diffuse infrared radiation. *Proceedings of the IEEE*, 67(11):1474 – 1486, 1979.

[GB79b] F.R. Gfeller and U. Bapst. Wireless in-house data communication via diffuse infrared radiation. *Proceedings of the IEEE*, 67(11):1474–1486, 1979.

[GB08] Michael C. Grant and Stephen P. Boyd. Graph Implementations for Nonsmooth Convex Programs. In Blondel Vincent, Boyd Stephen, and Kimura Hidenori, editors, *Recent Advances in Learning and Control*, pages 95–110. Springer London, London, UK, 2008.

[GC18] Amit Kumar Gupta and Ananthanarayanan Chockalingam. Performance of MIMO Modulation Schemes With Imaging Receivers in Visible Light Communication. *Journal of Lightwave Technology*, 36(10):1912–1927, may 2018.

[GPR12] Z. Ghassemlooy, W. Popoola, and S. Rajbhandari. *Optical wireless communications: system and channel modelling with Matlab®*. CRC Press, 2012.

[GZK14] Divya Ganti, Weizhi Zhang, and Mohsen Kavehrad. VLC-based indoor positioning system with tracking capability using Kalman and particle filters. In *2014 IEEE International Conference on Consumer Electronics (ICCE)*, pages 476–477. IEEE, jan 2014.

[HCWZ15] R Hou, Y Chen, J Wu, and H Zhang. A Brief Survey of Optical Wireless Communication. In *13th Australasian Symposium on Parallel and Distributed Computing (AusPDC 2015)*, volume 163, pages 41–50, Sydney, Australia, 2015.

[HKJ14] Andrej Hrovat, Gorazd Kandus, and Tomavz Javornik. A Survey of Radio Propagation Modeling for Tunnels. *IEEE Communications Surveys & Tutorials*, 16(2):658–669, 2014.

[HLC+15] Xingxing Huang, Jiehui Li, Nan Chi, Yiguang Wang, Yuanquan Wang, and Chao Yang. Experimental demonstration for high speed integrated visible light communication and multimode fiber communication system. *IET Optoelectronics*, 9(5):207–210, oct 2015.

[HNP+15] Naveed Ul Hassan, Aqsa Naeem, Muhammad Adeel Pasha, Tariq Jadoon, and Chau Yuen. Indoor Positioning Using Visible LED Lights. *ACM Computing Surveys*, 48(2):1–32, nov 2015.

[HPF+15] F. Hammer, M. Pichler, H. Fenzl, A. Gebhard, and C. Hesch. An acoustic position estimation prototype system for underground mining safety. *Applied Acoustics*, 92:61–74, 2015.

[HY16] Phat Huynh and Myungsik Yoo. VLC-Based Positioning System for an Indoor Environment Using an Image Sensor and an Accelerometer Sensor. *Sensors (Basel, Switzerland)*, 16(6):783–799, may 2016.

[JK04] S. Jivkova and M. Kavehrad. Shadowing and blockage in indoor optical wireless communications. In *GLOBECOM '03. IEEE Global Telecommunications Conference (IEEE Cat. No.03CH37489)*, pages 3269–3273. IEEE, 2004.

[Jud88] Scott M. Juds. *Photoelectric sensors and controls : selection and application*. M. Dekker, 1988.

[JWLL18] Ruonan Ji, Shaowei Wang, Qingquan Liu, and Wei Lu. High-Speed Visible Light Communications: Enabling Technologies and State of the Art. *Applied Sciences*, 8(4):589, apr 2018.

[KB97] J.M. Kahn and J.R. Barry. Wireless infrared communications. *Proceedings of the IEEE*, 85(2):265–298, 1997.

[KKC95] J.M. Kahn, W.J. Krause, and J.B. Carruthers. Experimental characterization of non-directed indoor infrared channels. *IEEE Transactions on Communications*, 43(2/3/4):1613–1623, feb 1995.

[KKY+13] Hyun-Seung Kim, Deok-Rae Kim, Se-Hoon Yang, Yong-Hwan Son, and Sang-Kook Han. An Indoor Visible Light Communication Positioning System Using a RF Carrier Allocation Technique. *Journal of Lightwave Technology*, 31(1):134–144, jan 2013.

[KMPB14] Georg Kail, Patrick Maechler, Nicholas Preyss, and Andreas Burg. Robust asynchronous indoor localization using LED lighting. In *2014 IEEE International Conference on Acoustics, Speech and Signal Processing (ICASSP)*, pages 1866–1870. IEEE, may 2014.

[KN04] Toshihiko Komine and Masao Nakagawa. Fundamental analysis for visible-light communication system using LED lights. *IEEE Transactions on Consumer Electronics*, 50(1):100–107, feb 2004.

[KVAS16] Nicolas Krommenacker, Oscar C. Vasquez, Miguel D. Alfaro, and Ismael Soto. A self-adaptive cell-ID positioning system based on visible light communications in underground mines. In *2016 IEEE International Conference on Automatica (ICA-ACCA)*, pages 1–7, Curico, Chile, oct 2016. IEEE.

[KZKP15] Dilukshan Karunatilaka, Fahad Zafar, Vineetha Kalavally, and Rajendran Parthiban. LED Based Indoor Visible Light Communications: State of the Art. *IEEE Communications Surveys & Tutorials*, 17(3):1649–1678, 2015.

[LAWA17] Shih Chun Lin, Abdallah Awadh Alshehri, Pu Wang, and Ian F. Akyildiz. Magnetic Induction-Based Localization in Randomly-Deployed Wireless Underground Sensor Networks. *IEEE Internet of Things Journal*, 4662(c):1–11, 2017.

[LDBL07] Hui Liu, Houshang Darabi, Pat Banerjee, and Jing Liu. Survey of wireless indoor positioning techniques and systems. *IEEE Transactions on Systems, Man and Cybernetics Part C: Applications and Reviews*, 37(6):1067–1080, 2007.

[LDY15] Shelei Li, Xueyong Ding, and Tingting Yang. Analysis of Five Typical Localization Algorithms for Wireless Sensor Networks. *Wireless Sensor Network*, 07(04):27–33, apr 2015.

[LLY+15] Dimitrios Lymberopoulos, Jie Liu, Xue Yang, Romit Roy Choudhury, Vlado Handziski, and Souvik Sen. A realistic evaluation and comparison of indoor location technologies. In *Proceedings of the 14th International Conference on Information Processing in Sensor Networks - IPSN '15*, pages 178–189, New York, New York, USA, 2015. ACM Press.

[LLZ14] Jian-hui Liu, Qing Li, and Xiao-yi Zhang. Cellular Coverage Optimization for Indoor Visible Light Communication and Illumination Networks. *Journal of communications*, 9(11):891–898, 2014.

[LPC+14] Li Liqun, Hu Pan, Peng Chunyi, Shen Guobin, and Zhao Feng. Epsilon: a visible light based positioning system. In *NSDI'14 Proceedings of the 11th USENIX Conference on Networked Systems Design and Implementation*, pages 331–343, Seattle, 2014.

[Lum] Lumileds. Lumen Maintenance and Reliability.

[LVd00] Cipriano R. Lomba, Rui T. Valadas, and A. M. de Oliveira Duarte. Efficient simulation of the impulse response of the indoor wireless optical channel. *International Journal of Communication Systems*, 13(7-8):537–549, nov 2000.

[LYC+14] Wu Liu, Chao Yang, Yiqin Chen, Qi Yang, and Dawei Zhang. An Indoor Positioning System Based on Cross-correlation in Visible Light Communication. In *Asia Communications and Photonics Conference 2014*, page AW3G.4, Washington, D.C., nov 2014. OSA.

[LYS+14] Hongbo Liu, Jie Yang, Simon Sidhom, Yan Wang, Yingying Chen, and Fan Ye. Accurate WiFi Based Localization for Smartphones Using Peer Assistance. *IEEE Transactions on Mobile Computing*, 13(10):2199–2214, oct 2014.

[LYWJ10] Yunhao Liu, Zheng. Yang, Xiaoping Wang, and Lirong Jian. *Location, localization, and localizability*, volume 25. Springer, New York, USA, 2010.

[LZZ+12] Penghua Lou, Hongming Zhang, Xie Zhang, Minyu Yao, and Zhengyuan Xu. Fundamental analysis for indoor visible light positioning system. *2012 1st IEEE International Conference on Communications in China Workshops, ICCC 2012*, pages 59–63, 2012.

[LZZ+14] Jinxing Li, Youping Zhao, Jing Zhang, Rui Jiang, Cheng Tao, Zhenhui Tan, and Information Engineering. Radio Channel Measurement and Characterization for

Wireless Communications in Tunnels. In *2014 IEEE/CIC International Conference on Communications in China (ICCC)*, pages 554–559. IEEE, oct 2014.

[Mau12] Rainer Mautz. Indoor Positioning Technologies, 2012.

[MC18] Mokhinabonu Mardonova and Yosoon Choi. Review of Wearable Device Technology and Its Applications to the Mining Industry. *Energies*, 11(3):547, mar 2018.

[Min] Mini Physics. The Electromagnetic Spectrum.

[MMJ18] Fadel Abdul-Zahra Murad, Ibrahim Abdullah Murdas, and Ali Raji Jabbar. Dust Effect on The Performance of Optical Wireless Communication System, 2018.

[MP78] J.N. Murphy and H.E. Parkinson. Underground mine communications. *Proceedings of the IEEE*, 66(1):26–50, 1978.

[MPS19] Shubham Mahajan, Davinder Prakesh, and Harjeevan Singh. Performance Analysis of Free Space Optical System Under Different Weather Conditions. In *2019 6th International Conference on Signal Processing and Integrated Networks (SPIN)*, pages 220–224. IEEE, mar 2019.

[MU15] Farshad Miramirkhani and Murat Uysal. Channel Modeling and Characterization for Visible Light Communications. *IEEE Photonics Journal*, 7(6):1–16, dec 2015.

[NJM13] Tuan Nguyen, Yeong Min Jang, and Yeong Min Jang. Highly Accurate Indoor Three-Dimensional Localization Technique in Visible Light Communication Systems. *The Journal of Korean Institute of Communications and Information Sciences*, 38, sep 2013.

[PFHM15] Parth H. Pathak, Xiaotao Feng, Pengfei Hu, and Prasant Mohapatra. Visible Light Communication, Networking, and Sensing: A Survey, Potential and Challenges. *IEEE Communications Surveys and Tutorials*, 17(4):2047–2077, 2015.

[PJRQ+11] R. Perez-Jimenez, J. Rufo, C. Quintana, J. Rabadan, and F. J. Lopez-Hernandez. Visible light communication systems for passenger in-flight data networking. In *2011 IEEE International Conference on Consumer Electronics (ICCE)*, pages 445–446. IEEE, jan 2011.

[PL18] Gregary Prince and Thomas Little. Two-Phase Framework for Indoor Positioning Systems Using Visible Light. *Sensors*, 18(6):1917, jun 2018.

[RGKR07] Jonathan Raper, Georg Gartner, Hassan Karimi, and Chris Rizos. Applications of location–based services: a selected review. *Journal of Location Based Services*, 1(2):89–111, jun 2007.

[RNSA14] Farshad Rashidi-Nejad, Fidelis Suorineni, and Bahareh Asi. Open pit or block caving? A numerical ranking method for selection. In *2014 SOMP Annual Meeting*, number 1, pages 183–199, South Africa, 2014.

[SA10] Zhi Sun and Ian F. Akyildiz. Channel modeling and analysis for wireless networks in underground mines and road tunnels. *IEEE Transactions on Communications*, 58(6):1758–1768, 2010.

[SDM14] Stephan. Sand, Armin. Dammann, and Christian. Mensing. *Positioning in wireless communications systems.* Wiley, 2014.

[sem] Nordic semiconductors. Single chip 433/868/915 MHz Transceiver nRF905.

[SES13] Se-Hoon Yang, Eun-Mi Jung, and Sang-Kook Han. Indoor Location Estimation Based on LED Visible Light Communication Using Multiple Optical Receivers. *IEEE Communications Letters*, 17(9):1834–1837, sep 2013.

[SGY+16] Ge Shi, Ge Shi, Yong Li, Li Xi, and Baitao Zang. A Robust Method for Indoor Localization Based on Visible Light Communication. In *2016 2nd IEEE International Conference on Computer and Communications (ICCC)*, pages 2154–2158, Chengdu, China, oct 2016. IEEE.

[SKS+16] Santosh Subedi, Goo-Rak Kwon, Seokjoo Shin, Suk-seung Hwang, and Jae-Young Pyun. Beacon based indoor positioning system using weighted centroid localization approach. In *2016 Eighth International Conference on Ubiquitous and Future Networks (ICUFN)*, pages 1016–1019. IEEE, jul 2016.

[SN07] S. M. Sze and Kwok Kwok Ng. *Physics of semiconductor devices.* Wiley-Interscience, 2007.

[The15] The National Institute for Occupational Safety and Health (NIOSH). Mining Topic: Illumination, 2015.

[TNH+15] Linus Thrybom, Jonas Neander, Ewa Hansen, Krister Landernas, and Krister Landernäs. Future challenges of positioning in underground mines. *IFAC-PapersOnLine*, 28(10):222–226, jan 2015.

[TSM+18] Prabhakar T, Vishwas Shashidhar, G S Aishwarya Meghana, R. Venkatesha Prasad, and Garani Vittal Pranavendra. Zero energy visible light communication receiver for embedded applications. *ACM SIGBED Review*, 15(2):37–43, jun 2018.

[TWL+15] Anagnostis Tsiatmas, Frans MJ Willems, Jean-Paul MG Linnartz, Stan Baggen, and Jan WM Bergmans. Joint illumination and visible-Light Communication systems: Data rates and extra power consumption. In *2015 IEEE International Conference on Communication Workshop (ICCW)*, pages 1380–1386. IEEE, jun 2015.

[Van08] Craig. Van Slyke. *Information communication technologies : concepts, methodologies, tools and applications.* Information Science Reference, New York, USA, 2008.

[VCZM12] Jayakorn Vongkulbhisal, Bhume Chantaramolee, Yan Zhao, and Waleed S. Mohammed. A fingerprinting-based indoor localization system using intensity modulation of light emitting diodes. *Microwave and Optical Technology Letters*, 54(5):1218–1227, may 2012.

[WAKS+17] Jia Wang, Ahmed Al-Kinani, Jian Sun, Wensheng Zhang, and Cheng-Xiang Wang. A path loss channel model for visible light communications in underground mines. In *2017 IEEE/CIC International Conference on Communications in China (ICCC)*, pages 1–5. IEEE, oct 2017.

[WAKZ+18] Jia Wang, Ahmed Al-Kinani, Wensheng Zhang, Cheng-Xiang Wang, and Li Zhou. A general channel model for visible light communications in underground mines. *China Communications*, 15(9):95–105, sep 2018.

[WC05] Damon W K Wong and George C K Chen. Optimization of spot pattern in indoor diffuse optical wireless local area networks. *Optics Express*, 13(8):317–324, 2005.

[WCL+17] Jhao Ting Wu, Chi Wai Chow, Yang Liu, Chin Wei Hsu, and Chien Hung Yeh. Performance enhancement technique of visible light communications using passive photovoltaic cell. *Optics Communications*, 392:119–122, jun 2017.

[Wer14] Martin Werner. *Indoor location-based services: Prerequisites and foundations*, volume 9783319106. 2014.

[Wis96] D.R. Wisely. A 1 Gbit/s optical wireless tracked architecture for ATM delivery. In *IEE Colloquium on Optical Free Space Communication Links*, volume 1996, pages 14–14. IEE, 1996.

[WWC+17] Lang Wang, Chunyue Wang, Xuefen Chi, Linlin Zhao, and Xiaoli Dong. Optimizing SNR for indoor visible light communication via selecting communicating LEDs. *Optics Communications*, 387(November 2016):174–181, 2017.

[WWY14] Shaoen Wu, Honggang Wang, and Chan-hyun Youn. Visible light communications for 5G wireless networking systems: from fixed to mobile communications. *Network, IEEE*, 28(December):41–45, 2014.

[XYY+17] Zirui Xu, Wei Yang, Kaiming You, Wei Li, and Young Il Kim. Vehicle autonomous localization in local area of coal mine tunnel based on vision sensors and ultrasonic sensors. *PLoS ONE*, 12(1):1–31, 2017.

[YGAM09] Serhan Yarkan, Sabih Guzelgoz, Huseyin Arslan, and Robin Murphy. Underground Mine Communications: A Survey. *IEEE Communications Surveys & Tutorials*, 11(3):125–142, 2009.

[YHV16] Muhammad Yasir, Siu-Wai Ho, and Badri N. Vellambi. Indoor Position Tracking Using Multiple Optical Receivers. *Journal of Lightwave Technology*, 34(4):1166–1176, feb 2016.

[YNA+17] Ali Yassin, Youssef Nasser, Mariette Awad, Ahmed Al-Dubai, Ran Liu, Chau Yuen, Ronald Raulefs, and Elias Aboutanios. Recent Advances in Indoor Localization: A Survey on Theoretical Approaches and Applications. *IEEE Communications Surveys & Tutorials*, 19(2):1327–1346, 2017.

[YZXZ15] Kun Yan, Haiyan Zhou, Hailin Xiao, and Xiangli Zhang. Current status of indoor positioning system based on visible light. In *2015 15th International Conference on Control, Automation and Systems (ICCAS)*, pages 565–569, Busan, South Korea, oct 2015. IEEE.

[ZB11] Seyed A Reza Zekavat and Michael Buehrer. *Handbook of Position Location: Theory, Practice, and Advances.* Wiley, 2011.

[ZCK14] Weizhi Zhang, M. I. Sakib Chowdhury, and Mohsen Kavehrad. Asynchronous indoor positioning system based on visible light communications. *Optical Engineering*, 53(4):045105, apr 2014.

[ZHQ+18] Yuan Zhuang, Luchi Hua, Longning Qi, Jun Yang, Pan Cao, Yue Cao, Yongpeng Wu, John Thompson, and Harald Haas. A Survey of Positioning Systems Using Visible LED Lights. *IEEE Communications Surveys and Tutorials*, 1(February):1963 – 1988, 2018.

[ZWW+15] Rong Zhang, Jiaheng Wang, Zhaocheng Wang, Zhengyuan Xu, Chunming Zhao, and Lajos Hanzo. Visible light communications in heterogeneous networks: Paving the way for user-centric design. *IEEE Wireless Communications*, 22(2):8–16, apr 2015.

Résumé

En raison des progrès des appareils électroniques et des technologies de communication, de nouvelles règles de sécurité doivent être appliquées afin d'exploiter les mines souterraines de façon sécuritaire et optimale. En 2006, le gouvernement américain a mis à jour ses politiques de sécurité et a adopté la PUBLIC LAW109-236. De ce fait, le suivi de personnel à l'intérieur des tunnels souterrains est aujourd'hui obligatoire pour l'exploitation des mines. Cette nouvelle réglementation établit que l'emplacement actuel, ou immédiatement avant l'accident, de tout le personnel souterrain doit être livré à une station de surveillance extérieure. Malgré les récents progrès des systèmes de suivi et de positionnement pour les environnements intérieurs, les mines souterraines constituent un cadre unique, qui impose des contraintes différentes aux technologies actuelles. Au cours des dernières années, les communications par lumière visible (Visible Light Communications - VLC) ont attiré l'attention des chercheurs, grâce principalement aux progrès récents dans la fabrication des diodes électroluminescentes (Light Emitting Diodes LEDs). Le développement rapide des systèmes VLC a encouragé les chercheurs à proposer des solutions de positionnement basées sur cette technologie. Le positionnement par lumière visible (VLP) présentent plusieurs avantages par rapport aux méthodes de positionnement traditionnelles. La plupart des méthodes VLP ont été évaluées dans des scénarios où il existe un réseau VLC dense et bien déployé. Les mines souterraines constituent de leur côté un environnement dynamique et dangereux par nature, et la plupart des hypothèses faites pour les environnements intérieurs traditionnels ne sont pas respectées. La faisabilité de l'utilisation d'un système VLP dans de telles conditions et capable de répondre aux exigences de positionnement reste une question ouverte. Par conséquent, le principal problème à résoudre dans la présente thèse est la conception et le développement de systèmes de positionnement pour mine souterraine, basés sur la communication par lumière visible. Le chapitre 2 vise à détecter les contraintes et limites des technologies de positionnement actuelles lorsqu'elles sont appliquées en milieu minier souterrain. En plus de cela, les exigences de positionnement basées sur la loi MINER sont présentées. Le chapitre 3, nous permet de présenter une évaluation de la performance des VLC en milieu souterrain. La mise en œuvre d'un simulateur de modèle de canal VLC pour les mines outerraines sert à déterminer les limites de plusieurs systèmes VLP dans les mines souterraines. Ainsi, au chapitre 4, une étude analytique des VLP pour les tunnels souterrains est réalisée afin de déterminer la meilleure architecture garantissant le service de positionnement tout en répondant aux exigences de localisation. A partir des principales limitations du VLP dans les mines souterraines et des exigences « utilisateur », un système de positionnement VLP est conçu et mis en œuvre. Le chapitre 5 utilise les limitations, les capacités et les exigences de positionnement pour concevoir une architecture de positionnement à faible coût et à grande échelle. En utilisant cette conception, nous avons développé une plate-forme réelle pour évaluer la performance des méthodes de positionnement par lumière visible. Au chapitre 6, une nouvelle méthode de positionnement robuste est présentée. Contrairement à la plupart des méthodes existantes dans la littérature, notre proposition n'est pas directement dérivée des méthodes basées sur les RF. L'algorithme proposé utilise les caractéristiques spéciales de la communication par lumière visible pour améliorer la performance de l'estimation de la position. La robustesse de notre méthode à plusieurs perturbations (erreurs dans la mesure de la hauteur, des angles d'inclinaison, et la propagation par trajets multiples à cause de réflexions de la lumière sur les murs) a été testée.

Mots-clés: Indoor positioning, Visible light communications, underground mines.

Abstract

Advances in electronics and communications technology have created new safety regulations that must be applied in order to operate underground mines safely and optimally. In 2006, the U.S. government updated its safety policies and adopted PUBLIC LAW109-236. As a result, monitoring of personnel inside underground tunnels is now mandatory for mining operations. This new regulation establishes that the current location, or immediately prior to the accident, of all underground personnel must be delivered to an external monitoring station. Despite recent advances in tracking and positioning systems for indoor environments, underground mines provide a unique environment that places different constraints on current technologies. In recent years, Visible Light Communications (VLC) has attracted the attention of researchers, mainly due to recent advances in the manufacture of Light Emitting Diodes (LEDs). The rapid development of VLC systems has encouraged researchers to propose positioning solutions based on this technology. Visible light positioning (VLP) has several advantages over traditional positioning methods. Most VLP methods have been evaluated in scenarios where a dense and well-deployed VLC network exists. Underground mines, on the other hand, are a dynamic and inherently hazardous environment and most of the assumptions made for traditional indoor environments are not met. The feasibility of using a VLP system under such conditions and capable of meeting positioning requirements remains an open question. Therefore, the main problem to be solved in this thesis is the design and development of positioning systems for underground mines, based on visible light communication. Chapter 2 aims at detecting the constraints and limitations of current positioning technologies when applied in an underground mining environment. In addition, the positioning requirements based on the MINER law are presented. Chapter 3, allows us to present an evaluation of the performance of VLCs in an underground environment. The implementation of a VLC channel model simulator for underground mines is used to determine the limits of several VLP systems in underground mines. Thus, in Chapter 4, an analytical study of VLPs for underground tunnels is carried out to determine the best architecture to guarantee the positioning service while meeting the location requirements. Based on the main limitations of the VLP in underground mines and the user requirements, a VLP positioning system is designed and implemented. Chapter 5 uses the positioning limitations, capabilities and requirements to design a low-cost, large-scale positioning architecture. Using this design, we have developed a real-world platform to evaluate the performance of visible light positioning methods. In Chapter 6, a new robust positioning method is presented. Unlike most existing methods in the literature, our proposal is not directly derived from RF-based methods. The proposed algorithm uses the special characteristics of visible light communication to improve the performance of position estimation. The robustness of our method to multiple perturbations (errors in the measurement of height, tilt angles, and multipath propagation due to light reflections from walls) has been tested.

Keywords: Indoor positioning, Visible light communications, underground mines.

Titre de la thèse:

Système robuste de localisation par lumière visible : application au domaine de l'exploitation des mines souterraines

(Robust localization system using Visible Light Communication technology for underground mines)

Présenté par M. Fabián Esteban SEGUEL GONZÁLEZ

Pour l'obtention du Doctorat de l'Université de Lorraine Mention Automatique, Génie Informatique.

Sous la direction de: Professeur Patrick CHARPENTIER et Maitre de conférences Nicolas KROMMENACKER

Introduction et Motivation

L'ouverture du système de positionnement global (global positioning system - GPS) à l'usage civil et l'arrêt de la selectivity availability (SA) en mai 2000 ont fait progresser l'industrie du positionnement et aux services basés sur la localisation (LBS). Alors que la Géolocalisation et Navigation par un Système de Satellites (GNSS) est devenu précis et omniprésent, il n'a pas été capable de surmonter les différents problèmes rencontrés dans les environnements intérieurs ou les scénarios métropolitains denses. Le signal en ligne de vue (line-of-sight - LOS) peut être bloqué par des bâtiments élevés dans les zones métropolitaines. Dans les scénarios d'intérieur, comme à l'intérieur des bâtiments et des tunnels, le signal est complètement perdu car les signaux GNSS ne peuvent pas pénétrer le béton, le métal ou le sol.

Alors que la navigation en extérieur est dominé par le GNSS, il n'existe pas de solution technologique unique pour les environnements intérieurs et de nombreuses technologies ont été proposées comme solutions possibles. La plupart des systèmes de positionnement intérieur (indoor positioning systems - IPS) que l'on trouve dans la littérature sont basés sur la technologie des radiofréquences (RF), des champs

magnétiques ou des signaux acoustiques [1]. Parmi eux, les IPS basés sur la technologie Wireless Fidelity (Wifi) sont la solution préféré car cette technologie est couramment intégrée dans les dispositifs disponibles sur le marché et réutilise l'infrastructures déjà disponible (points d'accès Wifi) pour fournir des informations de position [2], [3]. Le principal inconvénient de l'IPS basé sur le Wifi est que des grandes erreurs de positionnement peuvent toujours être trouvées (par exemple 6 m 8 m) dans le positionnement purement Wifi même si une précision raisonnable peut être obtenue [4].

En raison des progrès des appareils électroniques et des technologies de communication, de nouvelles règles de sécurité doivent être appliquées afin d'exploiter les mines souterraines de façon sécuritaire et optimale. En 2006, le gouvernement américain a mis à jour ses politiques de sécurité et a adopté la PUBLIC LAW109-236 [5]. De ce fait, le suivi de personnel à l'intérieur des tunnels souterrains est aujourd'hui obligatoire pour l'exploitation des mines. Cette nouvelle réglementation établit que l'emplacement actuel, ou immédiatement avant l'accident, de tout le personnel souterrain doit être livré à une station de surveillance extérieure. Malgré les récents progrès des systèmes de suivi et de positionnement pour les environnements intérieurs, les mines souterraines constituent un cadre unique, qui impose des contraintes différentes aux technologies actuelles.

Au cours des dernières années, les communications par lumière visible (Visible Light Communications - VLC) ont attiré l'attention des chercheurs, grâce principalement aux progrès récents dans la fabrication des diodes électroluminescentes (Light Emitting Diodes LEDs). Le développement rapide des systèmes VLC a encouragé les chercheurs à proposer des solutions de positionnement basées sur cette technologie. Le positionnement par lumière visible (visible light positioning - VLP) présentent plusieurs avantages par rapport aux méthodes de positionnement traditionnelles.

La plupart des méthodes VLP ont été évaluées dans des scénarios où il existe un réseau VLC dense et bien déployé. Les mines souterraines constituent de leur côté un environnement dynamique et dangereux par nature, et la plupart des hypothèses

faites pour les environnements intérieurs traditionnels ne sont pas respectées. La faisabilité de l'utilisation d'un système VLP dans de telles conditions et capable de répondre aux exigences de positionnement reste une question ouverte. Par conséquent, le principal problème à résoudre dans la présente thèse est la conception et le développement de systèmes de positionnement pour mine souterraine, basés sur la communication par lumière visible.

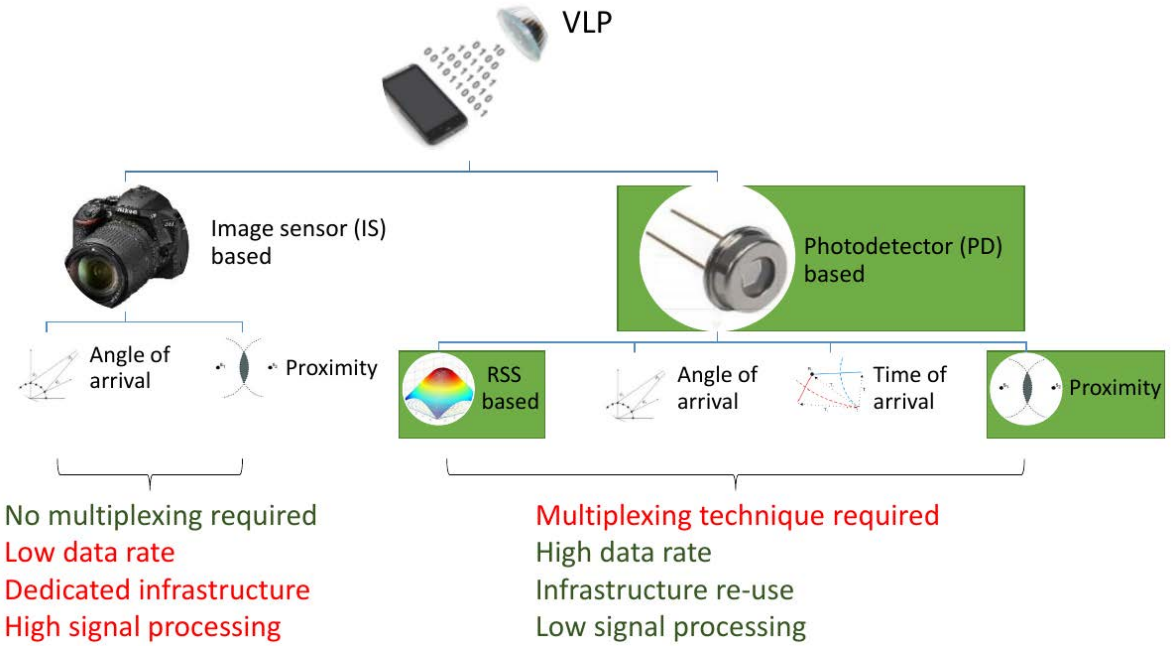

Figure 1 Classification des systèmes VLP

Contribution de l'étude

Sur la base de la classification des systèmes VLP de la figure 1, nous présentons la principale contribution de cette thèse. L'objectif de cette thèse est de fournir un système VLP pour les mines souterraines capable de répondre aux exigences particulières présentes dans cet environnement dangereux. Nos principales contributions sont résumées ci-dessous :

I. Évaluation des technologies de positionnement actuelles pour l'environnement des mines souterraines. Nous proposons, pour la première fois dans la littérature, une étude analytique des technologies actuelles qui

ont été proposées pour fournir de positionnement aux mines souterraines. A travers une classification et une analyse rigoureuses de plusieurs technologies, nous présentons les principaux avantages et inconvénients de chaque système.

II. Évaluation des besoins des utilisateurs en matière de systèmes de positionnement des mines souterraines. Nous dérivons les principales exigences des utilisateurs pour les systèmes VLP dans les mines souterraines en nous basant sur les caractéristiques particulières de cet environnement et, en utilisant la loi publique américaine 109-236 de 2006 [5]. De cette analyse, nous obtiendrons les principaux évaluateurs de performance pour évaluer les résultats des VLP.

III. Mise en œuvre d'un simulateur de modèle de canal VLC pour les mines souterraines. Nous proposons un modèle générique de canal VLC dans les mines souterraines. Ce modèle de canal prend en compte plusieurs caractéristiques des mines souterraines qui ne sont pas présentes dans les modèles traditionnels (températures plus élevées, non orthogonalité des parois, blocage partiel et total du signal, etc.) Le simulateur peut être utilisé non seulement pour évaluer les systèmes VLP, mais aussi les performances des VLC dans les mines souterraines.

IV. Étude analytique de la VLP dans l'environnement des mines souterraines. En utilisant le modèle de canal proposé pour les mines souterraines, nous développons, pour la première fois dans la littérature, une étude analytique des performances de la VLP dans les mines souterraines.

V. Conception d'une topologie de système de positionnement optimisée pour le VLP dans les mines souterraines. Nous concevons une topologie de système de positionnement afin de répondre aux exigences de l'utilisateur en matière de VLP dans les mines souterraines. Cette conception est utilisée afin de développer une implémentation matérielle réelle d'un système VLP. Cette contribution est détaillée au chapitre 4.

VI. Mise en place d'un système de VLP à faible coût et à grande échelle. Nous mettons en œuvre un système VLP à faible coût et à grande échelle pour les

mines souterraines. Différents systèmes VLP sont évalués à l'aide de cette mise en œuvre matérielle. La plate-forme peut être utilisée pour tester non seulement les méthodes proposées dans cette thèse, mais aussi des développements ultérieurs

VII. Conception et mise en œuvre d'une méthode VLP robuste sans gamme. Nous fournissons la première méthode VLP sans gamme conçue en utilisant les caractéristiques de réutilisation spatiale des systèmes VLC. Nous avons mis en œuvre et évalué notre méthode en utilisant le matériel à faible coût et à grande échelle proposé dans cette thèse. Notre proposition est comparée à d'autres méthodes traditionnelles à portée libre conçues pour les communications RF. Les contributions \textbf{(1)} et \textbf{(2)}, détaillées au chapitre 2, présentent les besoins des utilisateurs et les caractéristiques de positionnement dans les mines souterraines.

VIII. Évaluation des exigences de robustesse des VLP. Nous étudions la robustesse de plusieurs méthodes de positionnement dans le cadre du scénario des mines souterraines. Nous comparons les résultats des systèmes que nous proposons avec une méthode de positionnement traditionnelle basée sur les radiofréquences. Notre évaluation fournit des informations essentielles pour choisir le système VLP adéquat dans l'environnement des mines souterraines.

Structure de la thèse

La figure 2 présente un diagramme de processus montrant la construction étape par étape de cette thèse.

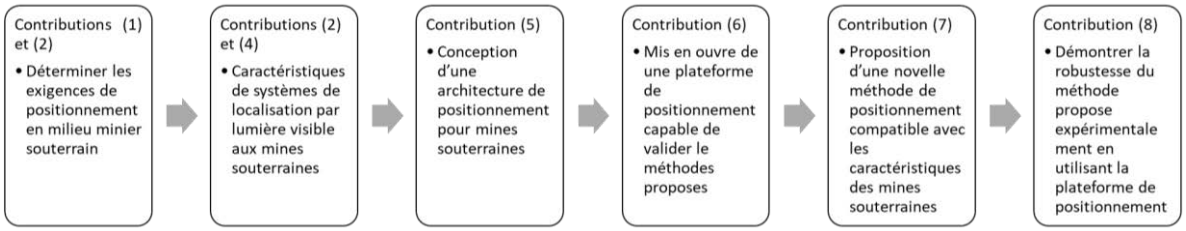

Figure 2 Structure de thèse: Diagramme de procèdes

La contribution **I,** présentée au chapitre 2, vise à détecter les problèmes des technologies de positionnement actuelles lorsqu'elles sont appliquées dans l'environnement des mines souterraines. Ensuite, la contribution **II**, livrée dans le même chapitre, est utilisée pour déterminer les spécifications de l'utilisateur pour ce scénario particulier. La conception correcte d'un système VLP doit être faite après une évaluation rigoureuse des exigences.

Plus loin, une fois que les exigences et les caractéristiques du positionnement souterrain sont établies, une évaluation de la performance du VLC en environnement souterrain est fournie. Les contributions **III** et **IV** sont utilisées pour déterminer les limites de plusieurs systèmes VLP dans les mines souterraines. Ces résultats seront comparés aux exigences découlant des contributions **I** et **II** afin de déterminer la meilleure architecture pour pouvoir garantir un service de positionnement dans le scénario proposé. Les contributions **III** et **IV** sont présentées respectivement aux chapitres 3 et 4.

Une fois que les principales limites du VLP dans les mines souterraines sont déterminées et que les exigences des utilisateurs sont établies, un système de positionnement VLP est conçu et mis en œuvre. Contribution **V** utilise les limitations, les capacités et les exigences des utilisateurs détaillées dans les chapitres 2, 3 et 4 pour concevoir une architecture matérielle à faible coût et à grande échelle pour les mines souterraines, qui est détaillée dans le chapitre 5. La contribution **VI**, livrée dans le même chapitre, exploite cette conception pour mettre en œuvre une plate-forme du monde réel qui sera utilisée pour évaluer les performances des méthodes de positionnement en lumière visible.

La contribution **VII** présente une nouvelle méthode robuste de positionnement sans portée. Contrairement à la plupart des méthodes existant dans la littérature, notre proposition n'est pas directement dérivée des méthodes basées sur les RF. L'algorithme proposé utilise des caractéristiques spéciales de la VLC pour améliorer les performances d'estimation de la position. Le chapitre 6 donne un aperçu de notre méthode.

Finalement, la contribution **VIII** évalue la performance de notre proposition en utilisant la plate-forme d'essai de la méthode à grande échelle/faible coût de la contribution **VI**. L'algorithme proposé utilise les caractéristiques spéciales de la communication par lumière visible pour améliorer la performance de l'estimation de la position. La robustesse de notre méthode à plusieurs perturbations (erreurs dans la mesure de la hauteur, des angles d'inclinaison, et la propagation par trajets multiples à cause de réflexions de la lumière sur les murs) a été testée.

Références

[1] D. Lymberopoulos, J. Liu, X. Yang, R. R. Choudhury, V. Handziski, and S. Sen, “A realistic evaluation and comparison of indoor location technologies,” in *Proceedings of the 14th International Conference on Information Processing in Sensor Networks - IPSN ’15*, 2015, pp. 178–189.

[2] X. Liu, H. Makino, S. Kobayashi, and Y. Maeda, “Design of an Indoor Self-Positioning System for the Visually Impaired - Simulation with RFID and Bluetooth in a Visible Light Communication System,” in *2007 29th Annual International Conference of the IEEE Engineering in Medicine and Biology Society*, 2007, pp. 1655–1658.

[3] N. U. Hassan, A. Naeem, M. A. Pasha, T. Jadoon, and C. Yuen, “Indoor Positioning Using Visible LED Lights,” *ACM Comput. Surv.*, vol. 48, no. 2, pp. 1–32, Nov. 2015.

[4] H. Liu, J. Yang, S. Sidhom, Y. Wang, Y. Chen, and F. Ye, “Accurate WiFi Based Localization for Smartphones Using Peer Assistance,” *IEEE Trans. Mob. Comput.*, vol. 13, no. 10, pp. 2199–2214, Oct. 2014.

[5] 109th Congress, “Mine Improvement and New Emergency Response,” *Public Law*. pp. 109–236, 2006.